Cato de Hullu

The effect of sediment grain size on dune erosion

a field experiment

TU Delft

Witteveen + Bos

The effect of sediment grain size on dune erosion

Experimental field study on the effect of sediment grain size on dune erosion at the Sand Engine by conducting manipulative field experiments

by

Cato de Hullu

In partial fulfilment of the requirement for the degree of Master of Science in Hydraulic Engineering at the faculty of Civil Engineering and Geosciences at Delft University of Technology to be defended publicly on May 10^{th} 2023

Thesis committee:

Chair:	Ass. prof. dr. ir. S. de Vries
Supervisors:	Prof. dr. ir. A. J. H. M. Reniers
	Ir. P. P. J. van Wiechen
	Ir. C. W. T. van Bemmelen
Place:	Faculty of Civil Engineering, Delft
Project Duration:	July, 2022 - May, 2023
Student number:	4542037

An electronic version of this thesis is available at http://repository.tudelft.nl/.

Hydraulic Engineering · Delft University of Technology

Preface

This master thesis finalises my MSc study Hydraulic Engineering at Delft University of Technology, with a specialisation in Coastal and River engineering. This study is only a small part of the extensive research on dune erosion in the coastal zone. This study is a collaboration between TU Delft and the engineering firm Wittenveen Bos. I am extremely grateful and still excited that I had the opportunity to conduct large-scale field experiments in September 2022 for this study. In this first section of this report I would like to express my gratitude to everyone who contributed to this study.

This master's thesis would not have been possible without the help of many people. I would like to thank all members of my graduation committee for dedicating their time and sharing their knowledge and positivity. I always looked forward to our committee meetings. First of all I would like to thank my chair, Sierd de Vries, for his accessibility and always making time for a thorough discussing. I also want to thank him for his enthusiasm and inviting me to interesting events where I was able to share this study. I would like to thank Ad Reniers for his experience and ciritical view on approaches which helped to bring this study to a higher level. I would like to thank Paul van Wiechen for the weekly meetings, patients, for all the help during the fieldwork and for letting me taste the differences between the university coffee machines. Finally, I would like to thank Cas van Bemmelen for all the brain storming, motivation and resolving python bugs.

I also want to thank Pieter van der Gaag, Arno, and Arie for supporting me in the first two months with all the preparations prior to the fieldwork. Creating such a successful week would not have been possible without their contributions and smart solutions. Additionally, I want to thank all the students who participated in this study during the fieldwork course. Despite the bad weather and the major setback, we had a great week with a lot of laughs.

Special thanks go to my support group of friends, including Tom, Mathieu, Eva, and Sophie, for their assistance with the pilot run. Last but not least, I am grateful to my parents and Marie for always supporting me and for trying to get me home with a calm work space and treats!

I really enjoyed working on this topic and was (almost) never not motivated to work on my thesis. I had a great time at the TU Delft!

Enjoy reading!

C.C. de Hullu
Delft, April 2023

Abstract

Along the Dutch coastline, coastal dunes act as the primary sea defence to protect the low-lying areas behind it from flooding. To ensure that these dunes are strong enough to meet national safety standards, models are used to assess their strength. Even though our modelling capabilities have significantly improved over the years, model uncertainties remain because specific processes are not yet fully understood.

One of those uncertainties is the effect of sediment grain size on dune erosion. The relative importance and effect of this parameter differs significantly among dune erosion models. It is however expected that this parameter influences the morphological response of dunes during storm conditions.

Manipulative field experiments to study the effect of sediment grain size on dune erosion were conducted from September 24 until September 27 2022. In total, six experiments were conducted in which four different grain sizes were tested. Two open shipping containers were placed in the intertidal zone and acted as coastal wave flumes. Inside both containers, artificial dunes were built, with median grain sizes ranging from 0.21 to 0.31 mm, and were subjected to wave attack during high water. Cameras were used to calculate erosion volumes at a high sampling frequency. Environmental conditions were measured to capture water levels and wave conditions.

Dune erosion was measured with cameras, providing a low-cost and user-friendly method. This method can accurately and continuously capture dune profiles, particularly when there is a distinct color contrast between the dune profile, incoming swash, and backdrop. Analysis of the profile development reveals that the dune toe linearly translates over time in both the cross-shore and vertical directions. The translation in the vertical direction is also correlated with the rising mean water level.

The analytical model derived by Larson et al. (2004) based on wave impact theory was used to relate measured erosion volumes to incoming hydrodynamic conditions and to isolate the relative importance of sediment grain size on dune erosion. The considered time interval used in this study differs from the original approach, as this study focuses on short-term timescales of subsequent events during the experiment rather than the total erosion of an experiment. The application of this newly introduced timescale requires less data and gives more insight into the involved processes for subsequent erosion events. A linear trend is obtained between erosion volume and hydrodynamic forcing but the model cannot be used as an accurate prediction model, it tends to overestimate erosion volumes. The effect of grain size is incorporated in the transport coefficient. The transport gradient decreases when the sediment grain size increases. A negative correlation that converges as grain size increases was found between the two parameters, demonstrating a non-linear, monotonic dependence.

This study reveals that erosion rates are smaller for dunes composed of coarser grains than finer grains. This is indicated by both the cumulative erosion volumes for identical hydrodynamic conditions and the values of the transport coefficient in the analytical model. Additionally, the formation of steeper slopes is observed for dunes composed of coarser grains. These findings could be attributed to the fact that coarser grains have larger fall velocities and therefore are less easy transported by the waves and currents. This study enhances our comprehension of the effect of sediment grain size, ranging from 0.21 to 0.31 mm, on dune erosion and can contribute in resolving discrepancies between model predictions and field measurements to improve future assessments of dune erosion with models.

Contents

List of symbols

Symbol	Unit	Description
α	[°]	Foreshore slope
C	[m^3/s]	Sediment concentration
C_{eq}	[m^3/s]	Equilibrium sediment concentration
C_L	[-]	Calibration factor
C_s	[-]	Empirical transport coefficient
D_{50}	[mm]	Median sediment grain size
η	[m]	Water level
η_0	[m]	Still water level
η_{surge}	[m]	Surge level
η_{tide}	[m]	Astronomic tide level
g	[m^2/s]	Gravitional accelaration
h	[m]	Depth
h_{dune}	[m]	Dune height
h_{toe}	[m]	Dune toe position
H_0	[m]	Deep water wave height
H_{0s}	[m]	Deep water significant wave height
H_{m0}	[m]	Spectral deep water significant wave height
L_0	[m]	Deep water wave length
m_{cr}	[-]	Critical slope angle
p	[-]	Porosity parameter
P	[-]	Person's value
r	[-]	Roughness parameter
R	[m]	Run-up height above the still water level
R_*	[m]	Run-up height above the dune toe
$R_{20\%}$	[m]	20% exceedence value of run-up height
$S_{20\%}$	[m]	20% exceedence value of swash height
σ	[-]	Standard deviation
$\triangle t$	[sec]	Event time period
t_0	[min]	Experimental start time (when water first reaches the dune)
T	[sec]	Wave period
$T_{m0-1.0}$	[m]	Spectral deep water wave period
T_{mean}	[m]	Spectral deep water wave period
T_s	[sec]	Adaptation timescale
u	[m/s]	Velocity
u_{cross}	[m/s]	Cross-shore velocity velocity
u_{long}	[m/s]	Alongshore velocity
ΔV_E	[m^3/m]	Erosion volume
w	[m/s]	Sediment fall velocity
x	[m]	Distance from the coastline
x_0	[m]	Zero x point new coordinate system
x_{RD}	[m]	X coordinate of RD-coordinates
y	[m]	Length scale of the profile
y_0	[m]	Zero y point new coordinate system
y_{RD}	[m]	Y coordinate of RD-coordinates
z_0	[m]	Elevation of the dune toe
z_b	[m]	Elevation between dune toe en crest

1 Introduction

This chapter gives a brief introduction to the research that will be conducted. The background and problem definition of this study will be introduced followed by the corresponding objective and research questions. Finally, a brief overview of the document outline is given.

1.1 Background

The Netherlands is heavily dependent on the protection of the beach and dune system, which forms the base of the Dutch sea defense system. There is a strong urge to protect the coastal regions, particularly since 25 percent of the Netherlands is located below sea level and a major part of the most densely populated areas are located in the lowlands behind the coast (van Gent et al., 2008). The relevance of defending the Dutch coast is reinforced by future influences of sea level rise and the increasing probability of the occurrence of more severe storms (Hapke et al., 2010).

To ensure the protection of the Dutch hinterland, the strength of the sea defense system is being assessed to meet national safety standards. A safety standard is obliged per dike segment. The normative conditions are defined as a change of failure, the coastal protection of the Dutch coastline ranges from 1/3,000 to 1/30,000 along the Dutch Coast (den Bieman, 2016). During design storm conditions dune retreat erosion rates of 80 to 100 meter are accepted within the existing design guidelines (Bosboom and Stive, 2021).

Untill now the sandy part of the Dutch coast was assessed with empirical models. Those models are based on the equilibrium profile method calibrated on laboratory experiments. This method assumes that over an average time period (years-to-decades) the shape of the active profile always returns to its equilibrium shape unless there is a gradient in transport along the coast (Bosboom and Stive, 2021). In most equilibrium models 2-dimensional processes are simplified to 1-dimensional processes. The empirical model DUROS is currently used to assess coastal regions. DUROS was developed by Vellinga in 1986, and was updated to DUROS+ by van Gent et al., 2008 to include the wave period. In the future, a switch will probably be made to process-based models. Process-based models are promising tools for risk assessment of dune erosion since 2-dimensional processes can be taken into account. A promising process-based model to assess coastal changes due to storms is XBeach. Currently XBeach is already used to assess the Belgium coast (Witteveen and Bos, 2022).

Even though our modelling capabilities have significantly improved over the years, model uncertainties remain because specific processes are not yet fully understood. One of these uncertainties is the effect of grain size (van Wiechen et al., 2023). The grain size distribution of dunes is a characteristic that deviates for each dune. This characteristic has an impact on the dune's robustness and its response to the waves and currents. In general, drag forces and fall velocities increase as grain size increases, while dune compactness and inter-particle friction decreases for larger grain sizes (Overton et al., 1994).

Model computations show that the current XBeach model is rather insensitive to changes in the grain size diameter (Quataert et al., 2018). It is however expected that this parameter strongly influences the morphological response of dunes during storm attack. It is not known however what this impact exactly is; an increase or a decrease of the response based on changes in diameter.

The Dutch coast consists of a wide range of grain sizes, different coastal formations and dune fronts. In spite of the growing attention for coastal protection strategies and methods, knowledge about storm impact is still lacking, especially near the dune face and with regards to morphological processes. Additionally, the question arises whether traditional hard structure measures are the only possible solutions. Nature-based solutions, such as (mega) sand nourishment's and natural reinforcement of dune systems, are receiving increasing attention as potential means to protect coastal regions. In order to develop general models that accurately represent nature, it is important to gain more knowledge about the extent of the influence of these uncertainties and therefore further research on these processes is required. The influence of these uncertainties can have a significant impact on dune erosion and the implementation of these processes in models.

This research focuses on dune erosion processes near the dune face within the collision regime, defined as erosion between the dune toe and the dune crest, and whether sediment grain size has an effect on erosion volumes. Large-scale manipulative experiments are conducted at the Dutch coast to gain insights into this effect. Manipulative field experiments are designed with a field setup that increases the likelihood of the occurrence of dune erosion under moderate conditions, thereby increasing the number of events and enhancing the chances of obtaining field data (van Wiechen et al., 2023). Two open shipping containers are used to establish a contained setup on the beach. An artificial dune is built inside each container during low tide. During rising tide, water enters both containers, turning them into an in-field wave flume. Using this setup, real conditions are utilized while simultaneously controlling the setup to exclude alongshore processes, to solely focus on the 1D processes. Multiple experiments are conducted, to perform tests with varying grain sizes. Several measurement techniques are employed to measure volumetric changes to the dune and the incoming wave conditions. The collected data is used to study the extent to which grain size influences dune erosion. The data collected from the experiments is analyzed to investigate erosion patterns and to determine whether the hydrodynamic forcing can be related to the amount of erosion volume. The analysis of this correlation aims to eliminate the effect of variable daily conditions to isolate the relative importance of sediment grain size.

Figure 1: Similair manipulative field experiments were conducted in 2021 by Scheijmans at the Sand Engine, Kijkduin, the Netherlands (Scheijmans, 2021).

1.2 Objective and research questions

Field experiments are conducted on the Sand Engine where artificial dunes are built inside open shipping containers to control the setup and focus solely on 1D processes. These experiments aim to investigate the effect of sediment grain size on dune erosion by exposing dunes composed of varying grain sizes to local conditions. The data collected from the experiments is analyzed to investigate erosion patterns and whether there is a correlation between hydrodynamic forcing and the amount of erosion volume. By investigating the collected data more insight is gained on the response of grain size to wave exposure to meet the research objective:

Investigate the influence of sediment grain size on erosion volumes within the collision regime by eliminating daily variable conditions through finding a relationship between wave impact and erosion volumes.

To further clarify the research objective, the study has been divided into one primary research question and three sub-questions:

> **What is the effect of varying sediment grain size on dune erosion within the collision regime in a 1D field setup?**
>
> 1. How are erosion volumes quantified using video observations, what are the advantages and disadvantages?
> 2. How do erosion volumes and dune toe positions develop over the experimental time?
> 3. To what extent can erosion volumes be accurately predicted based on analysis of hydrodynamic processes?

1.3 Document outline

To achieve the objective and answer the research questions, this report is divided into 7 chapters. **Chapter 1** introduces the research topic and its relevance. Furthermore, the problem statement is described and the research objective and questions are framed. **Chapter 2** provides a theoretical background based on a literature study. It describes definitions used in this study along with a description of experiments already conducted within this topic. **Chapter 3** gives an overview of the field site, local conditions, a description of the conducted experiments, experimental setup, and measurement instruments employed. **Chapter 4** presents the methodology used for the data analysis. The data analysis is split into three parts, erosion volumes, wave impact theory and the effect of sediment grain size. In **Chapter 5** the results of the data analysis of field campaign are presented. This chapter follows the same structure as the previous chapter, consisting of three parts. Experimental observations, physical limitations and the results are further discussed in **Chapter 6**. Final **Chapters 7 and 8** end with the conclusions and recommendations of this study.

Five appendices have been added to this study. **Appendix A** provides more detailed results about the general field conditions. In **Appendix B**, a side study is conducted to investigate whether infra-gravity waves had any influence on the occurrence of events and the amount of erosion volume. **Appendix C** describes the wave impact theory of Fisher et al., 1986 (1986) that was tested for this study but ultimately not used. **Appendix D** includes pictures of selected events from two experiments to provide a better understanding of the erosion events. Finally, **Appendix E** gives a brief literature study about the effect of dune erosion, which is not further used in this study but can be used as guideline in further studies.

2 Theoretical background

This research focuses on the effect of sediment grain size on dune erosion. This chapter will elaborate on the processes involved during dune erosion, provide a brief overview of previously conducted experiments on dune erosion, and describe various types of dune erosion models. Furthermore, previous studies on the effect of sediment grain sizes are described and the current implication of this effect in models is presented.

2.1 Definitions

2.1.1 Coastal region

The offshore boundary of the furthest coastal region is typically referred to as the depth of closure, from this boundary sediment transport is assumed to be absent. Moving closer onshore, the subsequent section is identified as the surf zone, in this area waves start to interact with the seabed and nonlinear effects start to develop. The zone near the dune face is called the swash zone, which is the region where sediment transport takes place due to both hydrodynamic forcing and bottom instabilities (van Wiechen et al., 2023). The region between the water and the dune face is called the foreshore.

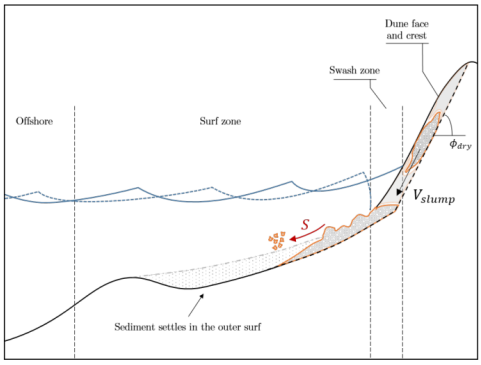

Figure 2: Dune erosion process in surf and swash zone. Where S indicates the sediment transport and the grey dotted profile indicates the initial dune profile (van Wiechen et al., 2023).

2.1.2 Water levels at dune face

During storms water levels tend to reach further onshore and run-up levels increase. Four definitions contributing to the total water level are described: astronomical tide, surge level, setup and vertical swash. The astronomic tide refers to the predictable rise and fall of the ocean's water levels due to the gravitational pull. Severe weather conditions cause water levels to rise higher than the predicted tide, this is called surge. Closer to the dune face setup and vertical swash occurs which together forms the run-up level (Figure 3). Setup is caused by the onshore movement of waves, which temporally rises the water level in shallow areas. Swash is the up-rush of flow onto the shore after waves have broken (Bosboom and Stive, 2021;Stockdon et al., 2006).

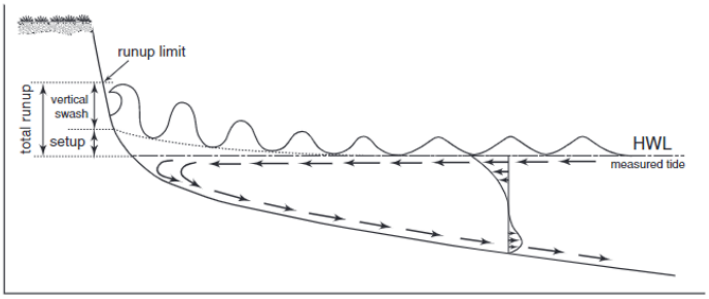

Figure 3: Schematized distinction of contributors impacting the dune face (Suanez et al., 2012).

2.2 Dune erosion

2.2.1 Impact regimes

Four impact levels are defined by Sallenger separating different phases of dune erosion: swash, collision, overwash and inundation regime. This research focuses only on reviewing dune erosion during the collision regime. The collision regime refers to a storm where the water level exceeds D_{low}, but does not exceed D_{high} (Figure 2.2.1). Net erosion is caused by incoming swash that reaches the area between the dune toe and crest.

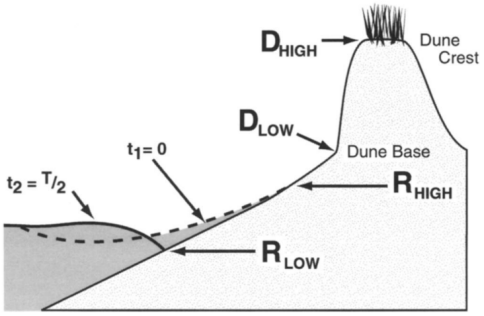

Figure 4: Schematic of boundaries of the four impact levels (Sallenger, 2000).

2.2.2 Dune erosion process

Incident waves move onshore, and typically break since the water depth decreases and the wave speed reduces causing the wave to steepen and eventually break. This process is called depth-limited breaking (Holthuijsen, 2007). In general, shorter waves are likely to break earlier than longer waves, since longer waves interact with the seabed at a later stage, allowing them to maintain their velocity and propagate further onshore. Longer waves tend to have more energy than shorter waves. Generally, short waves are responsible for the upstirring of sediment and long waves for the transport of this stirred up sediment. This is because short waves usually have less energy and interact more with the seabed, by for example wave breaking, making them efficient to stir up sediment. Longer waves are less affected by the seabed and travel further making them more efficient in transporting sediment (van Wiechen et al., 2023).

During storms the surge levels rise and the water level increases. This rise enables the waves to break further onshore as they feel the bottom later and more wave energy is able to reach the dunes. The incident wave train exist out of waves of different wave lengths. Approaching the dune face, the process of depth limited breaking has already dissipated the majority of the shorter waves. This leaves long waves, particularly infra-gravity waves, to deliver the dominant forces when the wave front reaches the dune. More wave energy reaches the dune and fewer waves are present to dissipate this expanded energy, resulting in larger run up levels (van Gent et al., 2008).

Sediment is removed from the dune face into the swash zone. In this zone sediment is stirred up due to the presence of the waves resulting in near-bed orbital velocities. Increasing wave skewness in this zone results in larger pressure gradients and bore induced turbulence. A net sediment transport is directed offshore to the inner surf zone and high concentrations of suspended sediment are transported by a strong undertow. The transport gradient reduces in a seaward direction and sediment settles further seaward, slowly increases the seabed. A new beach profile is developed, which is more capable of dissipating the incoming wave energy. This new beach profile results in decreasing run up levels and reducing dune erosion rates (Bosboom and Stive, 2021; van Gent et al., 2008; van Wiechen et al., 2023).

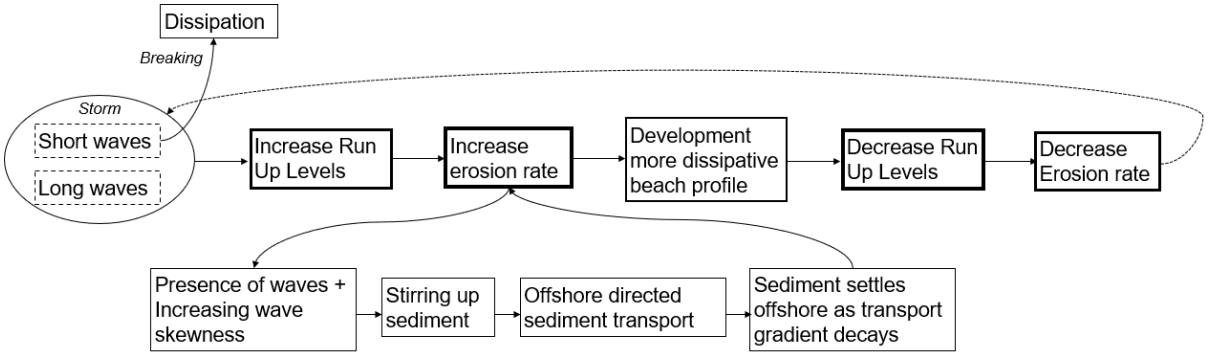

Figure 5: Brief overview of the processes contributing to dune erosion during storms.

2.2.3 Physical quantities that affect dune erosion

Several parameters are discovered to have an influence on dune erosion. First of all, the magnitude and duration of wave exposure is known to affect dune erosion. Wave breaking and run-up in the swash zone, causes water to infiltrate the dune face, resulting in saturation and increased cohesion of the sand. This increases the weight of a part of the dune face, which eventually slumps down when it becomes to heavy (Palmsten and Holman, 2011). This increase of cohesion also causes the slope of the dune face to become steeper than the angle of repose of dry sediment, which is approximately 45 ° (van Wiechen et al., 2023).

Furthermore, wave energy is also known to be highly dynamic in the swash zone and affects dune erosion. The wave height, wave steepness and wave period are parameters that determine the extent of dune erosion (van Wiechen et al., 2023; Stockdon et al., 2006; van Thiel de Vries et al., 2008; Masselink and Puleo, 2006).

Geotechnical aspects have been found to influence dune erosion as well. Previous studies indicate that the shape and slope of the beach profile have a considerable effect on the amount of erosion (Stockdon et al., 2006). Also the height and steepness of the dune face appear to also have a significant effect on dune erosion rates (van Wiechen et al., 2023; van Thiel de Vries et al., 2010).

2.2.4 Dune erosion stages

Dune erosion can be divided into two stages. The first stage or initial stage mobilizes sand of the lower part of the dune, leading to drag-induced erosion and steepening the slope of the dune face. This processes creates a very unstable dune face and can continue until the dune face has a nearly vertical profile. In the second stage slumps of dune erode from the dune face due to soil instabilities. This is also referred to as avalanching. A bulk of sediment breaches down and the entire dune face is moving landward (van Wiechen et al., 2023).

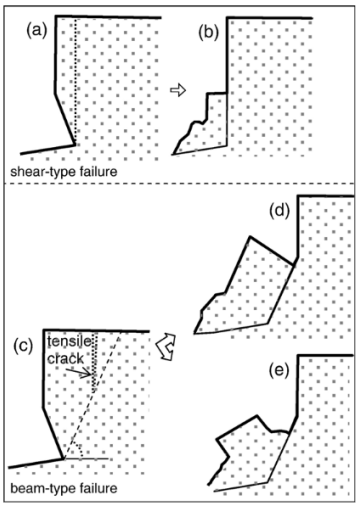

Figure 6: Schematized visualization of two failure mechanisms due to soil instabilities. Shear-type of failure (top panel) and beam-type of failure (bottom panel).

Two types of failure of the dune volume can be distinguished for this second erosion stage where avalanching occurs: shear-type of failure and beam-type of failure. According to Erikson et al. (2007) shear-type of failure occurs when a sediment volumes slides down since the weight of the volume exceeds the shear strength. Beam-type of failure occurs when negative earth pressures develops a tension crack landwards from the dune face. This crack moves downward, causing a sediment volume to slide down (Erikson et al., 2007). Both failure types are dependent on the saturation of the dune volume, as the weight of the sediment increases and the internal friction between particles reduces (Scheijmans, 2021).

2.2.5 Dune regression

Erosion of the dune face leads to a landwards regression of the dune. Erosion events are particular triggered due to soil instabilities and a potential notch over the dune toe. Generally, erosion start with the initial erosion stage, where sand is mobilized and the dune toe is eroded. The second stage, avalanching, initiates more severe erosion events as bulks of sediment shear down. Cumulative erosion curves typically follow a s-shaped curve, showing that first relative small erosion events occur and later when the dune becomes more unstable, larger events occur with shorter time intervals in between (Rueda et al., 2011).

Subsequent erosion events are also dependent on the negative feedback mechanism between hydrodynamics and morphodynamics. This mechanism is time-dependent and involves the process where waves induce erosion of the dune face which accumulates on the foreshore. This accumulation temporally protects the dune from incident waves by the more dissipative profile (van Wiechen et al., 2023).

As the dune regresses in landward direction, the dune toe moves landward as well. Previous experiments reveal that the elevation of the dune toe also increases. They found that this increase is related to the increasing water levels during the experiments (Bonte and Levoy, 2015; van Bemmelen et al., 2020; Scheijmans, 2021).

2.3 Experimental investigations on dune erosion

The importance of protecting vulnerable hinterlands against storms and future sea level rise, calls for a better understanding of the influence of specific processes effecting dune erosion. Formerly, primarily wave flume tests were conducted to investigate dune erosion (Van de Graaff, 1977; Vellinga, 1986; Overton et al., 1988; Overton et al., 1994; van Gent et al., 2008; van Thiel de Vries et al., 2008; Kobayashi et al., 2013; Figlus et al., 2014; Martinez et al., 2016; Silva et al., 2016; Mendoza et al., 2017; R. Feagin, 2022).

Despite all successful studies performed in wave flumes, conducting experiments in wave flumes is very expensive and those experiments are not able to represent all the underlying physical processes that are appearing in natural conditions. Disadvantages are particularly encountered for the following three matters: scale problems, the replication of hydrodynamic conditions and long-shore processes (Scheijmans, 2021). In scaling, the main problem is the scale of the sediment itself, since the coefficient with which the grains can be reduced is limited by the Reynolds criterion. The Reynolds number is the ratio of inertial to viscous forces. When the sediment grain becomes too fine, cohesive forces start to dominate, causing the interaction between the water and sediment to act differently (Brandenburg, 2010). Hydrodynamics are simulated using wave generators. Those generators are installed at certain settings, and it is difficult to simulate the non-linear effects. Finally, long-shore processes cannot be replicated accurately because a wave gauge is quite small and coastal currents are usually not modeled.

Conducting dune experiments in the field is an alternative, wave simulators are not required and operations are less expensive. However in the field it is difficult to exclude specific processes. Long-shore sediment transport is one of the hard to separate processes that has a major impact on the interaction between erosion and deposition in a coastal cross-sectional (van Bemmelen et al., 2020).

Manipulative field experiments bridge the gap between laboratory tests and general performed field work. Manipulative field campaigns built a field setup in such way that erosion is forced under moderate conditions. This setup enables to include all natural processes, conduct experiments in safe conditions and decrease the costs (van Wiechen et al., 2023). By conducting the tests in a contained setup, it is possible to exclude long-shore sediment transport, allowing this research to focus on specific individual processes (Scheijmans, 2021).

2.4 Modelling dune erosion

Many tools are developed to assess dune erosion under extreme conditions. A distinction can be made between analytical models, behavior-based models and process-based models.

2.4.1 Analytical models

This section introduces the two classical approaches commonly used to estimate the effect of storms on dunes. The first approach is referred to as the equilibrium profile approach, this approach is refined by Vellinga in 1986 and further improved by Kriebel and Dean in 1993 with numerical models (Larson et al., 2004). This approach is based on empirical relations and on the principal that a beach will evolve towards an equilibrium state. Such principal is concerning long term time scales, since it takes a longer time interval to restore a post-storm profile to its stable equilibrium state.

The second approach is known as the wave impact theory developed by Fisher et al. in 1986. This approach is based on the linear relation between the force of the uprush at the dune exerting by the wave and the volume eroded (Fisher et al., 1986). The swash force is associated with the amount of sand eroded from the dune. This principal is suited for shorter timescales and episodic events, where the equilibrium profile is not yet reached and dune profiles vary in shape.

Overton et al. (1988) (1994) and Larson et al. (2004) further investigated the wave impact theory. Overton et al. (1988) (1994) found a linear relation between swash and erosion. The swash force is computed as a magnitude of bore velocity and bore depth. Larson et al. (2004) derived an analytical model to predict recession distance and eroded volume of coastal dunes during severe storms over time. The

model only considers the dune face and foreshore, and does not account for the profile further seaward. The theory assumes that there is a linear relation between swash force and erosion volumes. The swash force is computed as a magnitude of run-up height and incoming waves (van Wiechen et al., 2023). Palmsten and Holman (2011) derived a method to predict erosion based horizontal infiltration into the dune.

2.4.2 Behavior-based models

Behavior-based models simulate one-dimensional alongshore uniform conditions, in such models an equilibrium is forced. Examples of behavior-based models are: Duros+, UnibestCL+ and Asmita. Till now mainly behavior-based models have been taken into account, these models are well adequate for coastal regions with a small long-shore variability. However, 1 dimensional models are not able to model physics-based processes for more complex situations where the shore is highly variable (van Wiechen et al., 2023).

2.4.3 Process-based models

Process-based models do not force an equilibrium but this follows from balance formulations. Examples of process-based models are Delft3D and XBeach. An upcoming shift toward process based 2 dimensional models is made, since analytical and behavior-based models are not able to model complex variable situations (Roelvink et al., 2009). The dune erosion model XBeach is a promising model and is currently used to asses the Belgium Coast (Witteveen and Bos, 2022).

XBeach is an open-source process based model, predicting dune erosion rates on sandy coasts for timescales of storms and domain size of kilometers. XBeach is a 2DH model, which describes the depth averaged velocity field and sediment concentration. Such models are promising for situations where the horizontal dimensions can be separated from the timescale of the morphological process. This model approach is well suited for small time scales where the cross-shore profile evolution is not of significant influence (these situations require an understanding of the 3D flow structure). As Xbeach is a process based model, it loops through the model set-up from bottom depth to waves to the hydrodynamics, sediment transport and finally computes the bottom change. This information is looped back and updates the bottom depth, whereas the loop starts again (de Vries S., 2021). The model is short wave averaged and long wave resolving. Therefore, the model is capable of describing low-frequency motions and modelling near shore processes where long waves play an important role (van Gent et al., 2008).

A special application is added to the morphodynamics near the waterline, allowing to model avalanching. This process is simulated by locally looking at the profile slope and imposing a critical slope angle. A different critical slope can be exposed for a wet or a dry slope, since areas with a higher moisture content are more subjected to avalanching than dry parts. When the critical slope is exceeded, sediment is transported to adjacent cells and the slope slumps down till the conditions meet the critical slope again (Roelvink et al., 2015).

2.5 Sediment grain size

Dune formation is the result of an accumulation of sand particles that settle or get trapped on the beach. Sediment is mainly transported to the dune front by aeolian transport. Along the Dutch coast sediment grain sizes are well composed and have typical values between 0.2 and 0.3 mm (Van Rijn, 1984). The process of dune formation leads to a coastal barrier of unique dunes consisting of different grain size distributions. Different grain sizes have other characteristics, as the shape, density and fall velocity vary. These parameters influence the robustness of the dune and thus its ability to withstand attacking waves during storms that cause the dune to erode. Many experiments have already been dedicated to the question, regarding the relationship between sediment grain size and dune erosion volume. However, most experiments are limited by scale effects and limitations of laboratory simulations. Different approaches are applied and studies found other outcomes, leaving the question still unresolved.

2.5.1 Previous studies

Several studies describing the effect of sediment grain size on dune erosion have been dedicated (e.g., Van de Graaff, 1977; Vellinga, 1986; Overton et al., 1994; Larson et al., 2004).

Van de Graaff (1977) performed a series of dune erosion test in a wind and wave flume. Two grain sizes were tested 225 and 150 µm. His research concluded that erosion volumes decrease for larger fall velocities, associated with coarser grains. Vellinga (1986) developed a model for beach profile changes. To verify his model, he derived a relation between the process in the field and the process within a scale model and conducted a series of scale model test. During his measurements it was observed that the erosion profile is affected by grain size. The results confirmed Van de Graaff's findings, as coarser material resulted in steeper slopes and decreasing erosion volume. The effect of sediment grain size is described in his model by the fall velocity of dune sediment (w) in the formulation of the length scale of the profile (y) (Equation 1).

$$y = 0.47\left((w/0.0268)^{0.56}x + 18\right)^{0.5} - 2.0 \tag{1}$$

Overton et al. (1994) investigated a relationship between swash force and erosion while varying the sediment grain size during the experiments. She conducted several test were she varied the sediment grain size for the same swash force. In contrast to Van de Graaff and Vellinga, she found that decreasing the sediment grain size resulted in decreasing erosion volumes. Overton et al. reasoned her findings by the higher negative pore pressure within dunes consisting out of finer grains, requiring an exertion of greater force to induce erosion. Larson et al. (2004) developed an analytical model to estimate retreat distance and erosion volumes during storms. The model is based on the wave impact approach and was validated using four data sets originated from laboratory and field experiments. In his model, he found an inverse dependence between an empirical transport coefficient and the wave height-to-grain size ratio. He fitted a trend between the different datsets, this trend has marked scatter and is drawn between the tipping points of the datasets. This transport coefficient is dependent on erosion volume, and therefore he states that an decrease in grain size should reduce the erosion volume for a similar wave event. He relates this finding to the matrix suction phenomenon, which implies that dunes composed of finer grains have greater strength under wave attack.

The main difference between the results found by Van de Graaff and Vellinga to the results of Overton et al. and the conclusions drawn by Larson et al. is that the studies are based on two different approaches. Van de Graaff's and Vellinga's experiments were based on the equilibrium profile approach, while Overton et al. based her experiments on single bore impacts penetrating a container on the beach, to which Larson followed this approach in developing his model.

Both theories are referring to a defined volume that slumps from the dune, even though this volume is based on a different time scale for all studies. As Van de Graaff (1977) and Vellinga (1986) look at the effect of the entire system during a storm, Overton et al. (1994) looks at the effect of a single bore and Larson et al. (2004) predicts erosion for a summation of single bores over varying surge duration's. Therefore it seems that the gradient of the erosion volume over time is an important parameter that can result in different outcomes.

2.5.2 Current implementation of sediment grain size in models

Several dune erosion models have been developed, these models are promising tools for risk assessment, but still encounter large model uncertainties. It is therefore important that these uncertainties are clarified and known to users. This section describes the current implementation of sediment grain size in the models DUROSTA and XBeach.

DUROSTA is based on the formulations for the erosion profile derived by van Gent et al. in 2008. The equation for the erosion profile is related to the sediment fall velocity, which depends on the nominal grain diameter (Equation 2). This sediment fall velocity can be determined according to the formulations derived by Van Rijn (1984) or can be investigated during laboratory experiments.

$$\frac{7.6}{H_{0s}} * y = 0.4714 * \left[\left(\frac{7.6}{H_{0s}} \right)^{1.28} * \left(\frac{10.9}{T_{m-1.0}} \right)^{0.45} * \left(\frac{w}{0.0268} \right)^{0.56} * x + 18 \right]^{0.5} - 2.0$$

$$x_r = 250 * \left(\frac{H_{0s}}{7.6} \right)^{1.28} * \left(\frac{0.0268}{w} \right)^{0.56} \tag{2}$$

$$y_r = 250 * \left(\frac{H_{0s}}{7.6} \right)^{1.28} * \left[0.4714 *^{0.45} * \left(250 * \left(\frac{10.9}{T_{m-1.0}} \right)^{0.45} + 18 \right)^{0.5} - 2 \right]$$

Within the model XBeach sediment grain size is of influence in three parameters: the equilibrium sediment concentration, the adaption timescale and the avalanching module. In XBeach sediment concentrations (C_{eq}) are modeled according to a depth-averaged advection diffusion scheme. The source term, right hand side of Equation 3, represent a mismatch between the equilibrium sediment concentration and the actual sediment concentration and determines if accretion or erosion takes place (Roelvink et al., 2015).

$$\frac{\partial hC}{\partial t} + \frac{\partial hCu^E}{\partial x} + \frac{\partial hCv^E}{\partial y} + \frac{\partial}{\partial x}\left[D_h h \frac{\partial C}{\partial x} \right] + \frac{\partial}{\partial y}\left[D_h h \frac{\partial C}{\partial y} \right] = \frac{hC_{eq-hC}}{T_s} \tag{3}$$

There are two possible transport formulation in Xbeach to calculate the equilibrium sediment concentration, the Soulsby-Van Rijn and the Van Thiel-van Rijn equations. By means of these formulas an attempt is made to model the effect of the grain size of the sediment. Both formulations are dependent on sediment characteristics. The formulas are quite extensive and can be consulted in the XBeach manual.

Additionally, sediment grain size is represented in the adaptation timescale (T_s), since this timescale is related to the sediment fall velocity (w_s) (Equation 4). This adaptation time scale represents the time lag of the model to adapt to a different condition. The fall velocity is calculated according to the formulas suggested by Hallermeier in 1981 (Equation 4) (Roelvink et al., 2015). A larger grain size will result in a larger fall velocity and a smaller adaptation time, implying that the sediment response is relative rapid.

$$T_s = \max\left(f_{Ts}\frac{h}{w_s}, T_{s,\min} \right) \quad \text{With: } w_s = \alpha_1 \sqrt{\Delta g D_{50}} + \alpha_2 \frac{\Delta g {D_{50}}^2}{v} \tag{4}$$

Also within the avalanching step in XBeach it is possible to apply modifications for different grain sizes. A different critical slope angle (m_{cr}) can be imposed for different grain sizes (Equation 5). Reducing this angle causes a slope to avalanche at an earlier stage, resulting in more dune erosion.

$$\left| \frac{\delta z_b}{\delta x} \right| > m_{cr} \tag{5}$$

2.5.3 Model discrepancies for varying sediment grain sizes

To investigate the response of varying grain sizes in the models XBeach and DurosTA model calculations are performed replicating conditions of flume experiments conducted in the Deltagoot in 2006 (Quataert et al., 2018). Results of erosion volumes for variable grain sizes ranging between 0.15 and 0.30 mm show significant deviations between model results (Figure 7). XBeach appears relative insensitive to changes in grain size, whereas the results of DurosTA show a considerable dependence on varying the sediment grain size.

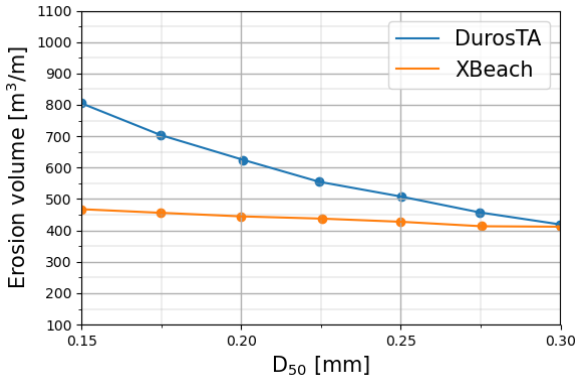

Figure 7: Effect of implementation of variable median grain sizes on dune erosion volumes after a 15 hour simulation with XBeach (orange line) and DurosTA (blue line) (Quataert et al., 2018).

To further investigate the sensitivity of XBeach to varying grain sizes, results of the model are compared to flume experiments conducted by Van de Graaff in 1977. The comparison reveals that XBeach typically underestimates erosion volumes. Furthermore, the horizontal lines connecting the results for the two grain sizes indicate that erosion volumes are relatively insensitive to changes in grain size (Figure 8). The underestimation of the erosion volumes increases for smaller median grain sizes (Quataert et al., 2018).

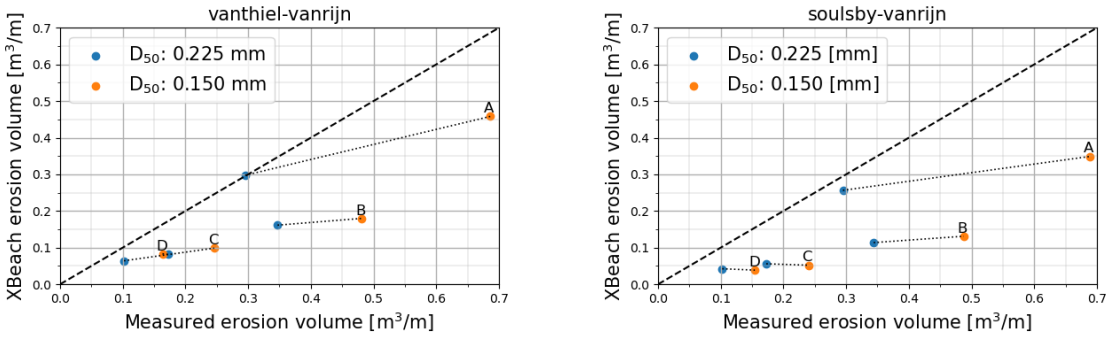

(a) (b)

Figure 8: Results of erosion volumes from XBeach for flume test of Van de Graaff (1977) compared to the erosion volumes found in the flume experiments. The results for the sediment transport equations of Vanthiel-vanrijn (a) and the Soulsby-vanrijn (b) (Quataert et al., 2018). Four test were compared (A, B, C, D). Results of median grain sizes of 0.225 mm (blue circles) and of 0.150 mm are indicated (orange circles).

2.6 Summary

Dune erosion is a complex process that involves various contributing factors. Wave energy, the magnitude and duration of wave exposure, and geotechnical aspects are the primary categories of parameters that affect this process. Dune erosion is generally initiated by soil instabilities, which is followed by avalanching, the breaching of a bulk of sediment. As the dune regresses in the landward direction, the dune toe also moves landwards and the toe elevation increases.

Already many studies are performed on dune erosion and several dune erosion models exists to predict erosion rates. There are two main approaches: the equilibrium profile approach and the wave impact theory. The equilibrium profile approach assumes that the beach profile always returns to an equilibrium state after a storm, and is based on long time intervals. The wave impact theory focuses on short timescales and relates individual swash forces to erosion volumes.

Differences in the results of the effect of sediment grain size are found. Van de Graaff (1977) and Vellinga (1986) found that coarser grains lead to steeper slopes and smaller erosion volumes than finer grains. On the other hand, Overton et al. (1994) and Larson et al. (2004) found that smaller grain sizes resulted in smaller erosion volumes. Remarkable was that the findings of Van de Graaff (1977) and Vellinga (1986) were based on the equilibrium profile approach and the findings of Overton et al. (1994) and Larson et al. (2004) were based on the wave impact theory and that all studies were based on different time intervals.

Also, in dune erosion models, there are differences in the response to varying grain sizes. The XBeach model seems to be rather insensitive to changes in grain size, while the DurosTA model shows more sensitivity. Therefore, it is important to conduct more research on the effect of sediment grain size and model discrepancies in order to improve our ability to predict erosion volumes accurately in the future.

3 Field site & instruments

This chapter presents the field site, local conditions and used instruments in this research. Field experiments are set up to gather data to be able to test the objective and answer the research questions. The first section of this chapter presents a brief description of the field site. The second section presents the general field conditions. In the third section, the design of the field experiments, planning, and approach are described. The last section outlines the data processing and includes a brief description of each instrument and the method used to clean the data.

3.1 Field site

The fieldwork is conducted at the Sand Engine on Saturday September 24th, Sunday September 25th and Monday September 26th. This name is given to the beach near Kijkduin after a mega sand nourishment, of approximately 21.5 million m^3 of dredged material, is deposited in front of the coast in 2011. The beach can be characterized as a dissipative beach, which is typically a beach with a wide surf and swash zone (Bosboom and Stive, 2021). The beach slope is quite mild and the variability along the coast is low. The sandy material consists of grains ranging from 0.2 mm up to 0.4 mm, which is coarser than other coastal regions along the Dutch coast (Ionescu et al., 2020). The Sand Engine is quite remote and not very crowded, which therefore provides a suitable location to conduct the fieldwork of this study.

Figure 9: The fieldwork is conducted at the Sand Engine near Kijkduin ("De Zandmotor", 2021).

The fieldwork location (Figure 9) is specifically chosen due to its higher bed elevation, which prevents flooding of the beach in between the sea and lagoon during high tides. Additionally, the location is situated in a relatively secluded area to minimize disruptions from visitors during experiments. Despite the remote setting, the site is readily accessible by quad, ensuring efficient transportation of necessary materials and supplies. The site's RD coordinates are 72.500 m (X coordinate) and 452.250 m (Y coordinate) for reference. To carry out the experiments, two containers were placed in the intertidal zone, where the sea reaches the shore between low and high tide.

3.2 Local conditions

General field conditions are briefly described in two sections: hydrodynamics and morphodynamics. These conditions are based on visual observations and results which are already obtained from processed data.

3.2.1 Hydrodynamic conditions

The experiment spanned 3 days and upon arrival a large surf zone is recognized where white capping could be observed further offshore. On Saturday and Sunday the waves are of similar size while on Monday the wave height increases considerably. It is also observed that as the tide increases over the duration of the experiment, waves break further onshore. This results in a rising still water level inside the container and more wave energy reaching the artificial dune.

Offshore measurements show variability in conditions between the different experimental days (Figure 10). The water levels follows a sinusoidal trend. The grey areas denote the specific time frames during which the experiments were conducted. Notably, the data shows considerably rougher conditions on Monday compared to Saturday and Sunday. Furthermore, the predominant wave direction is from the North-West.

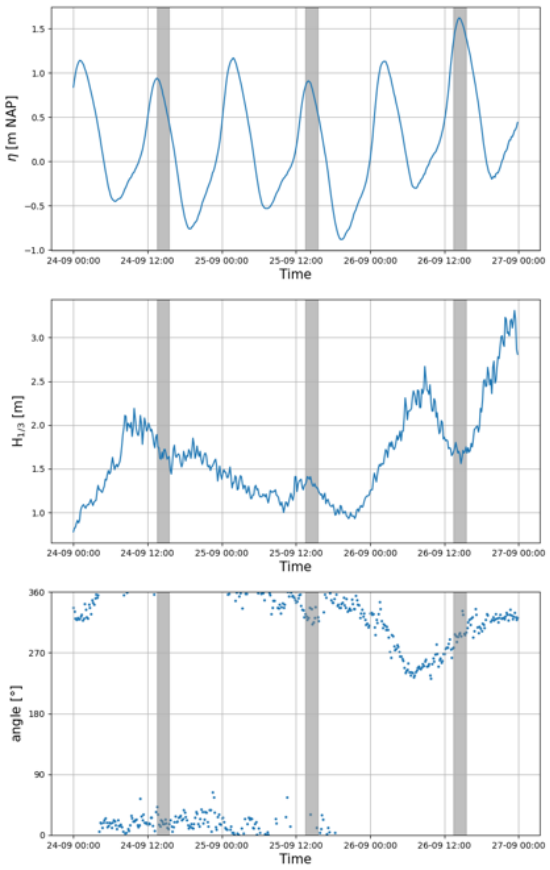

Figure 10: Offshore conditions measured at EuroPlatform, the water level (top panel), wave height (middle panel), wave angle relative to North (bottom panel). The grey areas indicate the time period where experiments were conducted for each experimental day.

Nearshore measurements at a distance of 1 meter in front of the container show that the water level on Saturday and Sunday gradually rose to about 1.2 m NAP. On Monday, the water rose significantly, nearly 0.6 meters higher than the levels on Saturday and Sunday. This increase is due to a rising spring tide and increasing setup. The magnitude of surface elevation fluctuation is rather similar for both containers on each day(Figure 11). However, the container with a later experimental start time (t_0) experiences a slightly higher forcing. The significant wave height and spectral period are obtained from the wave spectrum (Appendix A). On Saturday, the significant wave height and peak wave period is measured to be respectively 0.42 meters and 7.35 seconds, which decreased slightly to 0.37 meters and 7.25 seconds on Sunday. Conditions became rougher on Monday, with a significant wave height of 0.47 meters and a peak wave period of 9.92 seconds.

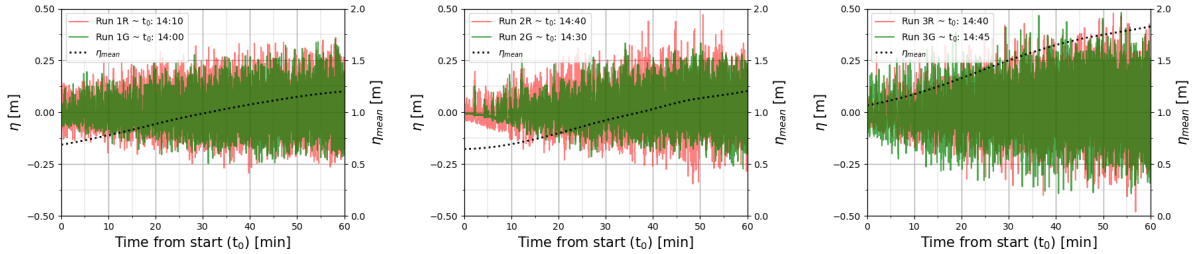

(a) Saturday 24-09-2022 (b) Sunday 25-09-2022 (c) Monday 26-09-2022

Figure 11: Surface elevation measured at a 1 meter offshore distance from the container opening. The magnitude of the surface elevation (η) (left axis), the mean water level (η_{mean}) (right axis).

The wave direction at a distance of 1 meter from the container opening is measured with velocity sensors (Figure 12). The dotted line represents the main direction of the velocity and the given angle equals the deviation of the velocity direction from the cross-shore velocity. It is shown that the alongshore velocity is quite small compared to the cross-shore velocity. This implies that the incoming waves are almost normal incident. Based on this finding, it is assumed that the alongshore component is negligible and that only 1-dimensional processes in the cross-shore can be considered.

The dominant wave direction is North-West, which confirms visual observations. Also, it can be seen that the wave direction varies around the North-West. The obtained data shows again that the conditions were rougher on Monday, as the velocity increases (Figure 12c).

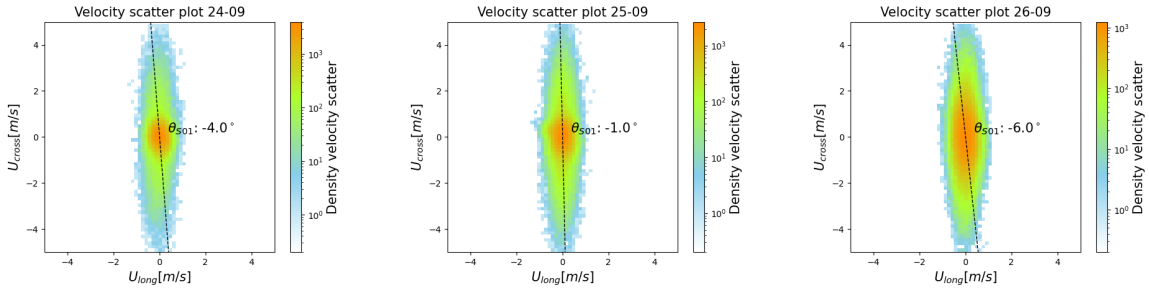

(a) Saturday 24-09-2022 (b) Sunday 25-09-2022 (c) Monday 26-09-2022

Figure 12: Velocity direction measured at a 1 meter offshore distance from the container opening. Alongshore velocities (U_{long}) are small compared to cross-shore velocities (U_{cross}).

3.2.2 Morphodynamic conditions

Regarding the morphodynamics, observations upon arrival reveal that the bed seems relatively flat with a mild slope which steepens moving offshore. The beach width is approximately 70 meters and the beach consists of medium to coarse sediment with ranging grain diameters between 0.20 and 0.35 mm. Rips develop along the shore after high tide, the rips appear along the entire beach, therefore it can be stated that this process is not caused by the implementation of the experiment.

It is very likely that the experiments affect the morphology around the containers. The Sand Engine is a highly dynamic beach, meaning that profile continuously changes. In addition, the initial profile is disturbed by the daily construction activities prior to each event. Also sediment from other locations is sampled and be added to the system where the experiments were conducted. Those actions change the morphodynamics.

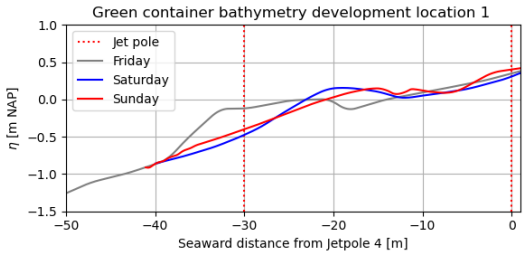

(a) Profile development green container

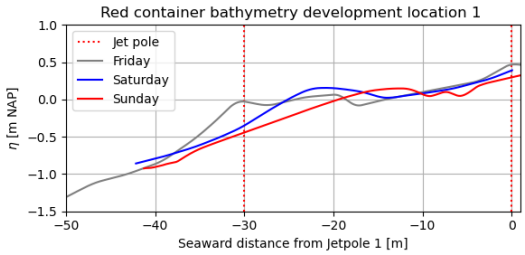

(b) Profile development red container

Figure 13: Measured bathymetry at the first location of both containers. The jet pole in front of the container is located at x = 0.

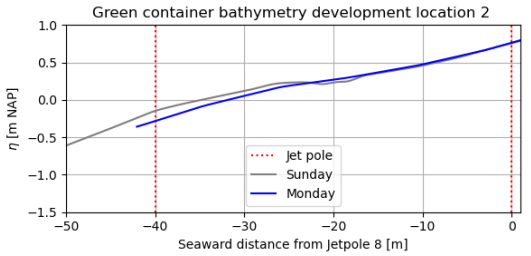

(a) Profile development green container

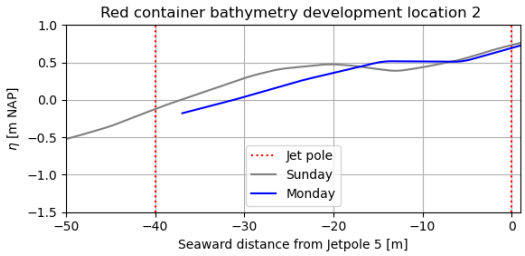

(b) Profile development red container

Figure 14: Measured bathymetry at the second location of both containers. The jet pole in front of the container is located at x = 0.

In Figure 13 and Figure 14, the cross-shore profiles are presented. They show that a bar is located around the middle jet pole and is moving onshore throughout the duration of the experiments. The size of the bar decreases significantly comparing the profile on Friday and Sunday. On Monday, the bar appears to be almost completely washed away. This can be related to the increase in wave energy, tidal elevation and setup starting on Sunday. The slope of the profile near the containers is rather constant over the time period of the experiments. The slopes in front of the container remain rather constant for all experiments, and therefore a foreshore of 1:33 is assumed for further analysis.

3.2.3 Overview local conditions

Day	η_{max} [m]	$\mathbf{H}_{m0}$ [m]	$\mathbf{T}_{m-1,0}$ [sec]	**Foreshore** [-]
Saturday 24-09-2022	1.2	0.43	7.35	1:33
Sunday 25-09-2022	1.2	0.37	7.25	1:33
Monday 26-09-2022	1.8	0.47	9.92	1:33

Table 1: Overview of the general field conditions for all three experimental days.

3.3 Field experiments

3.3.1 Concept & planning

For this study, a new experimental method is used to investigate dune erosion in the field. Specifically, 40-foot sea containers with an open top are utilized to replicate an in-field wave flume. This method has been validated in an earlier study through conducting several experiments (Scheijmans, 2021). In this method, artificial dunes are constructed inside the containers, which are exposed to waves. However, Scheijmans (2021) notes the limitations of this approach, such as the influence of the container wall. These limitations will be carefully considered throughout the study and taken into account during data processing.

Table 2 provides an overview of the experiments carried out during the fieldwork. Two experiments are conducted each day, one in the green container and one in the red container. Each container is defined as an individual experiment, meaning that a total of six experiments are performed during the fieldwork, referred to as run 1G, 1R, 2G, 2R, 3G and 3R. During low tide, preparations for the experiments were undertaken, and measurements were conducted during high tide. The artificial dunes were constructed using different grain sizes to test the objective of this study.

To enable comparisons of measurements taken from the green and red containers on a daily basis, both containers should experience the same conditions. This is achieved by analyzing measurements taken in a comparable time interval where hydrodynamic forcing is of equal magnitude and by building similar initial dunes inside both containers. The experiments start when water first reaches the dune toe, which is defined as t_0. The start time slightly varies per container because they are not placed at the exact same level. Despite the slight variation in starting times (t_0), measurements show that the hydrodynamic forcing is of similar magnitude during the experimental time. Each day, similar initial dune profiles are constructed with equal height, slope, and toe position. Based on these factors, it is reasonable to assume that the daily runs can be compared within their experimental time interval since they occur under similar conditions and regimes.

Run	**Day**	**Container**	$\mathbf{t}_0$ [-]	$\mathbf{H}_{m0}$ [m]	$\mathbf{T}_{m-1.0}$ [s]	$\mathbf{h}_{dune}$ [m]	$\mathbf{D}_{50}$ [mm]	$\mathbf{h}_{toe}$ [m NAP]
1G	Sat 24-09-2022	Green	14:00	0.77	7.35	1.5	0.21	0.75
1R		Red	14:10	0.77	7.35	1.5	0.27	0.80
2G	Sun 25-09-2022	Green	14:30	0.76	7.25	1.4	0.24	0.60
2R		Red	14:40	0.76	7.25	1.4	0.27	0.45
3G	Mon 26-09-2022	Green	14:45	1.25	9.92	1.6	0.31	1.35
3R		Red	14:40	1.25	9.92	1.6	0.27	1.32

Table 2: Overview of the executed experiments for three experimental days. The experiments start (t_0) when the water first reaches the dune toe. H_{m0} and T_{m0} are deep water wave conditions measured in front of the container. The dune height (h_{dune}), median grain size (D_{50}) and the initial elevation of the dune toe (h_{toe}) are characteristics of the constructed dunes.

3.3.2 Sediment sampling locations

Figure 15: The four sediment sampling locations at the Sand Engine (left panel). A sand ruler used on-site to estimate grain size characteristics (right panel).

For each experiment, the dunes contained a different type of sediment. The goal is to sample as large a difference in size as possible within 1 km of the site. Prior to the fieldwork, sediment samples are taken during field visits. This preliminary survey found that in order to retrieve the finest sediment, aeolian sand must be sampled. Among other places, aeolian sand is found at the edge of the Sand Engine lagoon (sample location 2). Sediment is driven towards the lagoon, where the sediment is trapped in the water. The moisture content of the sediment might be higher. Aeolian sand can also be sampled by scraping away only the top layer of sediment at spots where there is a lot of aeolian transport (sample location 3). The coarse sand is found mainly around the Argus mast (indicated by the red dot in Figure 15). This area has a relatively high shell content, which is not desirable as it is not typically found in natural dunes. Therefore, a location with a relatively low shell content (sample location 4) is selected for the study. The artificial dune in the green container is constructed using three different sediment bulks for the three experimental days. A reference dune is constructed in the red container that consisted of the same sediment each day obtained from sampling location 1. The sediment collected for the reference dune should be between the finest and coarsest grains sampled during fieldwork.

The median grain size of the sediment samples is derived by sieving the sediment using a sieving tower. The results of the cumulative sediment grain size distribution can be found in Appendix A.

Location	$\mathbf{x}_{RD}$ [m]	$\mathbf{y}_{RD}$ [m]	$\mathbf{D}_{50}$ [mm]	**Description**
1	73.200	452.300	0.27	Medium-coarse sediment (reference dune)
2	72.700	452.250	0.21	Fine sediment, may have a higher moisture content
3	72.510	452.230	0.24	Fine sediment, only the top layer is used
4	72.520	452280	0.31	Coarse sediment with a higher shell content

Table 3: The coordinates of the four sample locations are given including the median grain size and a description of the sample characteristics.

3.3.3 Design artificial dune

The study focuses on the collision regime, which means that the water level is constrained to the area between the dune toe and crest. Sediment transport over the dune crest is not permitted. An ideal design involves conducting measurements within the collision regime for as long as possible. Therefore, it is necessary to determine the location of the artificial dune in such a way that during high tide, the slope of the dune is exposed to water, but not to such an extent that it leads to overwash.

In order to minimize disturbances to the hydrodynamics caused by the container, it is essential to ensure a smooth transition between the beach and the container. This is achieved by maintaining the slope of the beach in the container area up to the toe of the artificial dune. This is rather difficult to accomplish due to the limited preparation time and the disturbances of the bed due to the use of large machines. Additionally, it is important to have a thick layer of sand in the initial part of the container to prevent the bottom of the container from being exposed. To achieve this, the sand at the front side is excavated by 0.5 meters prior to its placement (Figure 16).

The dune is constructed with a slope of 1:1, which is equivalent to the angle of repose of wet sand. The height of the dune varied between 1.5 to 2 meters, depending on the daily changing water level. As each dune contained a distinct grain size, the containers need to be emptied before each experiment, thus limiting the total volume that could be added. Since the height of the dune is more important than the crest width, it is necessary to reduce the crest width to ensure optimal height. As such, the crest width of the dunes is restricted to between 0.5 and 1 meter.

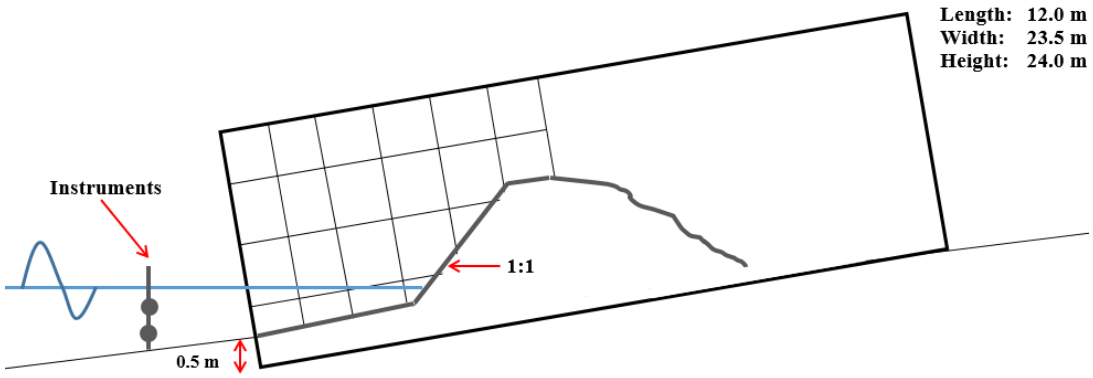

Figure 16: Schematic side view of the container setup.

The experiments are conducted during rising high tides, therefore the timing of the experiments is adjusted according to astronomical tidal predictions and water level predictions. Three components are considered in the design: the tide, setup, and run-up. Tidal, water level, and wave predictions are retrieved from RWS (2022). The run-up level is calculated according to the run-up equation derived by Stockdon et al. (2006) (Equation 6). These calculations are based on a normal distribution. One of the input values is a percentile, which gives a statistical approximation for the run-up that occurs a specific number of percent. To estimate the location of the dune toe, the $R_{20\%}$ is calculated. Previous field work at the site has shown that this is a reliable estimation of the water's reach. Predicted values of the astronomic tide, wave setup and run-up are combined to calculate the position of the dune toe (RWS, 2022). The calculations indicate that the container needs to be relocated on Monday due to a rise in tidal activity and an accompanying increase in predicted wave height.

$$R_{20\%} = 1.1 \cdot [< \eta > + \frac{S_{20\%}}{2}] \tag{6}$$

3.3.4 Experimental setup

Two locations are distinguished, as the location of the containers is changed on Monday. The location of the containers on Saturday and Sunday is referred to as Location 1 and the location for the experiments on Monday is referred to as Location 2. Instruments are replaced from jet poles 1, 2, and 4 to jet poles 5, 6, and 8. However, due to rough conditions, it is not possible to reach jet pole 3 on Monday. Therefore, it is decided to keep the instruments on this jet pole and measure offshore conditions from this point. It is assumed that the offshore measurements from jet pole 3 resemble the offshore measurements that would have been measured on jet pole 7.

The setup of the fieldwork consists of two 40 ft containers. The walls on both sides of the containers are restrained by parallel dunes. The parallel dunes serve to strengthen the container, hinder water flow around it, and thereby secure it in place. Moreover, the dunes exert opposite pressure on the container walls to prevent them from bending when the dune is constructed. The strengthening also creates a walkway along the container edges, facilitating measurements.

The container is situated near the high-water mark, which minimizes water flow around it. The artificial dune inside the container is constructed as far away from the opening of the container as possible, ensuring that the inside of the container is still visible. This way, more time is provided to allow any disturbances caused by the container to be rectified.

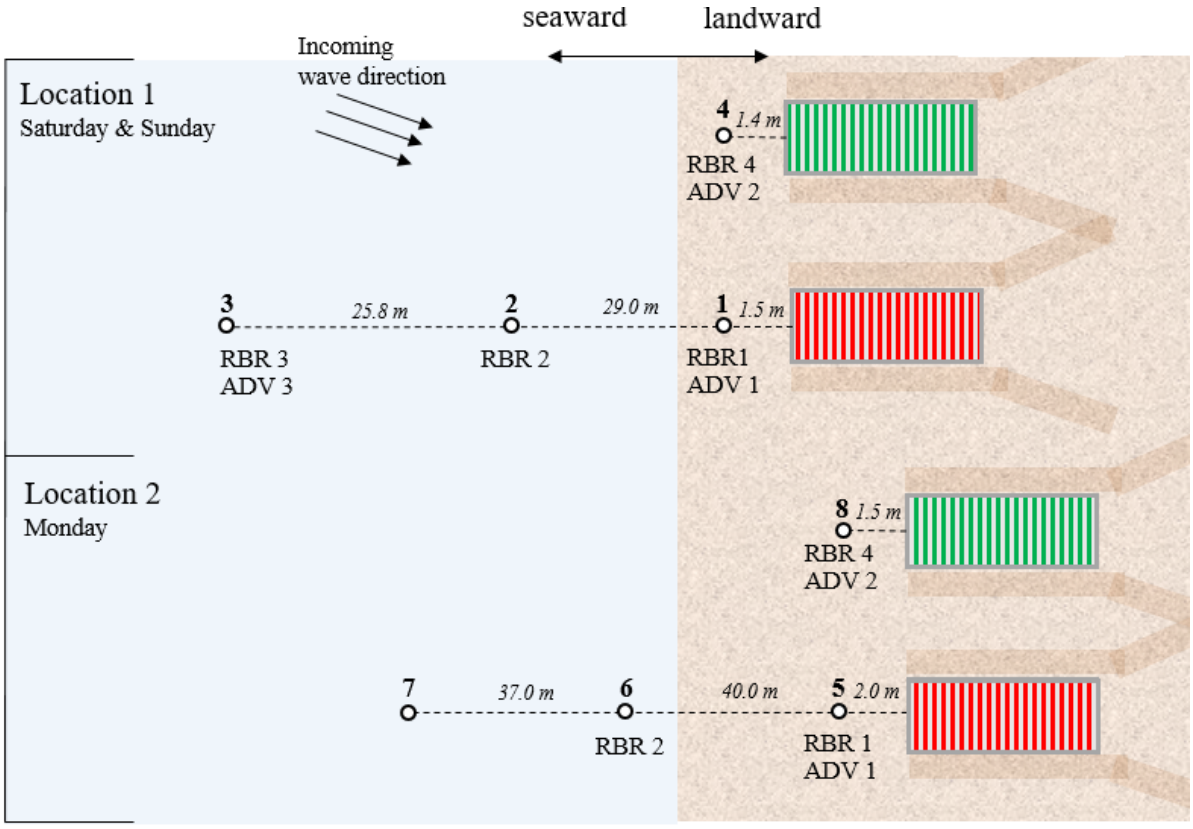

Figure 17: Schematic top view of the experimental setup with location 1 for the experiments on Saturday and Sunday and location 2 for the experiments on Monday. Jet poles were placed to install measurement instruments. The prevailing wave direction is indicated by the top arrows.

3.4 Instrumentation & data processing

This section provides a brief overview of the key processing steps undertaken. The main instrumentation used during the fieldwork are the pressure sensors (RBR), acoustic Doppler sensors (ADV), Global positioning systems (GPS) and video images (GoPro) in combination with a grid. All instruments will be briefly introduced.

(a) Jet pole in front of container

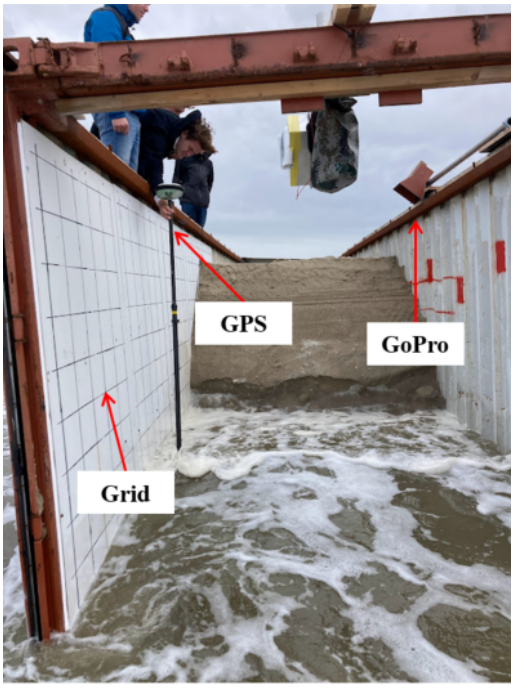

(b) Container opening

Figure 18: The instrumentation utilized during the field work to measure local conditions and dune profile development. The seaward outside of the container (left panel), the inside of the container (right panel)

3.4.1 RBR

The RBRs measure pressure measurements, where from water levels can be derived. From this data, the wave field and spectrum can be obtained. These pressure sensor measure with a sampling frequency of 8 Hz. To ensure that the instruments begin measuring as soon as they are submerged during rising tide, the pressure sensors are installed as close to the bed as possible (Figure 18a).

To process the data obtained from the RBR, the pressure signal is initially detrended using a 10-minute window. Subsequently, the pressure signal is transformed into a surface elevation by dividing the signal by the gravitational acceleration (9.81 m/s^2) and the density of seawater (1025 kg/m^3) and by performing an inverse Fourier transformation. Frequencies above 1 Hz are specified as noise and are removed in this transformation. Waves are identified by a zero-up crossing, where the wave height and length are calculated between upcoming crests. These four steps are presented in Figure 19.

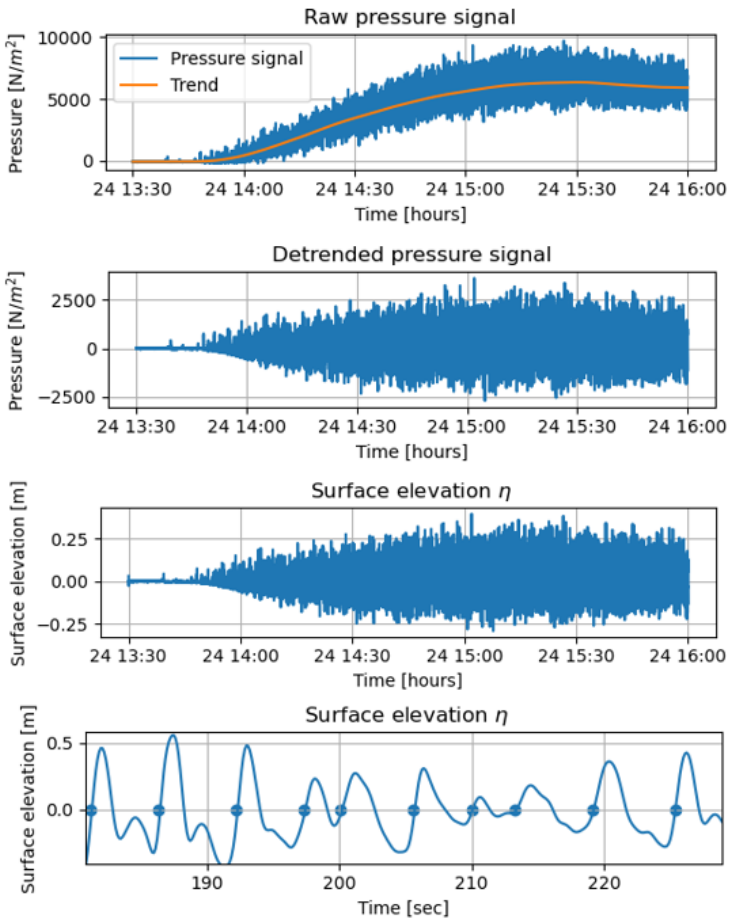

Figure 19: Example of processing pressure signal for RBR 1 on Saturday 24-09-2022. The unprocessed pressure signal (top panel), the pressure signal with its trend extracted (second panel), the surface elevation after the pressure signal has been converted (third panel), a segment of the surface elevation over time with the wave height and length determined by zero-up-crossing between the blue dots (bottom panel).

To obtain wave conditions, the next step is to extract the wave spectrum from the processed pressure signal. To accomplish this, time series are divided into 30-minute blocks to obtain a realistic observation while still including long waves. A Fourier series is used to transform the data for each block, and a variance density spectrum is calculated to determine the energy per frequency.

3.4.2 ADV

Velocity measurements are employed to determine the incoming wave direction and to validate the 1-dimensional assumption that solely cross-shore processes are considered (Chapter 3.2.1). The ADV measures velocities. The ADV data is processed similarly to the RBR data. First, the velocity data is detrended (Figure 20). Subsequently, for quality control purposes, a Fourier transform is performed to cut off frequencies above 1 Hz. Finally, the velocities are rotated in a new coordinate system so that the cross-shore velocity aligns with the container walls (Figure 21). The ADVs installed in front of both containers (jet pole 1,4,5 and 8) are aligned with the container entrance so no rotation is required and the measured cross-shore velocity coincides with the cross-shore velocity in the framework of the container.

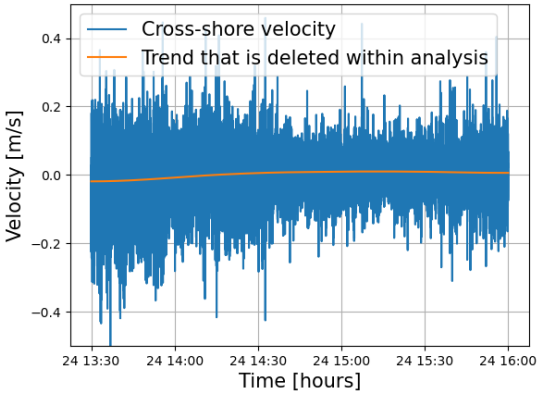

Figure 20: Example of data processing velocity signal for ADV2 on Saturday 26-09-2022, with the extracted trend from the signal (orange line).

3.4.3 GPS

The GPS is used to measure the bathymetry and the profile development of the dunes inside the container. Daily measurements of the bathymetry are taken, one prior to the experiments and the other after the experiments. Dune profile transects are taken during the experiments with the GPS after significant erosion events are observed. The GPS data is first filtered on measurement errors and then transformed to a new local coordinate system. Data with an error of 0.08 meter or higher is removed from the dataset. A different coordinate system is established for each container and location. The coordinates x_0 and y_0 are defined as the reference points at the jet pole in front of the container. The coordinates are transformed and interpolated to correct for any GPS measurement errors, allowing for the analysis of transects along straight lines.

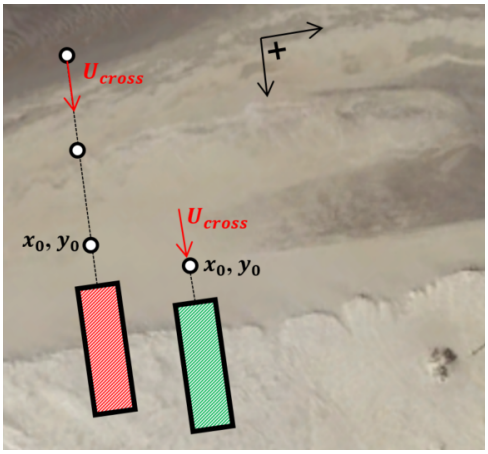

Figure 21: The new local coordinate system is obtained with the positive direction of the new local coordinate system (top black arrows).

Location	**Green container**		**Red container**	
	x_0 [m]	y_0 [m]	x_0 [m]	y_0 [m]
1	72.458	45.2203	72.467	452.330
2	72.458	45.2203	72.437	452.180

Table 4: RD-coordinates x_0 and y_0 of the new coordinate systems.

3.4.4 GoPro

GoPro images are used for two main purposes: to capture dune profile development in order to determine erosion volumes and to estimate run-up heights. The GoPros were set to take pictures every 0.5 second on Saturday 24-09-2022 and every 1 second on Sunday 25-09-2022 and Monday 26-09-2022. The GoPro is pointed at a 20 cm by 20 cm grid painted on the inside wall of the container in order to quantify erosion volumes. GoPros are relative cheap instruments and a much larger sample frequency can be achieved compared to the GPS. Therefore, erosion profiles are derived from the GoPro data. The GPS data is used as verification and to identify the elevation relative to NAP.

First, the images must be rectified to remove the GoPros fish eye effect. To create a rectified image, four points were manually selected and optimized by iteration (red dots in Figure 22a). The image is rendered within the new boundaries in such way that the grid in the container coincides with plotted grid lines (Figure 22b). To extract the contour lines from the rectified image, the pixels in the images are transformed to a grey scale (Figure 23). A pixel threshold needs to be defined in order to return a list of contour values. This threshold replaces the pixels below this value with black pixels and above this value with white pixels, allowing the white line to be extracted from the plot. For some days it is impossible to find a suitable value for the threshold, here the contours are manually selected. On Sunday, the GoPro in the red container (run 2R) stopped working during the test. For this run, dune profile development is extracted from GPS measurements.

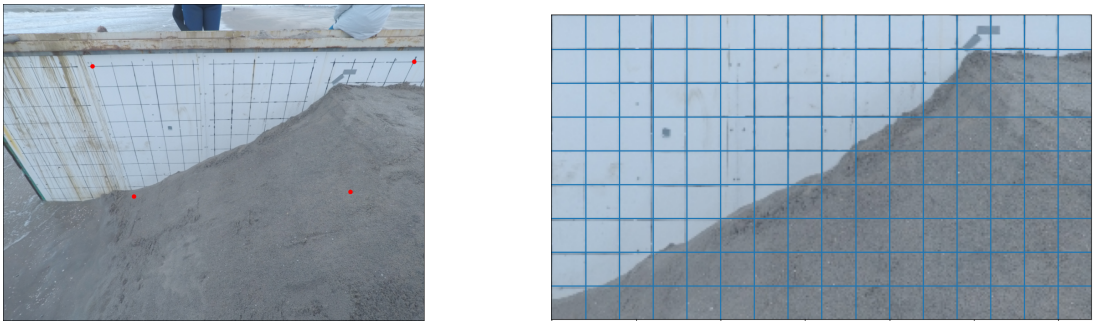

(a) Original image

(b) Rectified image

Figure 22: Rectification of GoPro images.

Figure 23: Extraction dune profile contour from GoPro image.
The pixels are transformed to gray scale (left panel), transformed to black or white pixels (middle panel), an a contour is extracted (right panel).

4 Data analysis

This chapter provides an overview of the methodology employed for the data analysis. The data analysis of this research is divided into three parts: analyzing erosion volumes, applying the wave impact theory, and investigating the effect of grain size on dune erosion. The methodology for each part is described separately. The results are presented within the specific parts and follow the same structure.

4.1 Part I data analysis: Erosion volumes

This section covers the first part of the data analysis, where erosion volumes are analyzed. Firstly, observations are made to determine which physical factors affect erosion during wave impact to get a better understanding of the processes involved. Secondly, profile transect are extracted from GoPro images to quantify erosion volumes and to compare the transects to GPS transects to evaluate the accuracy of the GoPro data. Lastly, cumulative erosion volumes are investigated in order to observe how erosion evolves over time and to compare the different experiments.

4.1.1 Physical quantities influence erosion

In order to gain more insight into the processes that affect the amount of dune erosion and trigger the occurrence of a new slump, GoPro images are examined. In Chapter 2.2.3, several quantities that are likely to influence erosion are described. Three main categories can be distinguished and these will be used as a guide. The images are analyzed to identify which quantities can be confirmed to affect dune erosion in the experiments conducted.

Three main categories:

1. Magnitude and duration wave exposure
2. Wave energy
3. Geotechnical aspects

4.1.2 Defining erosion volumes

Erosion volumes are extracted from profile measurements by comparing two profile transects and determining the difference in volume within two bounds. Profile transects are measured with the GPS and by images taken with GoPros. GPS measurements are very accurate and measure elevation relative to NAP. GoPro images are taken with a very high sampling frequency allowing to determine erosion volumes during the entire experiment. To assess the accuracy of the extracted profiles from the GoPro, the root mean square error is calculated by comparing the extracted profiles to GPS transects. This calculation is performed for each run to provide a better understanding of the margin of error in the data processing and to increase confidence in the measured values.

Erosion volumes are determined between time intervals on an event scale. Events are manually selected by scrolling through the data set retrieved from the GoPro. An event is identified as a clear difference in profile visible to the eye. The erosion volume is calculated by comparing the profile transect just after a slump with the profile just after the subsequent slump (Figure 24). This method allows for the identification of the processes that lead to the initiation of a new event during a given time period. All relevant quantities that contribute to the new event and affect the magnitude of such an event are captured within this time interval. The established erosion volumes on event scale serve as an input parameter in part II of the data analysis.

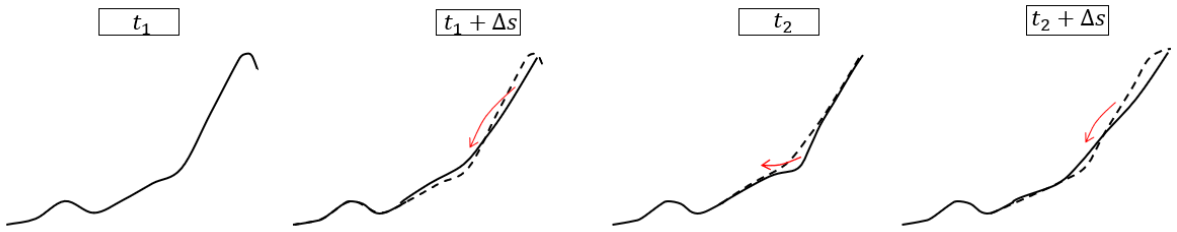

Figure 24: The erosion volume is determined as the difference between the profile just after a slump ($t_1 + \triangle s$) and the profile just after a subsequent slump ($t_2 + \triangle s$). The profiles just before slumps are t_1 and t_2. The sediment transport is indicated by the red arrow.

This study focuses on the collision regime and compares how dunes with different grain sizes respond to wave impact. Therefore the slump volume is the relevant measure of erosion (the purple area in Figure 25). The study does not consider sediment accumulation on the foreshore (the light blue area in Figure 25), as its focus is only on the impact of waves on the dune slope.

The erosion volume between two transects is bounded by two vertical lines. The left boundary is determined by the intersection of both profiles, whereas the right boundary is defined at the maximum vertical retreat distance of the crest (red lines in Figure 25). For each erosion volume, the left boundary is selected manually, while the right boundary remains constant throughout the experiment. This is because it represents the maximum retreat of the crest within the collision regime, and any reduction in the crest within this section is still considered as erosion.

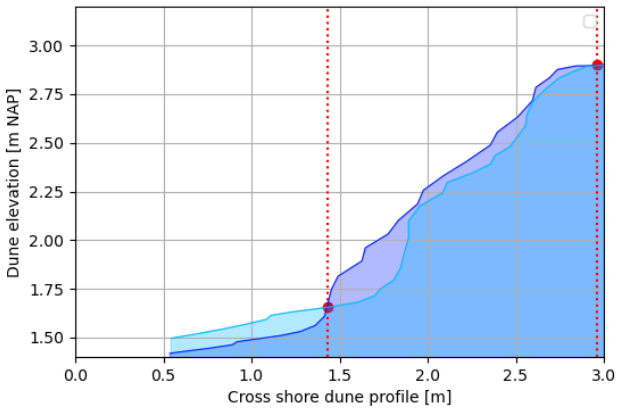

Figure 25: Cross-shore dune profile during one of the experiments. Vertical lines show the horizontal bounds for the erosion volume and the erosion volume is depicted in purple.

4.1.3 Comparing daily erosion measurements

Similar daily conditions are simulated by constructing similar initial dunes and by analyzing measurements during a comparable time interval where hydrodynamic forcing is of equal magnitude (Chapter 3.3.1). This enables direct comparison of daily erosion measurements. Cumulative erosion patterns of the reference dune, which is composed of the same sediment every day (red container) are compared to cumulative erosion patterns of the dunes composed of different sediment sizes (green container).

4.2 Part II data analysis: Wave impact theory

This section covers the second part of the data analysis. The application of an adaptation of the wave impact theory is analysed, where swash force is associated with the amount of erosion volume. This section introduces the method used for predicting erosion volumes based on hydrodynamic processes. The predicted erosion volumes are compared to the measured erosion volumes derived in part I of the data analysis to develop a wave impact relation based on previously established models.

4.2.1 Application analytical model based on wave impact theory

Two potential methods of the wave impact theory are tested in order to find a correlation between erosion volumes and wave impact: 1) Fisher et al. (1986) and 2) Larson et al. (2004). In the theory of Fisher et al. (1986) the erosion volume is related to the frequency and intensity of individual bores. In the theory of Larson et al. (2004) the magnitude of erosion volumes is associated to run-up and incoming wave exposure. The theory of Fisher et al. (1986) appeared not to be qualified for this study as the setup and gathered data were inadequate for testing this theory (Appendix C). The theory established by Larson et al. (2004) is better suited for this study, since the input variables are easier to measure from the setup and input variables resemble visual observations. This method is selected for the continuation of this study.

In this theory an analytical model is derived that predicts dune erosion ($\triangle V_E$) based on a quantification of wave impact (Equation 7). The used analytical model relies on five parameters to determine the solution:

$$\Delta V_{\mathrm{E}} = 4C_{\mathrm{s}} \left(R - z_{\mathrm{o}}\right)^2 \frac{\triangle t}{T} \tag{7}$$

Parameter		**Definition**
C_s	[-]	Empirical transport coefficient
ΔV_{E}	$[m^3/m^2]$	Erosion volume
R	[m]	Run-up height
z_0	[m]	Elevation of the dune toe
$\triangle t$	[sec]	Event time period
T	[sec]	Wave period

Table 5: Description of variables used in the analytical model by Larson et al. (2004).

Larson et al. (2004) found an agreement between the analytical model and four data sets originating from laboratory and field experiments. The analytical model was used to predict the total erosion that would occur during the surge period, these predictions were compared to the actual measurements of total erosion. Datasets of field experiments had an experimental time span of 10 to 24 hours, while the datasets of laboratory tests ranged from 20 to 70 minutes. The focus of this research, however, is to estimate the erosion volumes that occur during selected time intervals within the experimental period. Erosion volumes will be predicted for selected events for time spans ranging from 30 seconds to 5 minutes.

Such a selected time interval is equal to the time expired between two erosion events and is defined as the event time period ($\triangle t$). The event time period varies per event depending on the selection of events. Erosion volumes (ΔV_{E}) are calculated based on this time interval and the dune toe elevation (z_0) remains constant over this time period. However, some parameters are measured per wave and are known at a more detailed time scale. These parameters are modified to a representative value in the event time period. Analysis of different representations were performed and results show that this is best accomplished by computing the root mean square of the run-up, and by taking the average value of the wave period.

4.2.2 Flowchart application analytical model

Figure 26 presents a flowchart illustrating the method used to derive a relation between the measured erosion volume (1) and the impact parameter (2). The measured erosion volumes are derived in the first part of the data analysis. To derive the impact parameter, firstly a run-up relation (2a) is derived to estimate the run-up height at all times. Secondly, the run-up parameter (2b) and wave counter (2c) are established. The run-up parameter is defined as the height that the water reaches above the dune toe. The wave counter indicates the number of incoming waves in a certain time frame. These two parameters are combined to an impact parameter. A linear relation is derived by a least-square fit of the measured erosion volumes to the predicted erosion volumes by the impact parameter (3).

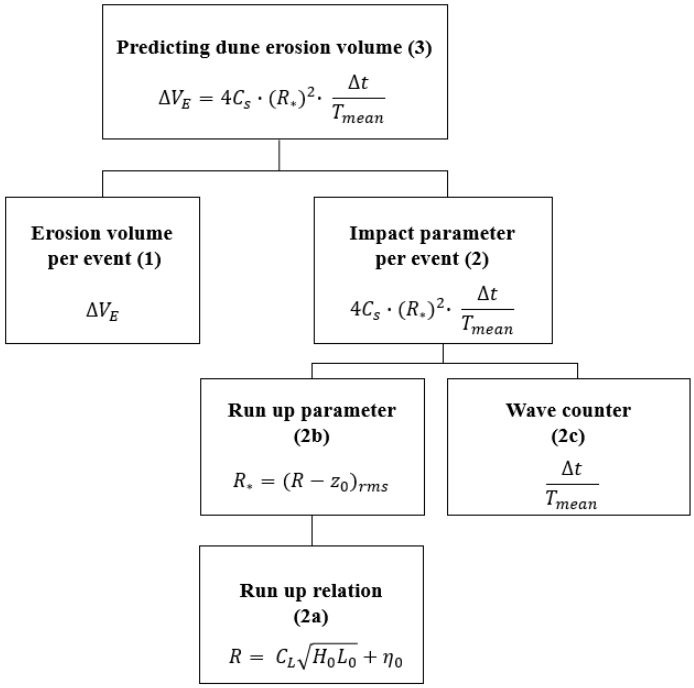

Figure 26: This flowchart provides an overview of the method used in this study based on the analytical model of Larson et al. (2004), with the predicted erosion volume (ΔV_{E}), a dimensionless transport coefficient (C_{s}), the run-up height (R), the difference between mean water level and dune toe (z_{o}), the event time duration ($\triangle t$) and the mean wave period (T).

4.2.3 Erosion volume per event (1)

Results of 'Part I data analysis: Erosion volumes' are used as input parameter. Erosion volumes are calculated as the profile change between two events (Chapter 4.1.2). An event is identified as a clear difference in profile visible to the eye. Events are manually selected and the time period between events varies.

4.2.4 Run-up relation (2a)

Run-up is defined as a measure of the height of individual water-level peaks above the still water level. The still water level (η_0) is defined as the sum of the level of the astronomical tide and surge. Contributions from wave setup and swash are integrated in the surge level.

$$\eta_0 = \eta_{tide} + \eta_{surge} \tag{8}$$

It is quite time-consuming to determine the run-up heights for each wave from GoPro images. Moreover, modeling the extraction of run-up height is challenging due to the variability of sunlight and the low sampling frequency of the GoPro camera, leading to uncertainty in whether a run-up or run-down is captured. Therefore, a run-up relation has been developed to estimate the run-up height at all times. This reduces the amount of time required to determine run-up heights from the GoPro images, because only a limited number of them need to be analyzed. Several methods are available to predict wave run-up. For this study, the formula by Hunt (1959) is chosen because run-up is quantified as a measure of offshore conditions and reliable measurements of these conditions were obtained during the fieldwork (Equation 9). This relation seems reasonable as higher offshore energy is typically expected to result in a higher run-up height at the artificial dune in the container. A more comprehensive run-up relationship, such as the one developed by Stockdon et al. (2006), could also have been utilized. However, there is not enough data to assume a normal distribution.

Input parameters of the run-up relation are derived by Hunt (1959) for specific beach slopes and grain sizes. The calibration factor C_L depends on the foreshore ($tan(\alpha)$), an indication of the roughness (r), and the porosity (p) of the beach. Steeper slopes lead to higher run-up and and larger grain sizes result in rougher and more porous beaches, attenuating the run-up. To use this formula for the Sand Engine, it is necessary to identify a comparable case study to determine the appropriate C_L value. Subsequently, the calculated value will be compared to run-up measurements taken at the Sand Engine to assess its accuracy.

$$R = C_L \sqrt{H_0 L_0} \tag{9}$$

$$C_L = 2.3 \cdot (\frac{2\pi}{g})^{0.5} \cdot \tan(\alpha)(r)(p) \tag{10}$$

It is challenging to accurately link a specific offshore wave condition to an observed run-up height inside the container due to measurement errors and the transformation of waves as they approach the shore. Therefore wave conditions and run-up heights are analysed in time intervals. The root mean square of 13 run-up heights is correlated with the root mean square of the measured offshore wave height and length during the same period. This is performed every 5 minutes, resulting in one data point every 5 minutes representing the root mean square of 13 measurements.

4.2.5 Run-up parameter (2b)

The analytical model of Larson et al. (2004) only accounts for run-up that reaches above the dune toe (R_* in Figure 27). It is important to acknowledge that, despite the notation of R as run-up height, the current description implies that R represents an indicator of the hydrodynamic impact on the dune. The run-up (R) is determined from the run-up relation and is known per wave, the still water level (η_0) at that specific time is summed up to know the water elevation relative to NAP. Finally the dune toe elevation, which is a constant for every specific event, is subtracted in order to only consider the run-up above the dune toe (R_*).

$$R_* = R + \eta_0 - z_0 \tag{11}$$

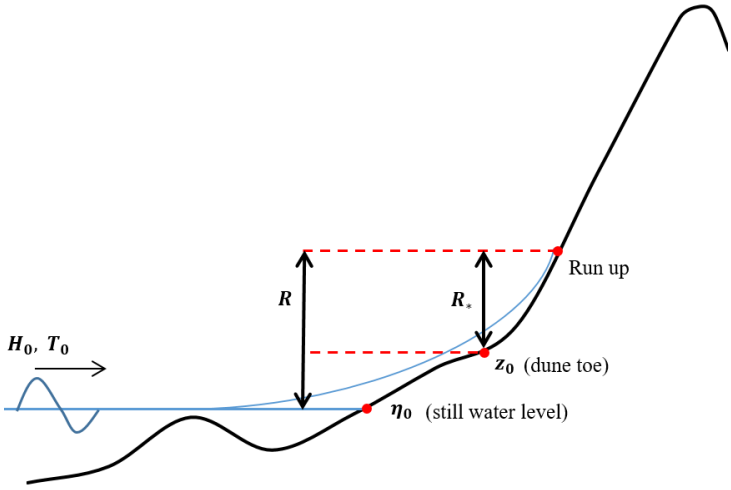

Figure 27: Definition of the run-up parameter (R_*), the run-up parameter is a measure of the height the water level reaches above the dune toe.

4.2.6 Wave counter (2c)

The wave counter represents the estimated number of incoming waves per event time period It is calculated by dividing the duration of the event ($\triangle t$) by the mean deep water wave period ($T_{0,mean}$).

4.2.7 Impact parameter per event (2)

The impact parameter is determined by combining the wave counter with the run-up parameter. This parameter calculates the predicted erosion volume.

4.2.8 Predicting dune erosion volume (3)

The predicted erosion volumes by the wave impact parameter are compared to the measured erosion volumes derived in Part I of the data analysis (Chapter 4.1). The transport coefficient (C_s) in this equation is a constant which is calibrated by least-square fitting a linear relation between actual measured erosion volumes and the predicted erosion volumes. An empirical solution is derived for each experimental run, except for run 2R, as no GoPro data is available for this run. Transport coefficients are determined for each run. This value includes the influence of several physical parameters that have not been explicitly considered, such as the impact of grain size and profile attenuation. The Pearson's correlation parameter is derived to indicate the level of correlation between the two parameters.

Transport coefficients (C_s) vary for every run and are compared to capture differences in erosion patterns. This parameter is validated by comparing them to values found by Larson et al. (2004). He discovered that the first three data sets had mean transport coefficient values of $1.4{\cdot}10^{-}3$, with a standard deviation of $0.74{\cdot}10^{-}3$, while other values were found for the storm field datasets of Birkemeier et al. (1988), respectively $1.4 \cdot 10^{-}4$ and $2.5{\cdot}10^{-}4$. All datasets showed marked scatter in the transport coefficients, especially the storm datasets of Birkemeier et al. (1988) which yielded significantly lower values.

4.3 Part III data analysis: The effect of sediment grain size

In the final part of the data analysis the effect of sediment grain size is investigated by comparing results of cumulative erosion volumes per day (part I) and by analyzing the results of the analytical model based on wave impact theory (part II).

Firstly, daily erosion measurements are compared to determine whether there is a deviation in erosion patterns that can be attributed to the effect of sediment grain size. Secondly, the results of the analytical model for each run are compared by examining the different values obtained for the transport coefficient (C_s). This coefficient considers physical parameters that are not explicitly accounted for in the model. The investigation focuses on whether there is a dependency of this parameter on the grain size. However, it is important to acknowledge that the transport coefficient is not only dependent on the grain size but also on several other parameters.

5 Results

This chapter presents the key findings of the data analysis. The data analysis exists of three parts and results will be presented separately for each part.

5.1 Part I data analysis: Erosion volumes

In this first part of the data analysis, observations reveal physical factors that affect dune erosion during wave impact. Furthermore, dune profile development is extracted from GPS and GoPro measurements and the cumulative erosion distribution is presented for each experiment.

5.1.1 Visual observations

The established three main categories (Chapter 4.1.1) appeared to have an impact on dune erosion: (2) the magnitude and duration of wave exposure; (1) wave energy; and (3) the geotechnical properties of the dune.

Firstly, based on several erosion events it seems as if run-up has a great impact on dune erosion. It seems that the effect of run-up is more prominent on the dune face compared to bore impact, as bore impact only occurs occasionally. One possible explanation for this is that the container was placed in the intertidal zone during moderate conditions, which forced dune erosion through run-up (Figure 28) and only occasionally through bore impact (Figure 29).

(a) (b) (c)

Figure 28: Run-up for run 3G on Monday 26-09-2022. (a) A wave front appears at the container opening. (b) Water runs against the dune face. (c) Water retreats and traces of the run-up are still visible.

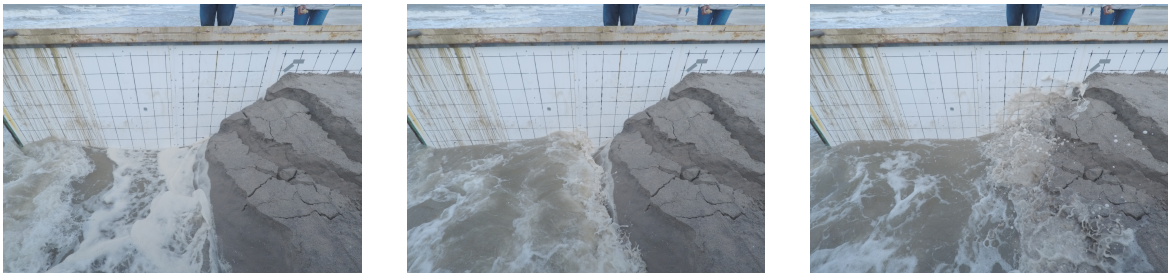

(a) (b) (c)

Figure 29: Bore impact for run 1G on Saturday 24-09-2022. (a) An incoming bore appears at the opening of the container. (b) The bore approaches the the dune toe. (c) The bore attacked the dune face.

Additionally, observations suggest that the wetting of the dune face by waves plays a significant role in dune erosion. As the sediment volume becomes wet, its weight increases resulting in higher gravitational force that can lead to avalanching. When a bulk of sediment slumps, it is frequently observed that the newly exposed sediment has a lighter color, indicating that mainly the saturated segment of the dune has slumped. This observation is consistent with the findings of laboratory studies (Palmsten and Holman, 2011).

Wave energy, the second category, appears to be a significant parameter in initiating dune erosion. Higher waves seem to have a greater impact and sediment transport capacity. Specifically, merging of bores was found to increase the wave energy in the container, resulting in higher run-up heights and more intense wave impact on the dune face. This phenomenon, where breaking wave fronts merge into a single wave front, is further elaborated by Bertin et al. (2018), who states that it leads to an increase in wave period and contributes to the transfer of energy from short wave frequencies to infragravity (IG) frequencies. This could be an indication of a wave with a longer period, which can penetrate further onshore without breaking and gives shorter waves the chance to travel on top of these waves.

A third significant factor contributing to dune erosion appears to be the geotechnical properties of the dune. Observations indicate that the dune face gradual steepens which leads to an unstable dune face and potential failure through shear-type or beam-type failure (Figure 30c). On the contrary, when eroded sediment accumulates in front of the dune face, it can create a temporary, more dissipative foreshore that protects the dune face from strong wave impact. It is also observed that dunes composed of coarser sediment tends to have steeper slopes, while those composed of finer sediment are not able to reach the same degree of steepness.

(a) Steepening of the dune face (b) Shear-type of failure (c) Beam-type of failure

Figure 30: Observations of geotechnical aspects influencing erosion mechanisms for run 3R on Monday 26-09-2022. (a) A very steep profile. (b) Shear-type of failure, when the weight excees the shear strength. (c) Beam-type of failure, when a tension crack is developed landwards.

5.1.2 Dune profile development

Dune profiles are extracted from the GoPro images to track the development of the dune profile. The extracted transects from the GoPro are compared to the measured transects obtained with the GPS (Figure 31). The comparison shows that the profile is accurately extracted from the images, with a RMSE of 5.81 cm for run 1G. Similar margins of error are observed for the other runs. So dune profiles can be extracted from the GoPro images every second, providing a high temporal resolution for the quantification of profile changes over time.

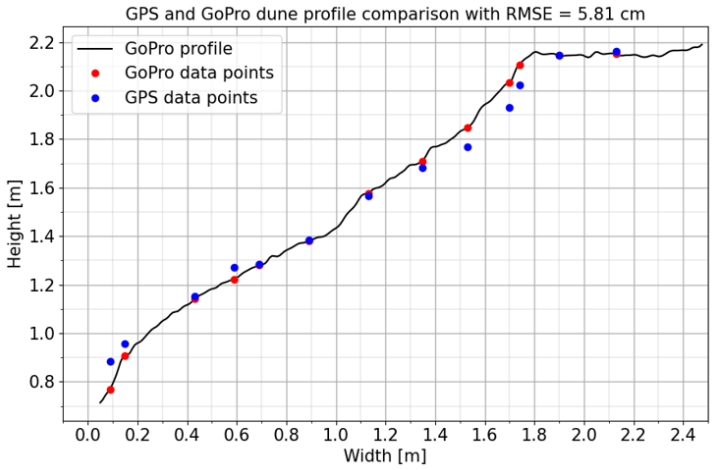

Figure 31: Comparing extracted GoPro transects with GPS transects for run 1G there is a RMSE of 5.81 cm.

Dune profile development is obtained for each day by plotting the transects for all events (Figures 32). The development shows that as the experiment progresses, the dune toe moves up and landward. Changes in the foreshore are also observed. In runs 1G, 1R, 2R and 3R, the foreshore remains nearly constant, while in run 2G and 3G, the slope becomes significantly milder. Additionally, it is obtained that the slope of the dune becomes gradually steeper till another slumping event occurs and that the crest of the dune decreases slightly. This reduction of the crest is the consequence of mass slumping and not overwash since the experiment only includes the collision regime.

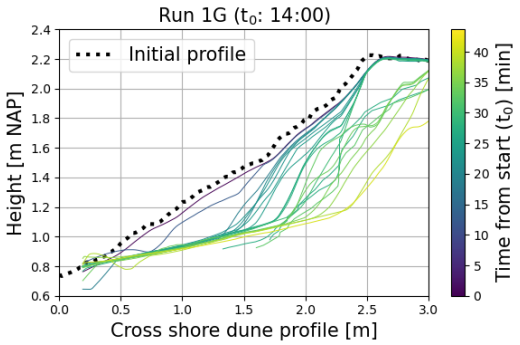

(a) Run 1G (D_{50}: 0.21 mm)

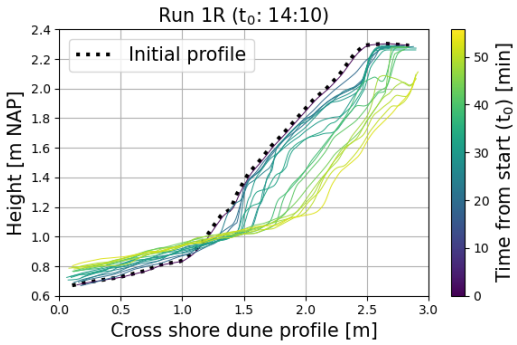

(b) Run 1R (D_{50}: 0.27 mm)

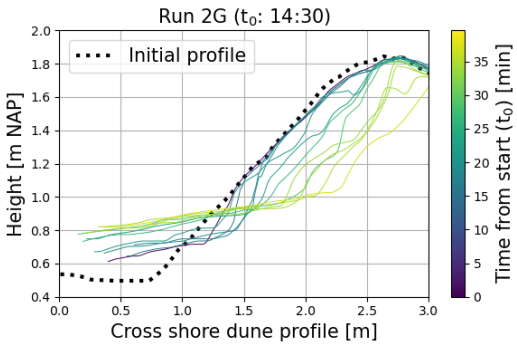

(c) Run 2G (D_{50}: 0.24 mm)

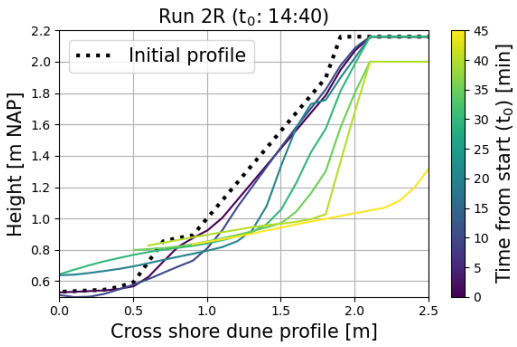

(d) Run 2R (D_{50}: 0.27 mm)

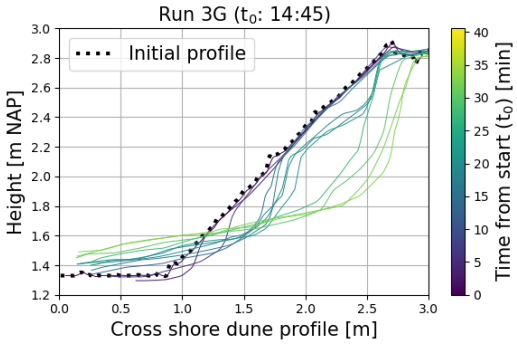

(e) Run 3G (D_{50}: 0.31 mm)

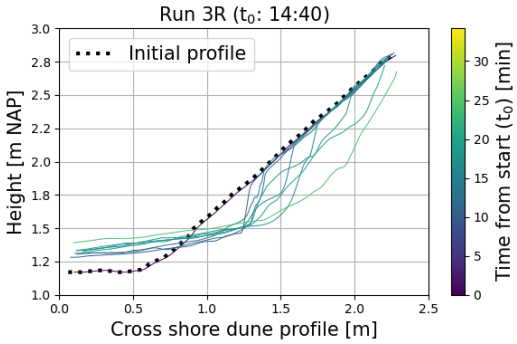

(f) Run 3R (D_{50}: 0.27 mm)

Figure 32: Dune profile development in the green and red container for all experimental days. Transects are measured using GoPro images, with the color of each transect indicating the time the measurement is performed.

5.1.3 Dune toe development

The dune toe regression for both cross-shore and vertical direction of the dune toe follow a linear trend backward and upward (Figure 33a). A strong trend is also observed between the dune toe elevation and the rising mean water level (Figure 33b). This linear trend of toe regression in cross-shore and vertical direction and the trend between the elevation of the dune and the mean water level hold for all runs.

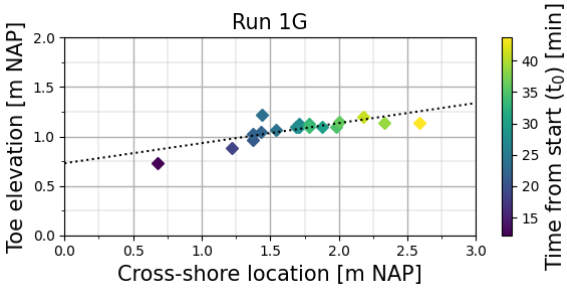

(a)

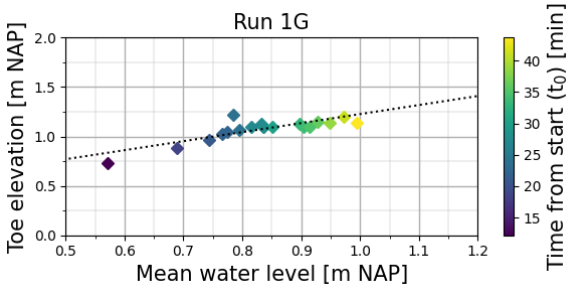

(b)

Figure 33: a) Trend upward dune toe position with respect to dune toe cross-shore position. b) Trend upward dune toe position with respect to the rising mean water level. The color of each transect indicates the time the measurement is performed.

On the one hand, it can be assumed that the dune toe continuous regresses in vertical direction following the linear trend. This approach allows to estimate the height of the dune toe at any time during the experiment (left figures in Figure 34). A slight deviation of the steepness of the lines is observed. The mean dune toe regression in the vertical direction over time could be estimated according to the linear trend: $y = 0.012x + 0.83$. On the other hand, computing a gradual relation is a more realistic approach, as it assumes that the toe only moves upward and backward after a slumping event has occurred (right figures in Figure 34). This Piece-wise approach to model the development of the toe provides a more accurate estimation of its height over time, as not every wave impact changes the toe location.

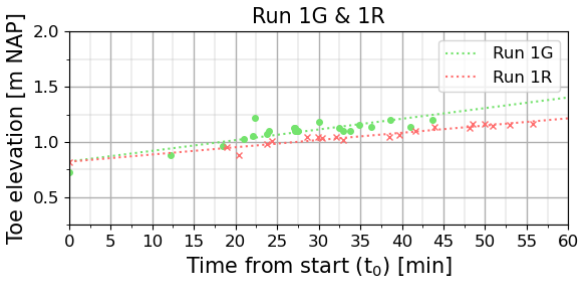

(a) Linear fit run 1G & 1R

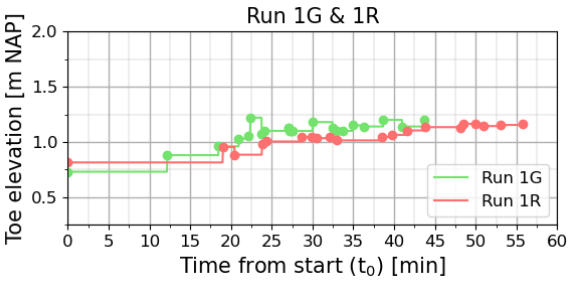

(b) Piece-wise fit run 1G & 1R

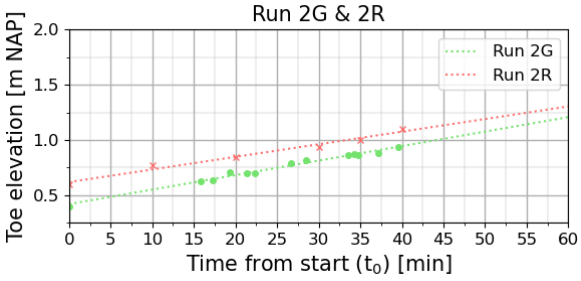

(c) Linear fit run 2G & 2R

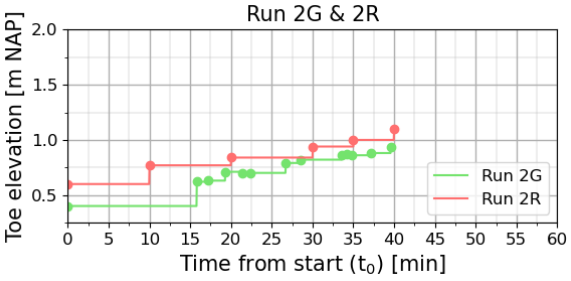

(d) Piece-wise fit run 2G & 2R

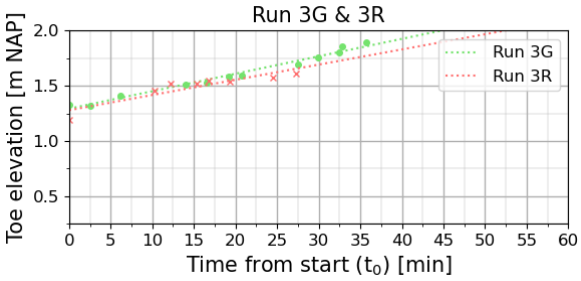

(e) Linear fit run 3G & 3R

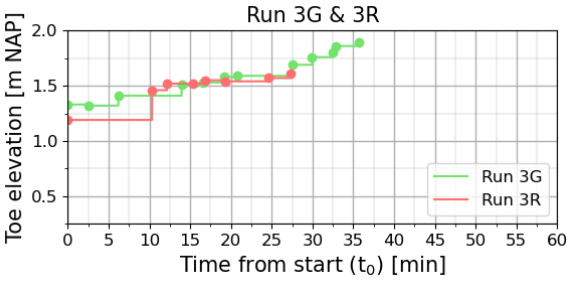

(f) Piece-wise fit run 3G & 3R

Figure 34: Development of the toe in vertical direction. (a) A linear fit through the toe elevation is drawn which assumes a continuous vertical regression of the dune toe in time. (b) A Piece-wise vertical regression of the dune toe assumes that the toe only moves upward after a slumping event.

5.1.4 Slump frequency

The frequency of slumps over time is investigated (Figure 35). It can be observed that at the beginning of the experiments, when the water first reaches the toe of the dune, there is a longer interval between erosion events and smaller volumes erode. In the middle of the experiment, erosion events occur in more rapid succession with larger volumes. This gradually slows down towards the end of the experiment period.

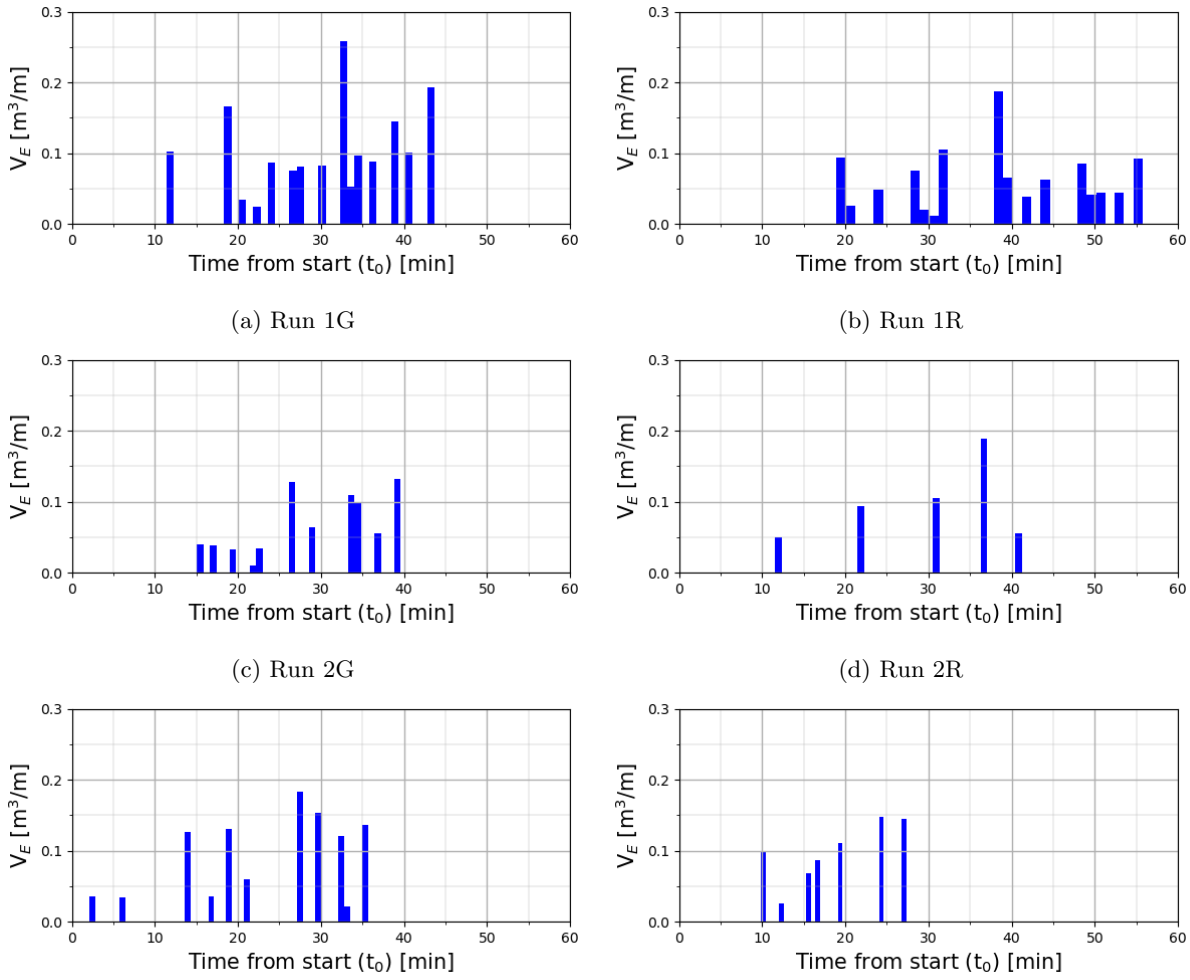

(a) Run 1G

(b) Run 1R

(c) Run 2G

(d) Run 2R

(e) Run 3G

(f) Run 3R

Figure 35: Plot of erosion volumes per event over time. Each blue bar represents an event, and the height of the bar indicates the amount of erosion that occurred during that event.

5.1.5 Cumulative erosion volumes

Erosion volumes are quantified from the GoPro images (Chapter 3.4.4). The development over time of cumulative erosion volumes typically follows a S-shaped curve (Rueda et al., 2011). This shape is clearly recognizable for runs 1G and 1R, while for runs 2D, 2R, 2G, and 3R, the S-shape is less pronounced. However, it is likely that these curves would have followed the same shape if the experiments had continued for a longer period of time, but they finished earlier due to overwash.

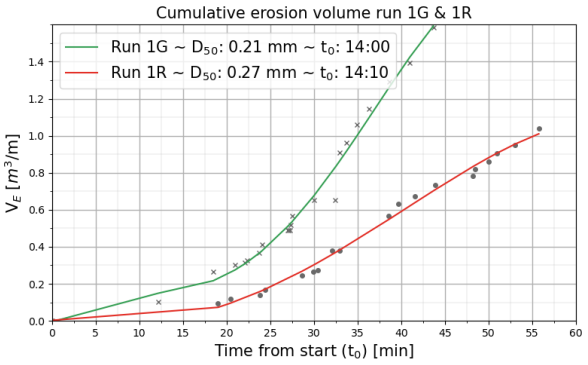

(a) Saturday 24-09-2022 (run 1G & 1R)

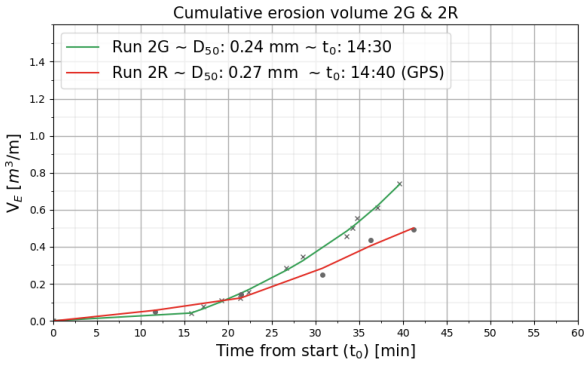

(b) Sunday 25-09-2022 (run 2G & 2R)

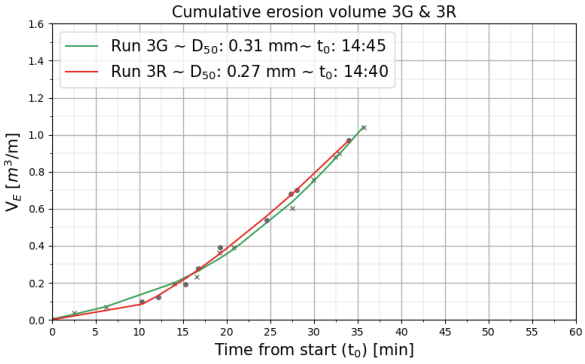

(c) Monday 26-09-2022 (run 3G & 3R)

Figure 36: The total erosion volume for each experimental day is calculated by adding up the erosion volumes from each individual event. This cumulative erosion data is plotted over time to show the overall evolution of the erosion volume.

5.1.6 Main results

The main results of the first part of the data analysis are the intermediate event erosion volumes for each experiment. These will serve as the input variables for the measured erosion volume in the second part of the analysis. In the third part of the data analysis, it is investigate whether the observed daily differences in erosion patterns can be explained by the use of different grain sizes.

Run	$\mathbf{t_0}$	**Surge duration** [min]	$\mathbf{H_{m0}}$ [m]	$\mathbf{T_{m1-0}}$ [s]	**Dune height** [m]	$\mathbf{D_{50}}$ [mm]	**Eroded volume** $[m^3/m]$
1G	14:00	43	0.77	7.35	1.5	0.21	1.60
1R	14:10	56	0.77	7.35	1.5	0.27	1.05
2G	14:30	40	0.76	7.25	1.4	0.24	0.75
2R	14:40	42	0.76	7.25	1.4	0.27	0.50
3G	14:45	36	1.25	9.92	1.6	0.31	1.05
3R	14:40	34	1.25	9.92	1.6	0.27	1.00

Table 6: Overview of the experimental conditions and results of 'Part I data analysis: Erosion volumes'.

5.2 Part II data analysis: Wave impact theory

The second part of the data analysis investigates whether there is a relation between measured erosion volumes and predicted erosion volumes by a wave impact parameter. Measured erosion volumes are derived in the results of the first part of the data analysis. Erosion volumes are predicted according to the analytical model derived by Larson et al. (2004) based on wave impact theory. Alternating timescales are applied from those used in the conservative method. First a run-up relation must be determined which is applicable to the field site. Followed by the determination of the impact parameters which predict erosion volumes. Subsequently, predicted erosion volumes by the impact parameter are compared to measured erosion volumes to identify any potential correlation between the two parameters. Finally, the accuracy of the analytical model in predicting erosion volumes is assessed.

5.2.1 Run-up relation

A run-up relation is derived to estimate the run-up height at all times. A Hunt-type of formula is used to predict the run-up inside the containers. Measured run-up heights are fitted to a quantification of offshore conditions to determine the calibration factor (C_L) (Chapter 4.2.4).

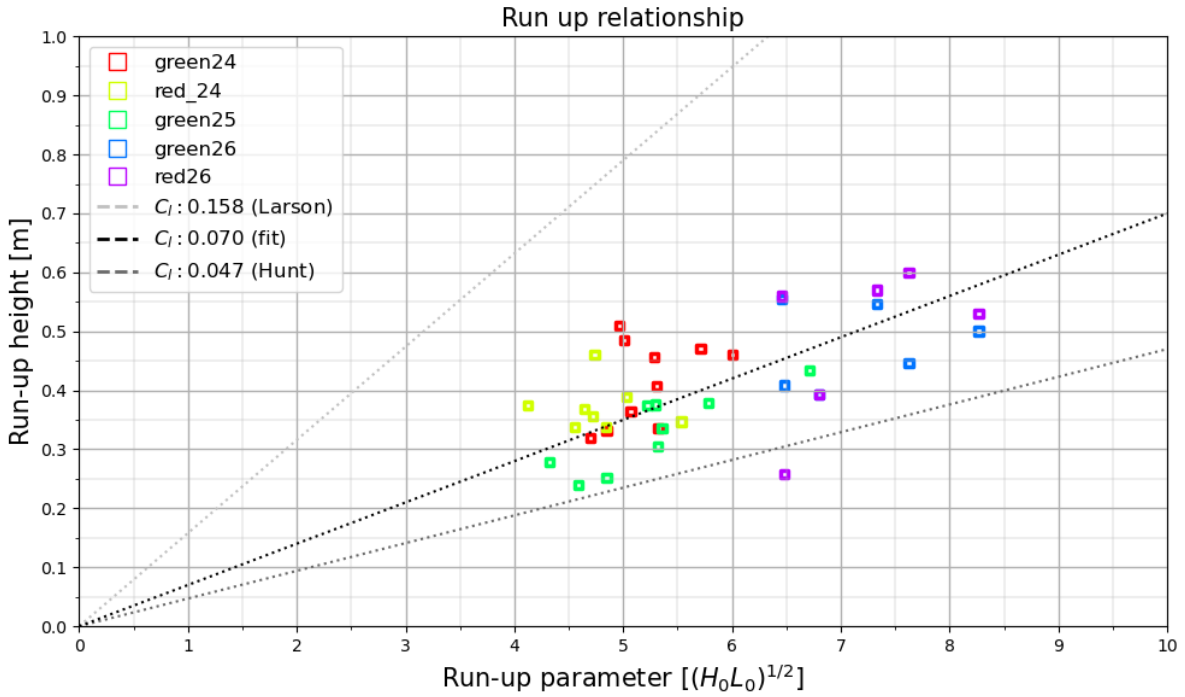

Figure 37: Estimation of the run-up at the field site using a Hunt-type of formula. Hunt (1959) suggest a C_L value based on the field sites properties of 0.047. Larson et al. (2004) uses a C_L value of 0.158 to predict the run-up at a beach with slope 1:7 and grain sizes ranging from 0.22 to 0.33 mm. A value for C_L of 0.070 is implemented to predict the run-up at the field site of this study.

Hunt (1959) derived values for the porosity (p) and roughness (r) parameters based on certain beach properties. The beach most similar to the field site had a slope of 1:30 and a grain size of 0.2 mm, for which he suggested a value of 0.77 for the roughness and porosity parameters ($r \cdot p$), resulting in a C_L value of 0.047. Larson et al. (2004) used a value of 0.158 for C_L to predict run-up levels based on a beach with slope 1:7 and grain sizes ranging from 0.22 to 0.33 mm.

Although Hunt (1959) suggests a value of 0.047 for a beach similar to the field site, run-up measurements at the field site indicate that a higher value of C_L predicts the run-up more accurately. This required higher value of C_L can be attributed to the fact that the beach slope, including a part in the surf zone, at the field site has a slope of almost 1:25. In addition, the grain size of the beach is somewhat coarser. The steeper slope indicates a higher value of C_L, although the increase in grain size indicates a decrease in the parameters for roughness and porosity ($r \cdot p$). This decrease is, however, almost negligible when comparing values suggested by Hunt (1959). Since this steeper slope results in a higher C_L value and the least square fit indicates that a higher value is required to accurately predict the run-up, a value of 0.070 is found to predict the run-up at the field site of this study.

5.2.2 Input parameter magnitudes over the experimental period

The input parameters of the analytical model within the period of the event include the root mean square of the run-up, the mean water level, a piece-wise constant value of the dune toe elevation, and an estimate of the number of incoming waves.

The values of the piece-wise dune toe position are shown in Figure 34, and the number of incoming waves is related to the time period of each event. The run-up parameter is determined by the run-up relation and depends on the mean water level, the offshore wave height, wave length, and the elevation of the dune toe (Equation 11). Throughout the experimental period, the offshore wave height and wave length show relatively consistent magnitudes. The mean water level demonstrates an increasing trend, which is strongly correlated with the increasing trend observed for the run-up (Figure 38). Again, it is obtained that conditions became rougher on Monday 26-09-2022.

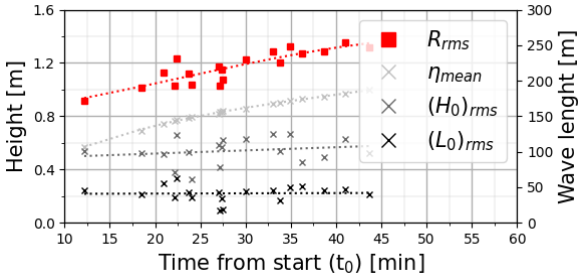

(a) Saturday 24-09-2022 (run 1G)

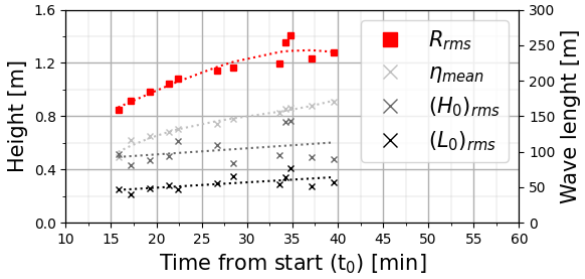

(b) Sunday 25-09-2022 (run 2G)

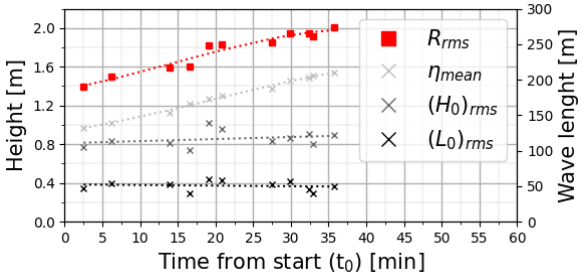

(c) Monday 26-09-2022 (run 3G)

Figure 38: The magnitude of input parameters is shown over the experimental period. While the offshore wave height and length remain relatively constant throughout the period, the mean water level and run-up show a similar increasing trend (fitted by a polynomial).

5.2.3 Solutions analytical model based on wave impact theory

Erosion volumes are predicted according to the analytical model derived by Larson et al. (2004) (Equation 7). Event time periods are determined based on the occurrence of manually selected events where significant changes are observed.

It is obtained that the selection of the event time period ($\triangle$t) used to calculate the impact parameter has a significant influence on the results. When a constant event time period is utilized, there is no correlation between the predicted and measured erosion volumes. This is because constant time periods lead to nearly constant values for the wave counter ($\frac{\triangle t}{T}$). The variability in the amount of incoming waves seems to be required in order to accurately predict erosion volumes by the impact parameter. When variable event time periods are used, there is a correlation between the predicted and measured erosion volumes. Variable time periods result in significant variability in the magnitude of the wave counter value, which has a significant impact on the solution. However there may be the need to restrict the time intervals between events, as it is important to consider that as the event time period increases, the representativeness of parameters known per wave becomes questionable. This is because certain quantities may be averaged out, resulting in a poor representation of the parameter. Furthermore, an extension of the event time period results in an increase of uncertainty added into the model, as the assumption of a constant dune toe (z_0) over the event period becomes questionable. On the other hand, time periods should be long enough to capture processes that trigger erosion events.

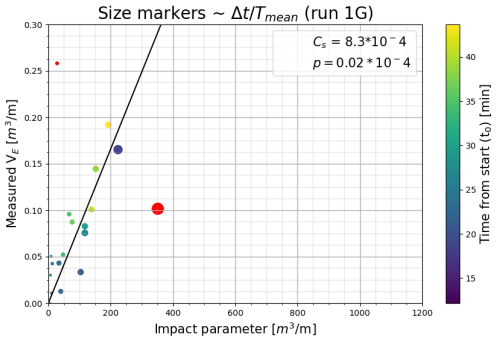

(a) Run 1G

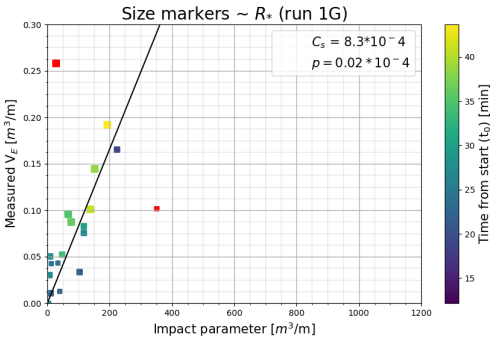

(b) Run 1G

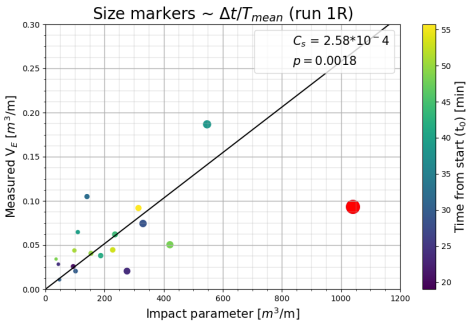

(c) Run 1R

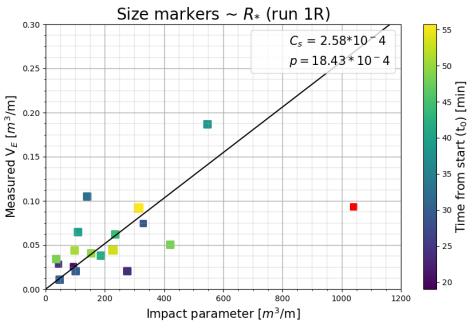

(d) Run 1R

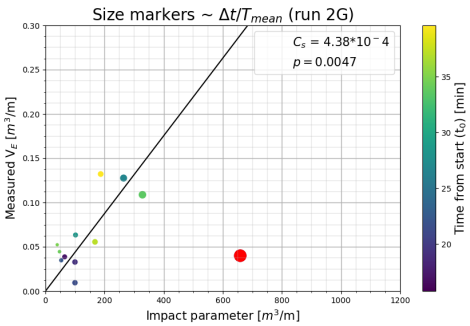

(e) Run 2G

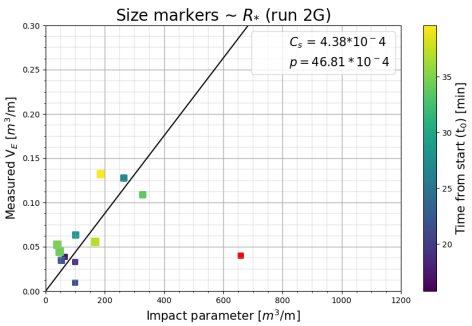

(f) Run 2G

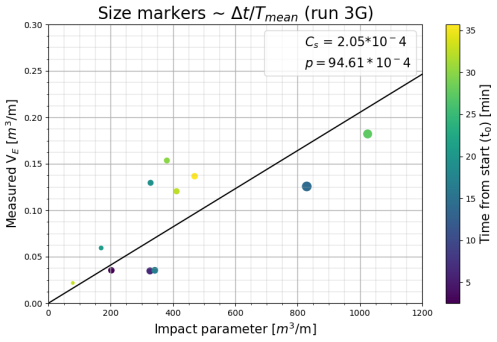

(g) Run 3G

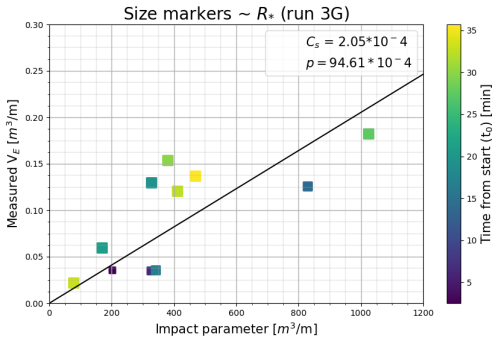

(h) Run 3G

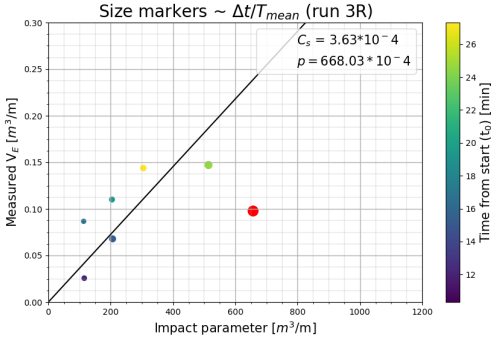

(i) Run 3R

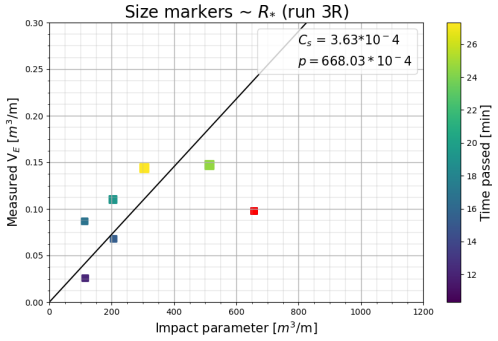

(j) Run 3R

Figure 39: Relation between eroded volume and a wave impact parameter calculated according to the analytical model derived by Larson et al., 2004 based on wave impact theory. C_s is a transport gradient and p is the Pearson correlation coefficient. The red scatter points indicate outliers and are neglected. The size of the scatter points varies depending on the magnitude of the wave counter ($\triangle t/T_{mean}$) for the left plots, and the magnitude of the run-up above the dune toe (R_*) for the right plots. The larger the size of the points, the higher the values are.

A linear trend is observed for all runs based on varying event time periods of manually selected events. Some runs exhibit outliers, these are attributed to contrasting event time periods. The size of the markers in the left plots reflects the number of incoming waves, with larger markers representing longer time intervals and a larger number of incoming waves (Figure 39). Considering longer time intervals has a significant impact on the predicted erosion volume and potentially leads to overshadowing the influence of other parameters. The size of the markers in the right plots reflects the run-up level above the dune toe (R_*), with larger markers representing higher run-up levels. Based on the figures, it is inferred that the number of incoming waves fluctuates more per run than the difference in magnitude of run-up above the dune toe. Furthermore, it is generally observed that higher impact parameters, and therefore larger erosion volumes, are associated with a greater number of incoming waves. These observations suggests a strong correlation between the amount of erosion volumes and the number of incoming waves, and a weaker correlation between the amount of erosion volumes and the magnitude of run-up above the dune toe.

When disregarding the outliers (red scatter points in Figure 39), the Pearson coefficient (p) indicates a strong correlation for all runs. Transport coefficients (C_s) are derived from the conducted experiments, ranging from $8.30 \cdot 10^{-4}$ to $2.05 \cdot 10^{-4}$.

5.2.4 Accuracy of analytical model in predicting erosion volumes

Erosion volumes are predicted using the analytical model based on wave impact theory derived by Larson et al. (2004) (Equation 7). To assess the accuracy of the model in predicting erosion volumes, the predicted cumulative erosion volumes are compared to the measured cumulative erosion volumes (Figure 40). A difference is observed between the two cumulative graphs, indicating that the analytical model cannot be used to accurately predict erosion volumes. The model tends to overestimate erosion volumes. Nevertheless, the model may still be useful for investigating different patterns of erosion behavior.

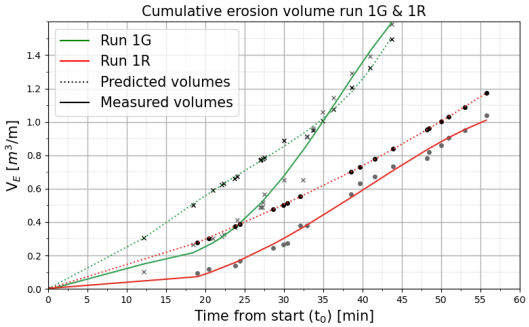

(a) Saturday 24-09-2022 (run 1G & 1R)

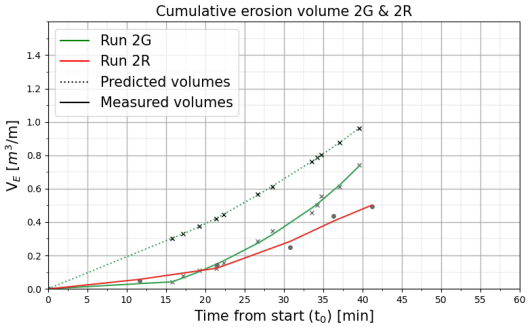

(b) Sunday 24-09-2022 (run 2G & 2R)

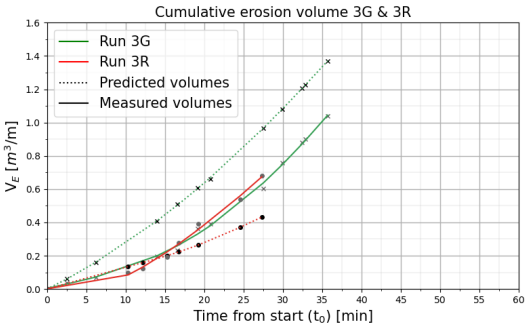

(c) Monday 26-09-2002 (run 3G & 3R)

Figure 40: The measured erosion volumes derived in part I are plotted against the predicted erosion volumes derived in part II.

5.2.5 Main results

The main results of the second part of the data analysis are the individual relationships between the measured erosion volumes and the impact parameter. A linear trend is observed in all runs, and each run has a unique transport coefficient that depends on aspects not explicitly accounted for in the analytical model. In the third part of the data analysis, it is investigated whether this coefficient is dependent on the median grain size.

Container	D50 [mm]	Cs [-]	σ [-]	Pearson's value [-]
1G	0.21	$8.30 \cdot 10^{-4}$	0.026	$1.7 \cdot 10^{-6}$
1R	0.27	$2.58 \cdot 10^{-4}$	0.030	$2.2 \cdot 10^{-3}$
2G	0.24	$4.38 \cdot 10^{-4}$	0.026	$4.80 \cdot 10^{-3}$
3G	0.31	$2.05 \cdot 10^{-4}$	0.040	$7.9 \cdot 10^{-4}$
3R	0.27	$3.63 \cdot 10^{-4}$	0.041	$120 \cdot 10^{-3}$

Table 7: Overview of the results of 'Part II data analysis: Wave impact theory'.

5.3 Part III data analysis: The effect of sediment grain size

In this section it is investigated whether the results of part I and II show an effect of utilizing different grain sizes. The two parts are investigated individually, beginning with analyzing the results of cumulative erosion volumes per day (Part I) and followed by analyzing the results of the analytical model based on wave impact theory (Part II).

5.3.1 Cumulative volumes

The results obtained from the cumulative erosion volumes per day show that, under nearly identical hydrodynamic conditions, dunes constructed from coarser grains exhibit smaller total erosion volumes than dunes constructed from finer grains (Figure 36). The dunes inside the green container for run 1G and 2G are constructed using smaller grains, respectively 0.21 mm and 0.24 mm. The reference dunes, 1R, 2R and 3R are composed of a medium grain size of 0.27 mm and the dune in run 3G is constructed from coarser material (0.31 mm). However, it is important to note that the comparison between erosion volumes per day should be interpreted carefully, as the hydrodynamic conditions varied to some extent each day (Figure 11). The run that started later (t_0) experienced slightly rougher conditions compared to the run that started earlier.

The results also demonstrate that the reduction in erosion volume is larger when increasing the median grain size from the lower range (0.21 mm) to the medium range (0.27) compared to the reduction when the median grain size increases from the medium range to the larger range (0.31 mm). This result suggest a convergence of the reduction in erosion volume within the used sediment range.

5.3.2 Wave impact theory

The transport coefficient (C_s) takes into account physical quantities that are not explicitly considered in Larson's analytical model, one of these dependent quantities is the effect of sediment grain size. To investigate this dependency, the transport coefficient is plotted against the median grain size of the dunes.

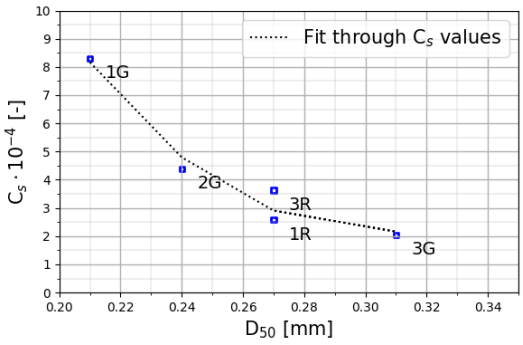

Figure 41: Transport coefficient C_s as a function of grain size for all runs.

It is obtained that transport coefficient decreases with an increase in grain size, suggesting that larger grain sizes lead to smaller erosion volumes. The reduction of the coefficient is non linear and follows a monotone trend. The relationship indicates that increasing grain sizes in the smaller range (0.21 to 0.27 mm) lead to a larger reduction of the transport coefficient than when grain sizes are increased to the larger range (0.27 to 0.31 mm). The results indicate that there is a converging trend for the transport coefficient as the grain size increases.

A decrease in the transport coefficient does not necessarily result in a corresponding decrease in erosion volume. The transport coefficient is also related to other involved parameters in the analytical model and to quantities that are not explicitly considered in this relation (Equation 7). Therefore, reducing the coefficient by a factor of almost 4 (difference between run 1G and 3G) does not imply that the erosion volume will decrease by the same factor (Figure 40).

6 Discussion

The main aspects of this study are briefly summarized:

1. Large scale manipulative field experiments were prepared and conducted at the Sand Engine, where two open shipping containers were placed in the intertidal zone and acted as coastal wave flumes.
2. Information about erosion volumes, dune profile development, and incident hydrodynamic conditions was gained from the gathered data.
3. The analytical model of Larson et al. (2004) based on wave impact theory was used to compare incident hydrodynamic conditions to measured erosion volumes to eliminate daily variable conditions.
4. The relative importance of sediment grain size on dune erosion is captured by comparing daily results of rather identical conditions and by comparing the solutions of the analytical model.

The uncertainties and limitations that arose for the experimental setup, the determination of erosion volumes, the wave impact theory and the effect of sediment grain size will be discussed.

6.1 Lessons learned of experimental setup

6.1.1 Hydrodynamics

Visual observations suggest that run-up, saturation, wave exposure and profile shape were the main processes that triggered dune erosion (Chapter 5.1.1). These parameters are typical processes that trigger dune erosion (Chapter 2.2.3). While manipulative field experiments can better replicate natural conditions than laboratory experiments, they still have physical limitations, particularly in terms of the ability to control the conditions and their magnitude. It is uncertain whether the test conditions can accurately replicate storm conditions, since the containers were placed in the intertidal zone and thereby forcing dune erosion through run-up. During storms more bore impact and steeper waves could be expected.

The container opening and walls may affect the incoming hydraulic conditions, and construction activities around the container could affect the initial bathymetry. Similar experiments, conducted by Scheijmans (2021), revealed that such influences were not measured. However some influences of the container were visible during the experiments of this study. Wave reflection was observed from the container walls, this was mainly observed for smaller waves with a low incoming velocity. For higher waves with a higher velocity, it seemed that the incoming wave power overruled the reflection. Additionally, at both sides of the container opening, scour holes became visible with falling tide, the effect of these scour holes on the solution is not known but is expected to be low inside the containers.

The artificial dunes inside the containers were constructed on top of the container floor, the container floor is impermeable and hinders seepage of rising groundwater flow. This ground water flow increases the saturation of the lower part of the dune, which may have two potential effects. Firstly, it can trigger slump events at an earlier stage due to the increased weight of the dune volume and bigger shear volumes could slump as the shear plane often appears at the boundary between wet and dry sediment. Secondly, groundwater flow could enhance cohesion of the dune face, leading to steeper profiles that exceed the angle of repose of dry sand (45 °) (Palmsten and Holman, 2012; van Wiechen et al., 2023). Those potential effects are expected to be small, since only the lower part of the dune face will experience ground water flow.

6.1.2 Geotechnical aspects

Sediment is collected from nearby locations at the beach to construct the artificial dunes inside the containers (Figure 15). Since sediment was collected locally, the resulting samples consist of a variety of grain sizes rather than a narrow distribution. This study examines the median grain size (D_{50}) of the sediment samples collected. It does not analyze the variability in grain size distributions or the extent to which the distribution width affects the sediment response. Additionally, some samples had a higher concentration of shells than expected in natural dunes. The influence of the sediment grain size distribution and shell content on dune erosion is unknown and may be relevant.

Sediment from the sample locations was deposited inside the containers and a dune was shaped and stamped to compact the sediment volume. The level of attention given to compaction varies per day, with slight greater care being taken on Monday (3G and 3R) compared to Saturday and Sunday (1G, 1R, 2G and 2R). The compactness of the dunes is not measured. It is possible that a lower level of compactness may increase erosion rates as sediment is more easily picked up and transported by the waves and currents. The impact of potential variations in dune compactness is unknown, but it is expected to be low between the different days due to the limited preparation time to establish compaction. However, natural dunes are likely to experience more compaction than the artificial dunes used in this study because they have been present for a longer time and have had more time to settle and become denser.

6.2 Quantification of erosion volumes

In this study, the definition of erosion volumes assumes that erosion events are independent events and are not influenced by previous slumps. Erosion volumes are quantified by comparing the profile just after one slump event to the profile just after a subsequent slump event. This approach was chosen because it enables analyses of the involved processes between events and it captures the time elapsed before a new event is initiated. However, erosion events may not be independent as previous events could affect the magnitude of subsequent events and the time interval between events. The negative feedback mechanism between hydrodynamics and morphodynamics is an example where this dependence could be obtained. This negative feedback mechanism refers to the process in which the accumulation of eroded sediment reinforces the front slope and reduces wave impact, resulting in a temporally more dissipative profile. The impact of this potential dependence is yet unknown. However, the gradient of sediment transport could be an important factor in determining the extent of this dependence. If this transport gradient is rather high, as in this study, sediment can be washed away more quickly, reducing the potential dependence and therefore having a smaller effect on subsequent erosion events. If this transport gradient is quite low, the influence of previous erosion events on subsequent events may be greater.

6.3 Evaluating wave impact theory

In this study, the analytical model of Larson et al. (2004) based on wave impact theory has been utilized with a different interpretation than its original application. The primary difference between the initial method and the method used in this study is the considered time interval. Larson utilizes his method to predict total erosion volumes over the duration of his experiments, which ranged from 30 minutes to 24 hours. This study employs the analytical model to predict erosion volumes within intermediate time intervals during the experiments, ranging from 10 seconds to 10 minutes. This approach investigates if there is also a relation between inter-mediate erosion events and hydrodynamic forcing. This way, less data is required and an attempt is made to get more insight in the processes involved for subsequent events.

Using varying intermediate event timescales rather than the entire experimental period creates a strong dependence of the solution on the magnitude of the intermediate event timescale (Chapter 5.2.3). On the one hand, it should be long enough to capture specific processes which influence the eroded volume. On the other hand, the timescale should be restricted with a maximum time interval, as a longer time scale introduces more uncertainty in the model. This is because the assumption of a constant position of the dune toe over an extended period becomes questionable, and the magnitude of the number of incoming waves may overshadow the influence of other parameters in the equation. Furthermore, some parameters are averaged over the varying timescale. Longer variable timescales may render different averaging of events than shorter timescales, this may lead to the averaging out of significant effects.

The model quantifies hydrodynamic forcing as a measure of run-up height and the amount of wave exposure. The model does not account for several physical quantities that are also known to affect dune erosion. Especially the influence of geotechnical properties of the dune and long waves, such as infragravity waves are not explicitly taken into account in the model (Erikson et al., 2007; van Gent et al., 2008). The model does not specifically account for important geotechnical properties such as sediment grain size, profile shape, and compactness of the dune. These effects are incorporated in the transport

gradient (C_s). Additionally, long waves cause a temporal rise in water level, which results in shorter waves grouping on the crest of these long waves, allowing them to reach further onshore and potentially leading to increased wave impact. The omission of these physical quantities in the model may be a reason for the limited ability to accurately predict dune erosion and potentially leads to the observed scatter in the relationships (40).

The run-up is predicted by a quantification of offshore conditions (Chapter 5.2.1). The calibration factor (C_L) is dependent on beach characteristics and fits the measured to the calculated run-up. Marked scatter was observed around the derived relation for predicting the run-up. A reason for this could be the less controlled field conditions and potential measuring errors. These errors could arise from difficulties in accurately determining the mean water level and excluding wave setup and swash from the measurements. Selecting a constant reference point could potentially reduce the scatter.

The model solutions showed significant variation in the transport coefficient (C_s) across all runs, ranging from $8.30 \cdot 10^{-4}$ to $2.05 \cdot 10^{-4}$. This order of magnitude corresponds to the values found by Larson et al. (2004) for the datasets of Birkemeier et al. (1988). These datasets consisted of field experiments conducted under storm conditions with a sinusoidal astronomic tide. The values obtained in this study are slightly higher than those found by Larson et al. (2004) for the datasets of Birkemeier et al. (1988). Possible explanations for these lower coefficients of the Birkemeier et al. datasets are the higher median grain size at this site, and the application of a sinusoidal run-up variation in time, which can overestimate the run-up values and results in higher impact parameters and a lower transport coefficient.

6.4 Capture the effect of sediment grain size

In order to compare cumulative erosion volumes per day, both containers should experience identical conditions, which can be achieved by measuring at comparable time intervals when the hydrodynamic forcing is of equal magnitude and by building similar dunes. Slight differences in conditions are obtained in the hydrodynamic forcing (Figure 11) and the elevation of the dune toes (Figure 34). Erosion volumes may be affected by these differences, and cannot solely be attributed to the effect of grain size. However the effect of these differences is expected to be low and the substantial differences in cumulative erosion volumes observed on Saturday (run 1G and 1R) and Sunday (run 2G and 2R) are expected to be primarily due to the use of different grain sizes.

The results of this study are consistent with the findings of previous studies by Van de Graaff (1977) and Vellinga (1986), which indicated that coarser sediment lead to steeper slopes and reduces erosion volume. Overton et al. (1994) found opposing results, which indicated that finer grains lead to smaller erosion volumes. This contradicting result could be explained by the fact that this study focused on the effect of individual bores and therefore, considers smaller time periods. Larson et al. (2004) also found opposite results, even though his analysis was based on longer surge duration's. Although the reason for these deviating results is unclear, two facts suggest that the findings of Van de Graaff (1977), Vellinga (1986), and Overton et al. (1994) should be given more consideration. Firstly, investigating the effect of grain size was not the primary objective of the study of Larson et al. (2004). Secondly, he compared results from different datasets with varying conditions and fitted a trend across them. However, this trend exhibited significant scatter and was drawn across the tipping point between datasets.

7 Conclusion

In this study, the effect of grain size on dune erosion within the collision regime was investigated through conducting manipulative fieldwork in open shipping containers. Inside both containers, artificial dunes were built with median grain sizes ranging from 0.21 to 0.31 mm, and were exposed to wave attack during high water. Video observations were used to capture dune development and offshore conditions were measured to relate incident hydrodynamic conditions to measured erosion volumes in time.

7.1 Effect of sediment grain size on dune erosion

The results of the cumulative erosion volumes per day indicate that for rather identical hydrodynamic conditions dunes composed of coarser grains have smaller total erosion volumes than dunes composed of finer grains (Figure 36). Wave impact theory (Larson et al., 2004) was used to isolate the relative importance of sediment grain size on dune erosion. The effect of grain size is incorporated in the transport gradient (C_s). A non-linear monotone dependence is found between the transport gradient and median grain size (Figure 41). This implies that a higher impact is required to erode the same volume for dunes composed of coarse sediment than for dunes composed of fine sediment. Earlier studies by Van de Graaff (1977) and Vellinga (1986) are consistent with this result, whereas the findings by Overton et al. (1994) differ. This discrepancy can be attributed to the fact that the latter study only focuses on the impact of an individual bore. The effect of grain size on dune erosion could be attributed to the fact that drag forces and fall velocities increase as grain size increases, making them less prone to be transported by waves and currents (Overton et al., 1994).

A clear difference between erosion is obtained comparing grain sizes ranging from 0.21 to 0.31, implying a significant effect of grain size on dune erosion for dunes composed of grains within this range. Both the results of cumulative erosion volumes and wave impact theory indicate that an increase in grain size to the higher range (0.31 mm) leads to a smaller reduction in erosion volume compared to an increase in erosion volume when the grain size is decreased to the lower range (0.21 mm). The trend observed for the dependence of the transport gradient on median grain size suggests convergence for larger grain sizes, which may imply that increasing the grain size beyond a certain point has a negligible effect on erosion volumes (Figure 41). Additionally, the formation of steeper slopes is observed for dunes composed of coarser grains.

7.2 Wave impact theory

The analytical model of Larson et al. (2004) based on wave impact theory finds a linear trend between erosion volumes and the impact of individual swash waves on the dune face. Individual swash waves are quantified as a measure of run-up height and the number of incoming waves. With this model the effect of variable daily conditions is eliminated and erosion patterns can be compared. The model cannot be used as an accurate predicting model for erosion volumes as it tends to overestimate measured erosion volumes.

The model is based on a dynamic relation, which means that an increase in a parameter does not necessarily result in a proportional increase in the solution. The transport coefficient's dependence on grain size cannot be directly related to the erosion volume, as this parameter is also associated with the evolution of the dune toe, the timescale of events and other quantities that are not explicitly included (Equation 7).

The considered time interval used in this study differs from the original approach. This study predicts erosion volumes over varying timescales, which are defined as the timescales between subsequent events, rather than entire surge periods. With this new approach less data is required and a better understanding of involved processes of subsequent dune erosion events can be obtained. The quantification of wave impact as a combination of measured run-up and the number of incoming waves confirms the concept of wave impact theory, which implies a linear relationship between swash force and erosion volume. A stronger trend is obtained between erosion volumes and the number of incoming waves, than for the dependency of erosion volume and run-up height. The transport gradient (C_s) attained similar values as found by Larson et al. (2004) for the storm datasets of Birkemeier et al. (1988). However, the

obtained values are slightly higher and marked scatter is obtained. Different explanations are possible for the higher transport gradient, for example, the dependency of the transport gradient on physical quantities that are not explicitly included in the model and the smaller median grain size measured at the field site compared to the site of Birkemeier et al. (1988).

Other theories, such as the wave impact model of Fisher et al. (1986) and the predition model of Palmsten and Holman (2011), are not investigated in this study, as the experimental setup was not sufficient in testing these models. In order to apply these models for the approach of this study, more elaborated research should be conducted in order to prepare an adequately setup. To test the model proposed by Fisher et al. (1986), it is necessary to measure bore heights and velocities. To test the model proposed by Palmsten and Holman (2011), dune saturation levels need to be measurable.

7.3 Capture erosion volumes with video observations

Dune profile segments were extracted from images captured by cameras, which provided a safe and effective means of collecting a large amount of data. The camera was positioned in a dry location, reducing the risk of breakdown and allowing easy access during the experiments. Additionally, the high frequency of data collection enables visual observations and therefore a more comprehensive understanding of the underlying processes. This approach offers a low-cost and user-friendly method for capturing dune profile development that is not labor-intensive.

Data analysis reveals that the dune toe linearly regresses over time in both the cross-shore and vertical directions (Figure 33a). The regression in the vertical direction correlates with the rising mean water level (Figure 33b).

Figure 42: Execution of experiments on Monday 26-09-2022 (run 3R).

8 Recommendations

8.1 Further research

It is recommended to perform further research by validating the results through performing laboratory experiments and by modelling the results in dune erosion models. Laboratory experiments should be performed to validate the findings on sediment grain size. These experiments allow for more specific research to be conducted without the without the interference of other field processes. Conducting laboratory experiments makes it possible to investigate the accuracy of the observed effect of sediment grain size and whether other parameters had a greater influence on the solution than anticipated in this study. In addition, laboratory experiments provide the opportunity to test with specific, selected sediment samples and therefore provides the opportunity to study sediment with either a narrow or wide grain size distribution. It is also recommended to model similar conditions in dune erosion models such as XBeach to assess the discrepancies between model predictions and field measurement. This way, the accuracy of models in predicting dune erosion is investigated and it is evaluated whether the effect of varying sediment grain sizes is incorporated accurately.

It is also recommended to conduct further research in better understanding the underlying mechanisms that drive slump events and their impact on dune erosion. This would help identify potential factors that have not yet been included in existing models in order to better predict erosion volumes and the time interval between erosion events. Examples of potential effects are the influences of profile attenuation over time and the negative feedback mechanism between hydrodynamics and morphodynamics, where the dune face is temporally strengthened by accretion of an eroded slump. A potential approach is to redefine erosion volumes by differentiating between primary and secondary erosion. Primary erosion can be defined as the erosion of the dune face, while secondary erosion refers to erosion of earlier deposited primary erosion on the foreshore which washes away gradually (Figure 43). This approach separates the slumping event itself from the volume that represents the negative feedback mechanism, which includes the time expired since the prior slump was washed away and the slope steepens. With the new approach of distinguishing between primary and secondary erosion, it becomes possible to conduct new analyses. For example, one could investigate whether erosion events are dependent and to what extent a previous slump influences a subsequent event. Additionally, it can be investigated whether the time intervals between events vary for different grain sizes.

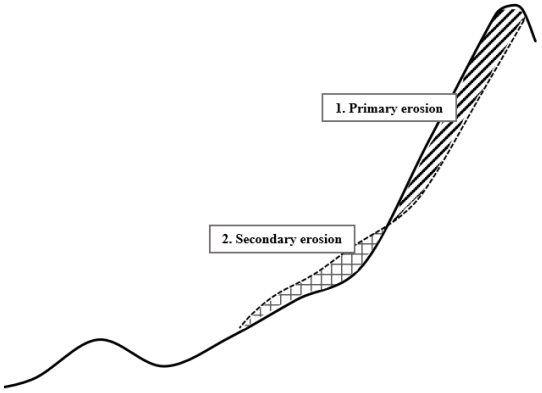

Figure 43: Redefinition erosion volumes between the initial profile (blck line) and the profile after an event (dotted line). Separating primary and secondary erosion.

Furthermore, it is recommended to use the method of manipulative field experiments for future studies as this methods enables large-scale experiments where no wave simulators are used. This method can provide valuable insights into the effects of specific processes on dune erosion. It can again be used to validate the findings related to the influence of grain size, but also allows for the investigation of other parameters, such as the impact of dune vegetation on erosion. For instance, small dunes that are prone to flooding in the upcoming storm season can be excavated and placed in the container to simulate a vegetated dune.

8.2 Implications for engineering purpose

It is recommended that engineers consider the finding of this study that dune erosion tends to increase non-linearly for smaller grain sizes, particularly when the grain sizes are in the lower range of this study (0.21 to 0.27 mm). Grain sizes beyond the range of 0.21 to 0.31 mm were not investigated in this research. Since engineers may not always have a choice of materials to work with, they should be aware of the findings of this study and can implement this awareness in their work by the use of a safety factor. For example, if models are used to assess a coastal area and the model weakly accounts for the influence of varying grain sizes on dune erosion, a safety factor can be used to mitigate potential risks. However, it is important not to directly implement the found dependency of the transport coefficient and the median grain size, as this difference in transport coefficient does not explicitly result in a proportional effect on erosion volume.

Furthermore, it should be taken into account that this study only focuses on sediment grain size, but the response of dunes depends on a combination of characteristics. The impact of other dune characteristics and their interaction with grain size is not considered. For instance, increasing grain size could have an effect on the growth of dune vegetation and therefor not necessarily results in a positive impact in reducing dune erosion rates.

8.3 Improvements experimental setup

The force of the sea should not be underestimated when performing manipulative field experiments and safety of participants and the setup should be ensured at all times. If rough conditions are expected, with waves higher than 1 meters in front of the container, it is advisable to position the container behind the high water line and postpone testing. This is because there is a potential risk that the container will collapse and starts drifting. This threat can be mitigated by reinforcing the container with long-shore beams, which reduces rotational forcing.

Some changes to the instruments are recommended to further optimize the setup. The GoPro cameras were directed towards a black and white checkerboard grid. This choice of colors was not optimal for distinguishing between the dune profile, the grid and incoming swash. This is because the color contrast between these aspects was not significant enough. It is recommended to use a grid with a significant color deviation from the other colors in the image. Four reference points should be present to enable the conversion of measurements relative to NAP. Additionally, it is advised to adjust the sampling frequency of the GoPro cameras to 8 Hz. This will make it possible to differentiate between incoming and outgoing waves, thereby enabling automatic determination of bore or run-up heights. Measurements of sediment concentration could be included in future setups to find a relation between sediment transport and wave impact. This eliminates the subjectivity of determining erosion events.

It is recommended to make some changes to the experimental setup as well. A potential mitigation against neglecting groundwater flow is to create a permeable under layer by drilling holes in the container floor. This allows water to infiltrate horizontally. A drawback of this approach is that it can reduce the strength of the container. To prolong the experimental time, it is recommended to increase the width of the dune crest of the artificial dune. In this study the containers had to be emptied between runs as different sediment grain sizes were used for testing. If this is not the case and this time limitation expires, it is recommended to increase the total volume of the dunes.

References

Bertin, X., de Bakker, A., van Dongeren, A. R., Coco, G., Andr'e, G., Ardhuin, F., Bonneton, P., Bouchette, F., Castelle, B., Crawford, W. C., Davidson, M., Deen, M., Dodet, G., Gu'erin, T., Inch, K., Leckler, F., McCall, R., Muller, H., Olabarrieta, M., ... Tissier, M. (2018). Infragravity waves: From driving mechanisms to impacts. *Earth-Science Reviews*, *177*, 774–799. https://doi.org/10.1016/j.earscirev.2018.01.002

Birkemeier, W. A., Savage, R. J., & Leffler, M. W. (1988). A collection of storm erosion field data. *Miscellaneous Paper*, (CERC-88-9).

Bonte, Y., & Levoy, F. (2015). Field experiments of beach scarp erosion during oblique wave, stormy conditions (Normandy, France). *Geomorphology*, *236*, 132–147. https://doi.org/10.1016/j.geomorph.2015.02.014

Bosboom, J., & Stive, M. M. J. (2021). *Coastal dynamics 1*.

Brandenburg, P. (2010). Scale dependency of dune erosion models performance assessment of the DUROS and XBeach model for various experiment scales. *Msc Thesis*.

De zandmotor. (2021). Provincie Zuid-Holland. Retrieved September 24, 2022, from https://dezandmotor.nl/

den Bieman, J. (2016). Hydraulische belastingen 2017 voor duinwaterkeringen.

den Heijer, C., Baart, F., & van Koningsveld, M. (2012). Assessment of dune failure along the Dutch coast using a fully probabilistic approach. *Geomorphology*, *143-144*, 95–103. https://doi.org/10.1016/j.geomorph.2011.09.010

de Vries S. (2021). Lecture notes: Lecture 4: Dune erosion and XBeach.

Erikson, L. H., Larson, M., & Hanson, H. (2007). Laboratory investigation of beach scarp and dune recession due to notching and subsequent failure. *Marine Geology*, *245*, 1–19. https://doi.org/10.1016/j.margeo.2007.04.006

Feagin, R. (2022). Private communication.

Feagin, R. A., Figlus, J., C.Zinnert, J., Sigren, J., Mart´ınez, M. L., Silva, R., Smith, W., Cox, D., Young, D. R., & Carter, G. (2015). Going with the flow or against the grain? the promise of vegetation for protecting beaches, dunes, and barrier islands from erosion. *Frontiers in Ecology and the environment*, (13(4)), 203–210. https://doi.org/10.1890/140218

Figlus, J., Sigren, J. M., Armitage, A. R., & Tyler, R. C. (2014). Erosion of vegetated coastal dunes. *Coastal Engineering Proceedings*, (34), 20. https://doi.org/10.9753/icce.v34.sediment.20

Fisher, J. S., Overton, M. F., & Chisholm, T. (1986). Field measurements of dune erosion. *Coastal Engineering*, *2*, 1107–1115. https://doi.org/10.1061/9780872626003.082

Guza, R., Thornton, E., & Holman, R. (1985). Swash on steep and shallow beaches, 708–723. https://doi.org/10.1061/9780872624382.049

Hapke, C. J., Reid, D., Richmond, B. M., Ruggiero, P., List, J. H., Hansen, M. E., & Farrar, D. (2010). Geomorphic and coastal process responses to sea-level rise in Southern California. *Oceanography*, *23*(4), 118–129.

Heineke, E. (2022). The potential of dune vegetation during storm conditions. *Msc Thesis*.

Holthuijsen, L. H. (2007). *Waves in oceanic and coastal waters*. Cambridge University Press.

Hunt, I. (1959). Design ofseawalls and breakwaters. *Journal ofthe Waterways and Harbors Division*, *85*(123-152). https://doi.org/10.1061/JWHEAU.0000129

Ionescu, A., de Schipper, M., & Storms, J. (2020). *Large observed grain size variability around the sand engine*. Retrieved January 9, 2023, from https://www.nck-web.org/boa-2020/373-large-observed-grain-size-variability-around-the-sand-engine

Kateman, I. (2007). Wave-impact driven dune face erosion processes. *Msc Thesis*.

Kobayashi, N., Grahler, C., & Do, K. (2013). Effects of woody plants on dune erosion and overwash. *Journal of Waterway, Port, Coastal and Ocean Engineering*, *139*(6), 466–472. https://doi.org/10.1061/(ASCE)WW.1943-5460.0000200

Kriebel, D., & Dean, R. (1993). Convolution method for time-dependent beach profile response. *Journal of Waterway, Port, Coastal, and Ocean Engineering*, *119*(2), 204–226. https://doi.org/10.1061/(ASCE)0733-950X(1993)119:2(204)

Larson, M., Erikson, L., & Hanson, H. (2004). An analytical model to predict dune erosion due to wave impact. *Coastal Engineering*, *51*, 675–696. https://doi.org/10.1016/j.coastaleng.2004.07.003

Martinez, M. L., Silva, R., Mendoza, E., Oderiz, I., & Perez-Maqueo, O. (2016). Coastal dunes and plants: An ecosystem-based alternative to reduce dune face erosion. *Journal of Coastal Research*, *1*(75), 303–307. https://doi.org/10.2112/SI75-061.1

Masselink, G., & Puleo, J. A. (2006). Swash-zone morphodynamics. *Continental Shelf Research*, *26*(5), 661–680. https://doi.org/10.1016/j.csr.2006.01.015

Mendoza, E., Oderiz, I., Martinez, M. L., & Silva, R. (2017). Measurements and modelling of small scale processes of vegetation preventing dune erosion. *Journal of Coastal Research*, *77*, 19–27. https://doi.org/10.2112/SI77-003.1

Overton, M. F., Fisher, J. S., & Young, M. A. (1988). Laboratory investigation of dune erosion. *Journal of Waterway, Port, Coastal, and Ocean Engineering*, *114*(3), 367–373. https://doi.org/10.1061/(ASCE)0733-950X(1988)114:3(367)

Overton, M., Pratikto, W. A., Lu, J. C., & Fisher, J. S. (1994). Laboratory investigation of dune erosion as a function of sand grain size and dune density. *Coastal Engineering*, *23*(1-2), 151–165. https://doi.org/10.1016/0378-3839(94)90020-5

Palmsten, M. L., & Holman, R. A. (2011). Infiltration and instability in dune erosion. *Journal of Geophysical Research: Oceans*, *116*(C10). https://doi.org/10.1029/2011JC007083

Palmsten, M., & Holman, R. A. (2012). Laboratory investigation of dune erosion using stereo video. *Coastal Engineering*, *60*, 123–135. https://doi.org/10.1016/j.coastaleng.2011.09.003

Quataert, E., van Santen, R., McCall, R., van Dongeren, A. R., & Steetzel, H. (2018). Aanloopstudie xbeach wbi.

Roelvink, D., Reniers, A., van Dongeren, A. R., van Thiel de Vries, J. S. M., McCall, R., & Lescinski, J. (2009). Modelling storm impacts on beaches, dunes and barrier islands. *Coastal Engineering*, *56*(11-12), 1133–1152. https://doi.org/10.1016/j.coastaleng.2009.08.006

Roelvink, D., van Dongeren, A. R., McCall, R., Hoonhout, B., van Rooijen, A., van Geer, P., de Vet, L., & Nederhoff, K. (2015). Xbeach manual.

Rueda, F., Gracia, V., Espejo, A., & Sanchez-Garcia, E. (2011). Beach-dune system erosion and accretion patterns on the high-energy Mediterranean coast (SW Spain). *Catena*, *87*(3), 382–391. https://doi.org/10.1016/j.catena.2011.06.003

RWS. (2022). *Waterberichtgeving*. Retrieved September 24, 2022, from https://waterberichtgeving.rws.nl

Sallenger, A. (2000). Storm impact scale for barrier islands. *Journal of Coastal Research*, *16*, 890–895.

Scheijmans, J. (2021). New method to measure dune erosion processes using a mobile, contained environment on a real beach. *Msc Thesis*.

Silva, R., Martinez, M. L., Oderiz, I., Mendoza, E., & Feagin, R. A. (2016). Response of vegetated dune-beach systems to storm conditions. *Coastal Engineering*, *109*, 53–62. https://doi.org/10.1016/j.coastaleng.2015.12.007

Stockdon, H. F., Holman, R. A., Howd, P. A., & Sallenger, A. H. (2006). Empirical parameterization of setup, swash, and runup. *Coastal Engineering*, *53*(7), 573–588. https://doi.org/10.1016/j.coastaleng.2005.12.005

Suanez, S., Cariolet, J., Cancouet, R., Ardhuin, F., & Delacourt, C. (2012). Dune recovery after storm erosion on a high-energy beach: Vougot Beach, Brittany (France). *Geormorphology*, *139-140*, 16–33. https://doi.org/10.1016/j.geomorph.2011.10.014

Van de Graaff, J. (1977). Dune erosion during a storm surge. *Coastal Engineering*, *1*, 99–134. https://doi.org/10.1016/0378-3839(77)90010-2

Van Rijn, L. C. (1984). Sediment transport, part iii: Bed forms and alluvial roughness. *Journal of Hydraulic Engineering*, *110*(12), 1733–1754. https://doi.org/10.1061/(ASCE)0733-9429(1984)110:12(1733)

van Bemmelen, C. W. T., de Schipper, M. A., Darnall, J., & Aarninkhof, S. G. J. (2020). Beach scarp dynamics at nourished beaches. *Coastal Engineering*, *160*, 103725. https://doi.org/10.1016/j.coastaleng.2020.103725

van Gent, M. R. A., van Thiel de Vries, J. S. M., Coeveld, E. M., de Vroeg, J. H., & van de Graaff, J. (2008). Large-scale dune erosion tests to study the influence of wave periods. *Coastal Engineering*, *55*(12), 1041–1051. https://doi.org/https://doi.org/10.1016/j.coastaleng.2008.04.003

van Thiel de Vries, J. S. M., van Dongeren, A. R., McCall, R., & Reniers, A. J. H. M. (2010). The effect of the longshore dimension on dune erosion. *1*, 49. https://doi.org/10.9753/icce.v32.sediment.49

van Thiel de Vries, J. S. M., van Gent, M. R., Walstra, D. J., & Reniers, A. J. H. M. (2008). Analysis of dune erosion processes in large-scale flume experiments. *Coastal Engineering*, *55*(12), 1028–1040. https://doi.org/10.1016/j.coastaleng.2008.04.004

van Wiechen, P. P. J., de Vries, S., Reniers, A. J. H. M., & Aarninkhof, S. G. J. (2023). Dune erosion during storm surges: A review of the observations, physics and modelling of the collision regime. *Submitted toitted to Coastal Engineering.*

Vellinga, P. (1986). *Beach and dune erosion during storm surges* (Doctoral dissertation). Delft University of Technology. https://doi.org/10.1016/0378-3839(82)90007-2

Witteveen & Bos. (2022). *Review of sea defences along the flemish coast.* Retrieved September 24, 2022, from https://www.witteveenbos.com/projects/review-of-sea-defences-along-the-flemish-coast/

A General field conditions

Wave characteristics

The significant wave height and the spectral period are extracted from the wave spectrum and calculated using equation 12 and 13. $T_{m-1.0}$ is calculated with respect to low-order moments. These moments are more sensitive to the low-frequency range of the spectrum and therefore give more weight to low-frequency waves (Holthuijsen, 2007). This consideration was made because van Gent et al. (2008) found that the presence of long waves is a significant contributor to the amount of dune erosion.

$$H_{m0} = 4\sqrt{m_0} \tag{12}$$

$$T_{m-1.0} = m_{-1}/m_0 \tag{13}$$

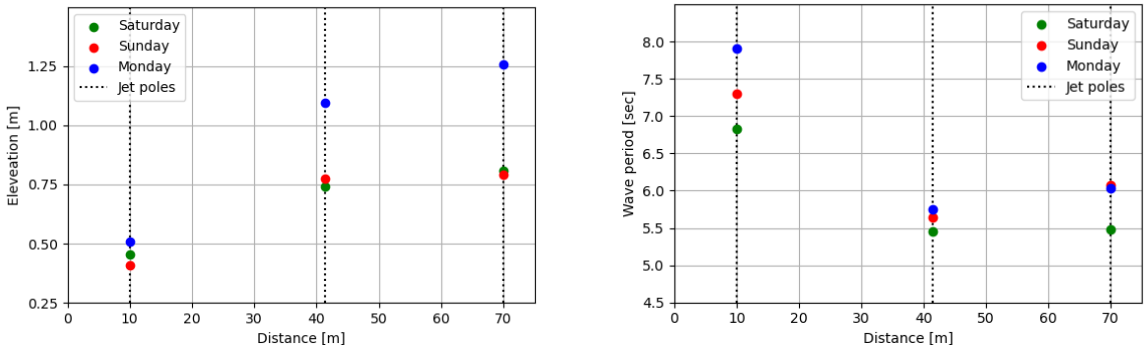

(a) Significant wave height (H_{m_0})

(b) Spectral wave period ($T_{m-1.0}$)

Figure 44: Wave conditions each day 14:30 - 15:00.

Wave energy & propagation

The measured wave conditions from the RBRs are presented in the wave spectra (Figure 45). The wave spectra of the different days are compared for the time period from 14:30 till 15:00 and show the total amount of incoming wave energy. On Monday a much larger amount of incoming energy is measured than on the other days.

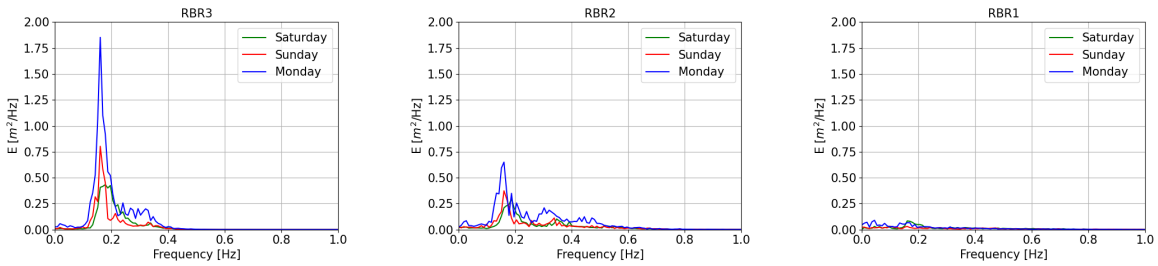

(a) Spectrum RBR3

(b) Spectrum RBR2

(c) Spectrum RBR1

Figure 45: Wave spectra 14:30 - 15:00.

Grain size distribution sediment samples

During the fieldwork, sediment samples were subjected to sieving using a sieving tower. This instrument consists of stacked sieves with varying diameters, which are agitated for 15 minutes. This process allows the sediment to move around and pass through the sieves, with smaller particles passing through finer mesh sieves and larger particles remaining on top of coarser mesh sieves. A cumulative distribution of

sediment grain size is then generated based on weight measurements, enabling the calculation of the d50 value

Sediment is sieved using a sieving tower of stacked sieves with grain size diameters of diameters in millimeters: 0.85, 0.6, 0.425, 0.355, 0.30, 0.25, 0.212, 0.15, 0.125, 0.063. The cumulative percentage of the sieves calculated in order to derive the median grain size (D_{50}). The grain sizes used in the experiment were varied each day, with finer grains (0.21 mm and 0.24 mm) used for runs 1G and 2G, and coarser grains (0.31 mm) used for run 3G. The reference dune in the red container was built using the same sediment (runs 1R, 2R, and 3R), and had a median grain size of 0.27 mm.

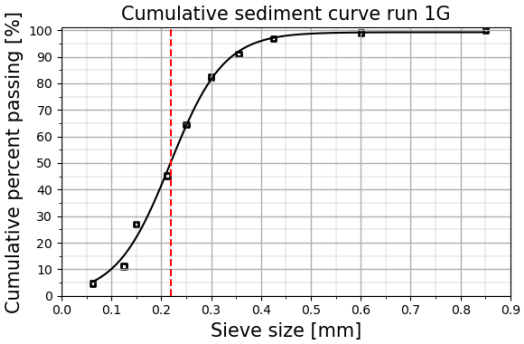

(a) Run 1G

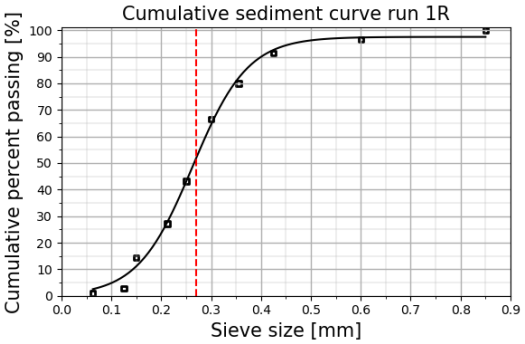

(b) Run 1R

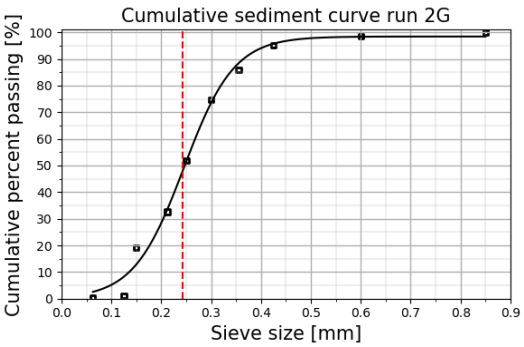

(c) Run 2G

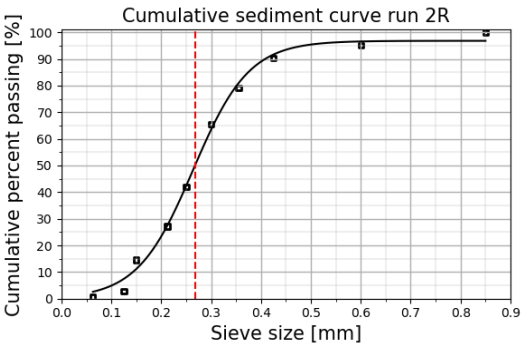

(d) Run 2R

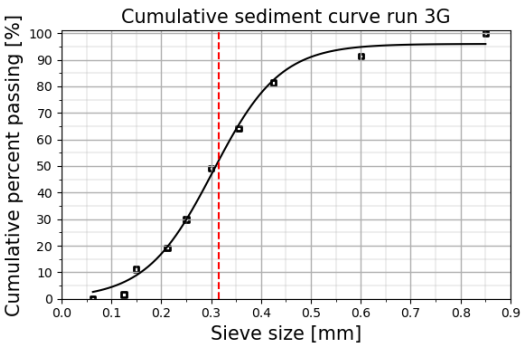

(e) Run 3G

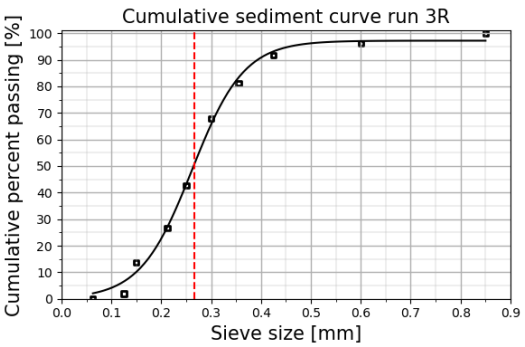

(f) Run 3R

Figure 46: Cumulative sediment sieving curves of the green and red container for all runs on the three experimental days.

Overview hydrodynamics

An overview of the hydrodynamic conditions are given for each day. Since wave characteristics are extracted from the pressure instruments in time intervals of half an hour, the wave heights and spectra are given in time intervals of half an hour for the period of 13:30 till 15:30.

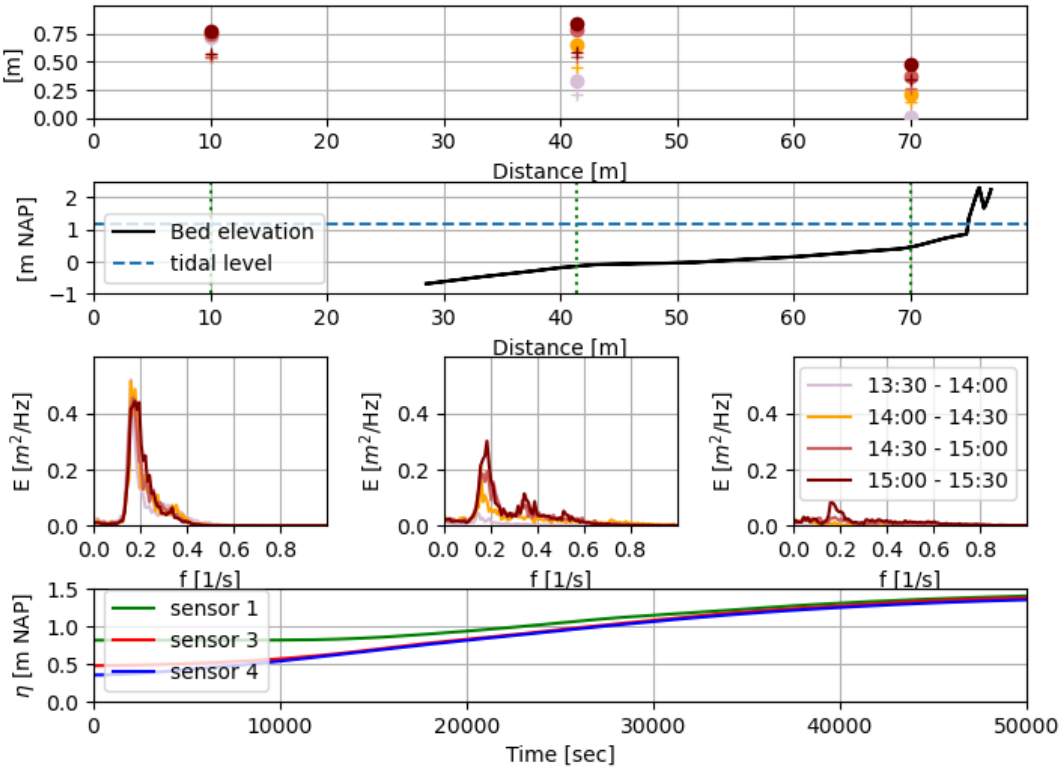

(a) Saturday 24-09-2022

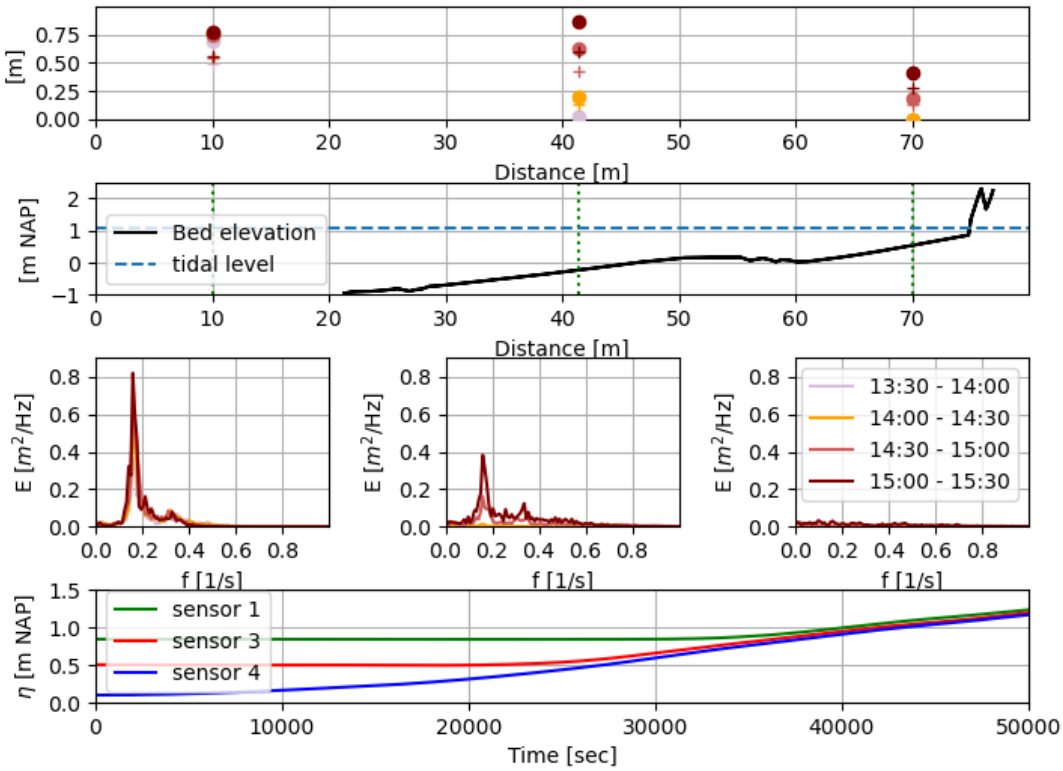

(b) Sunday 25-09-2022

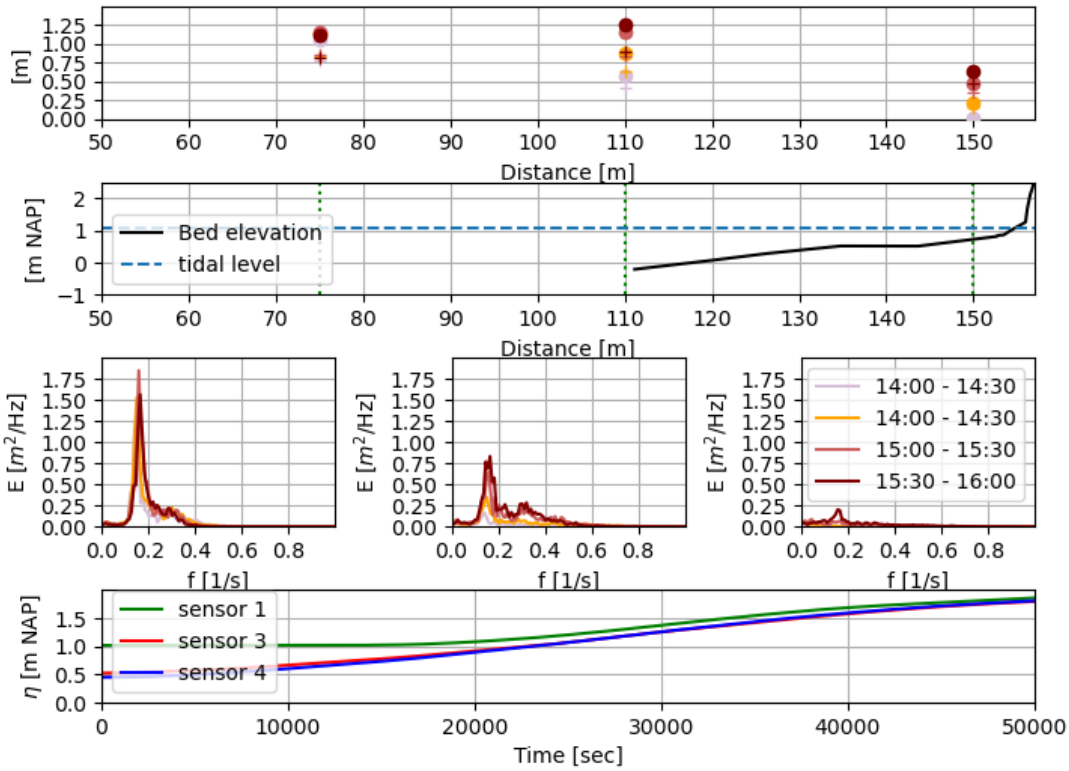

(c) Monday 26-09-2022

Figure 49: Overview of the hydrodynamic conditions for each day. The wave heights are illustrated for the different time intervals (top panel). The bathymetry of the dune (second panel). The wave spectra in station order of offshore, intermediate water depth and in front of the container (third panel). The water level measured at the three sensors (bottom panel).

B Effect of infra-gravity waves

The time period of waves is known to contribute to the amount of dune erosion. According to van Gent et al., infra-gravity waves (waves with periods ranging from 0.033 to 0.33 Hz) have a significant impact on dune erosion. To investigate this effect in this study, the infra-gravity waves are extracted from the total wave signal and plotted over time (Figure 50).

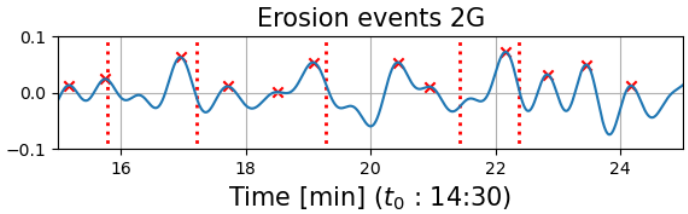

Figure 50: Time segment of run 2G where the infra-gravity wave signal is plotted over time. The red dotted lines represent the time when erosion events occur.

It is investigated whether events occur at the peak of the infra-gravity waves. The events are tallied and grouped into bins to determine the wave segment (peak or crest of the waves) in which the events occur (Figure 51). However, no clear trend is found, and the results rather indicate that slightly more events occur in the trough ($\eta_{IG} < 0$) of the wave signal than in the crest ($\eta_{IG} > 0$). However, no clear conclusion of this effect can be drawn from the results.

In addition, the amount of maxima within each event time period is counted and it is investigated whether the amount of maxima is related to the magnitude of the erosion events (Figure 52). It may be expected that the more infra-gravity waves occur during an event period, the higher the erosion volume. However, no clear trend between the parameters is observed.

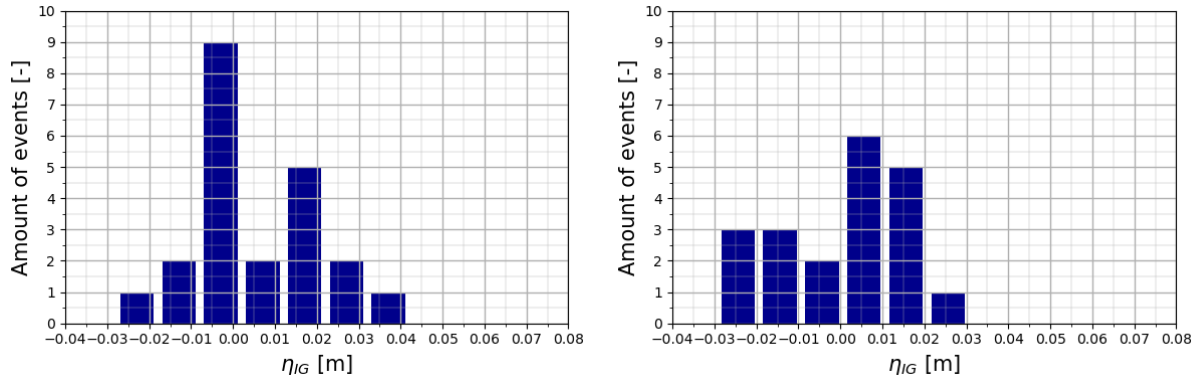

(a) Run 1R

(b) Run 1G

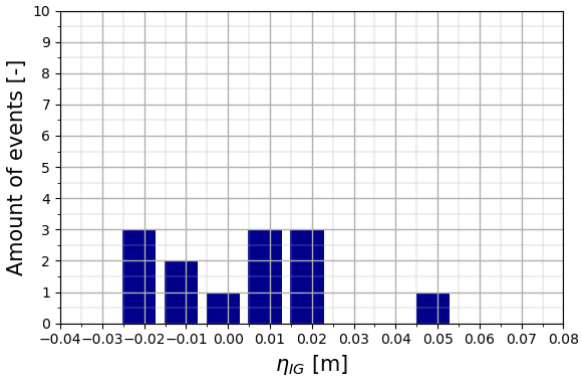

(c) Run 2G

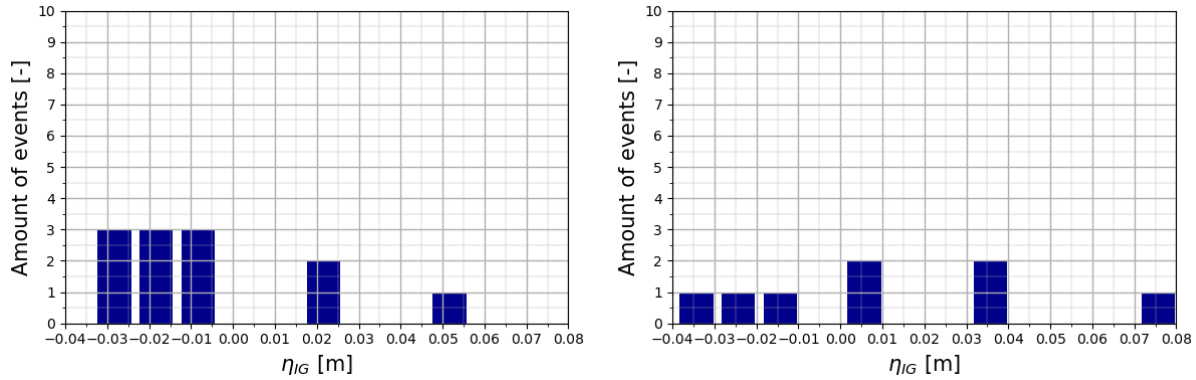

(d) Run 3G

(e) Run 3R

Figure 51: Histograms show the distribution of occurrence events based on the surface elevation level of the infra-gravity wave signal, denoted by η_{IG}.

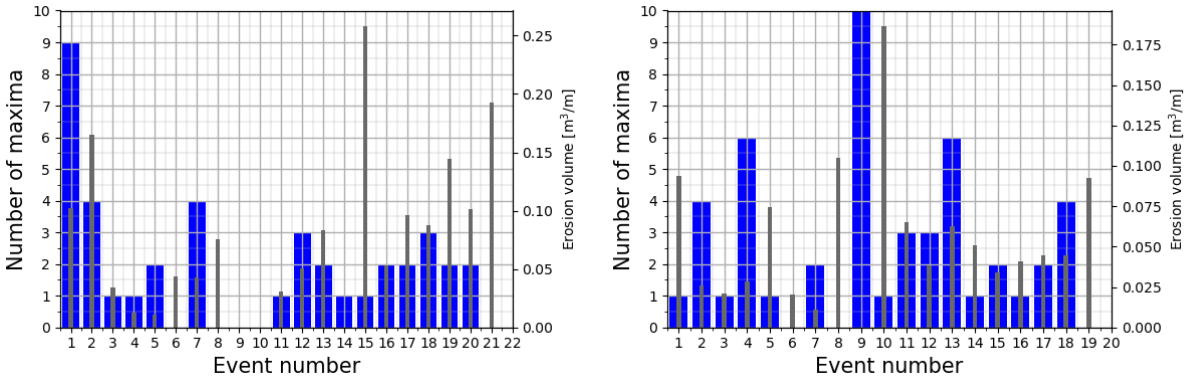

(a) Run 1R

(b) Run 1G

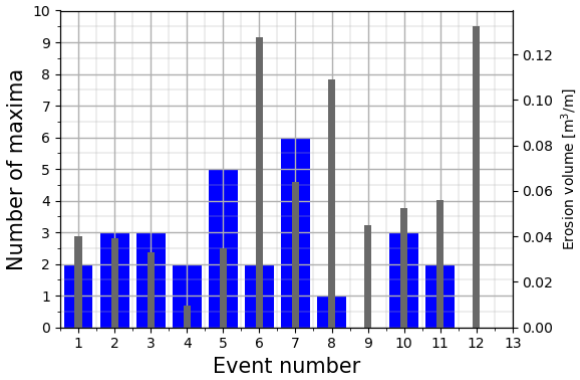

(c) Run 2G

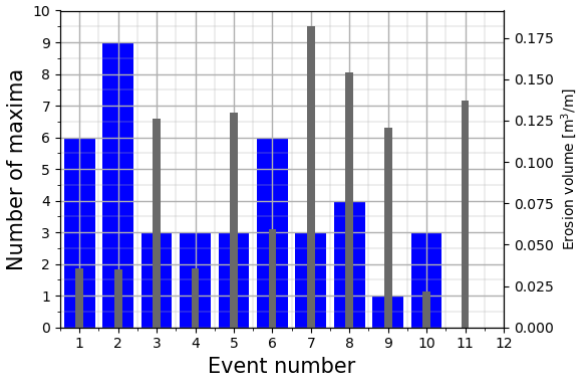

(d) Run 3G

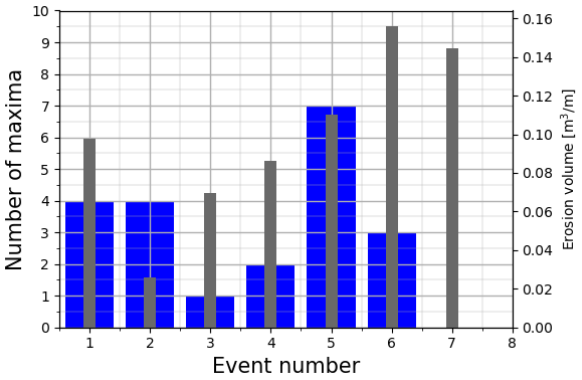

(e) Run 3R

Figure 52: Histograms show the distribution infra-gravity wave maxima that occurred within the time interval of an event. The left axes shows the number of maxima and the right axes shows the amount of erosion volume.

C Wave impact theory according to Fisher et al. (1986)

Wave impact theory

The wave impact theory proposed by Fisher et al. in 1986 relates impact from individual swash bores to erosion volumes. Impacts are described as a change in momentum flux and are related to erosion volumes as a function of frequency and intensity of these impacts. Further research conducted by Overton et al. validated this theory in 1988 and 1994. The main reason why this theory was hard to use for this study, was that it was hard to extract the incoming bore height and velocity from the measurements. First a decomposition of the total signal to an incoming and outgoing signal was required. The applied methodology and initial findings of this theory will be briefly described in this section.

Specific force

The wave impact is quantified as a specific force, which is dependent on the incoming swash forces. These swash forces are determined by the height (h_{swi}) and velocity (u_{swi}) of the incoming bore (Equation 14.

$$SF = \rho\overline{h_{swi}u_{swi}^2} \tag{14}$$

Decomposition wave signal

Since the specific force is calculated for individual waves, a wave-by wave analysis is required. The theory solely focuses on the incoming wave signal and measured hydrodynamic conditions at jet pole 1 and 5 (Figure 17) consists of a combination of incoming and reflective waves, a decomposition of the wave signal is required. Several methods exist to separate incoming from outgoing wave signals. The method of Guza et al. was found to be successful for similar studies of Kateman in 2007. The method to decompose the signal is using collocated velocity and surface elevation measurements. This decomposition method is based on the relation between kinematic relation between discharge and surface elevation.

The kinematic relation uses shallow water theory to separate the incoming and outgoing signal. The discharge is a function of the wave group celerity (c_{group}) and the surface elevation (η).

$$Q_{\text{in}} = c_{group} \cdot \eta_{\text{in}} \quad \text{and} \quad Q_{\text{out}} = \sqrt{gh_0} \cdot \eta_{\text{out}} \tag{15}$$

The assumption above is implemented in a formulation of the incoming and outgoing surface elevation. h_0 represents the still water level and g the gravitational acceleration.

$$\eta_{in} = \frac{\sqrt{gh_0} \cdot \eta + Q_{in}}{c_{group} + \sqrt{gh_0}} \quad \text{and} \quad \eta_{in} = \frac{c_{group} \cdot \eta - Q_{out}}{c_{group} + \sqrt{gh_0}} \tag{16}$$

Assuming that the total velocity signal consist of $u = u_{in} + u_{out}$ and the total surface elevation signal consist of $\eta = \eta_{in} + \eta_{out}$ and that the group velocity is equal to the wave celerity $c_{group} = \sqrt{gh_0}$ the equation is reduced to:

$$\eta_{\text{in}} = \frac{\eta + u\sqrt{\frac{h_0}{g}}}{2} \quad \text{and} \quad \eta_{\text{out}} = \frac{\eta - u\sqrt{\frac{h_0}{g}}}{2} \tag{17}$$

$$u_{in} = \eta_{in}\sqrt{\frac{g}{h_0}} \quad \text{and} \quad u_{\text{out}} = \eta_{\text{out}}\sqrt{\frac{g}{h_0}} \tag{18}$$

Application of this theory resulted in decomposed signals (Figure 53). This theory was applied by Kateman to decompose the wave signal in flume experiments. However, remarkable is that when this formula is used for field measurements the formula seems not to work as when the still water level (h_0) rises, the velocity decreases. In reality it is expected that with rising water levels, velocities increase since more wave energy reaches the measurement location. Therefore it seems that this theory is not applicable for this study.

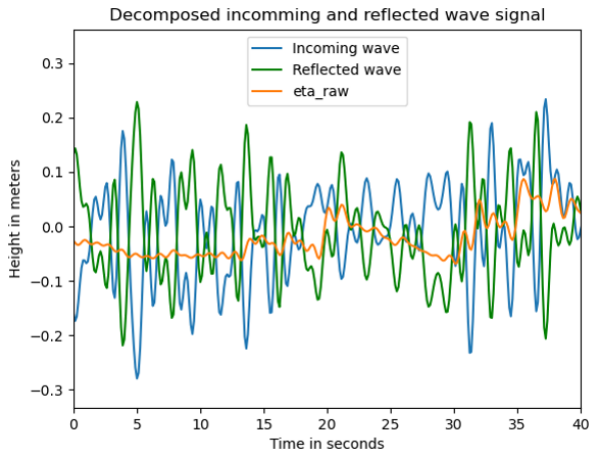

Figure 53: Segment of a decomposed wave signal. The raw signal is indicated by the orange line. The blue line represents the incoming wave signal and the green line the reflected waves. Since the application of the described decomposition method is questionable for this study, it is not certain if these signals are representative.

Application theory in this study

Despite multiple attempts to apply the wave impact theory to field data, it was found that the available data and set-up were inadequate for testing this theory. The primary challenge was to accurately determine the height and velocity of incoming swash bores. Measurements taken at jet pole 1, located 1 meter outside the container, were insufficient in representing the impact on the artificial dune, and also suffered from significant noise due to the time required for instruments to become fully submerged. In addition, it was complicated to separate the incoming and outgoing waves measured by RBR1, which required a challenging process of analyzing the wave signals. Accounting for the upcoming tide made this process even more complex.

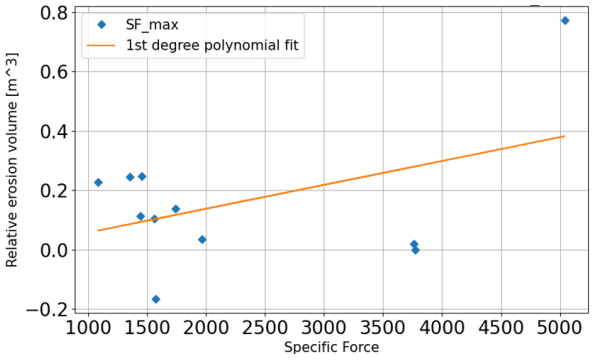

Figure 54: The measured erosion volumes are plotted against the calculated specific force. No clear trend and large scatter is obtained.

D Selected events for run 1G and 3G

To give a better perspective on the evolution of dune erosion during the experiment, selected events for two runs are visualized.

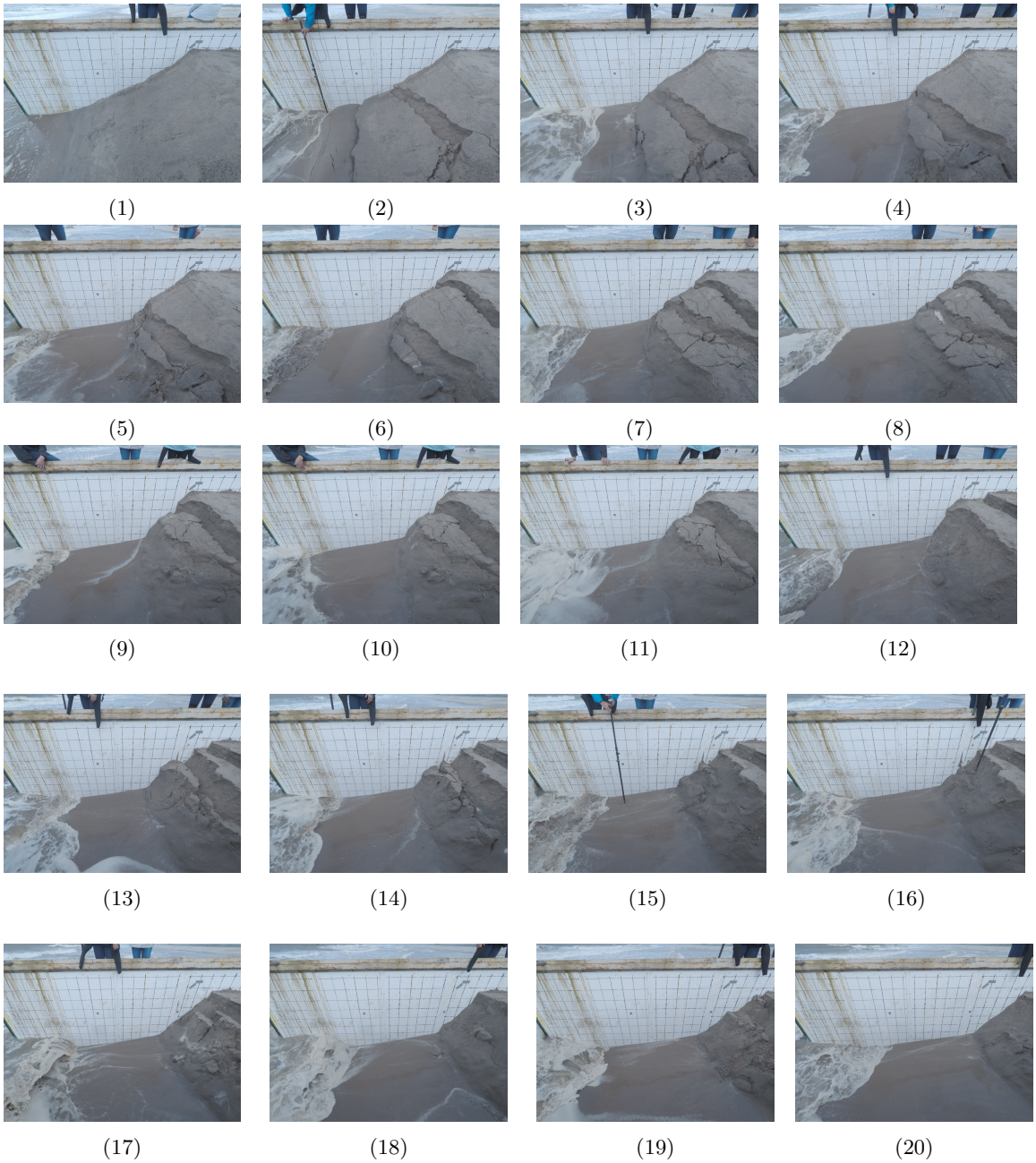

Figure 55: Erosion events Green container 24-09.

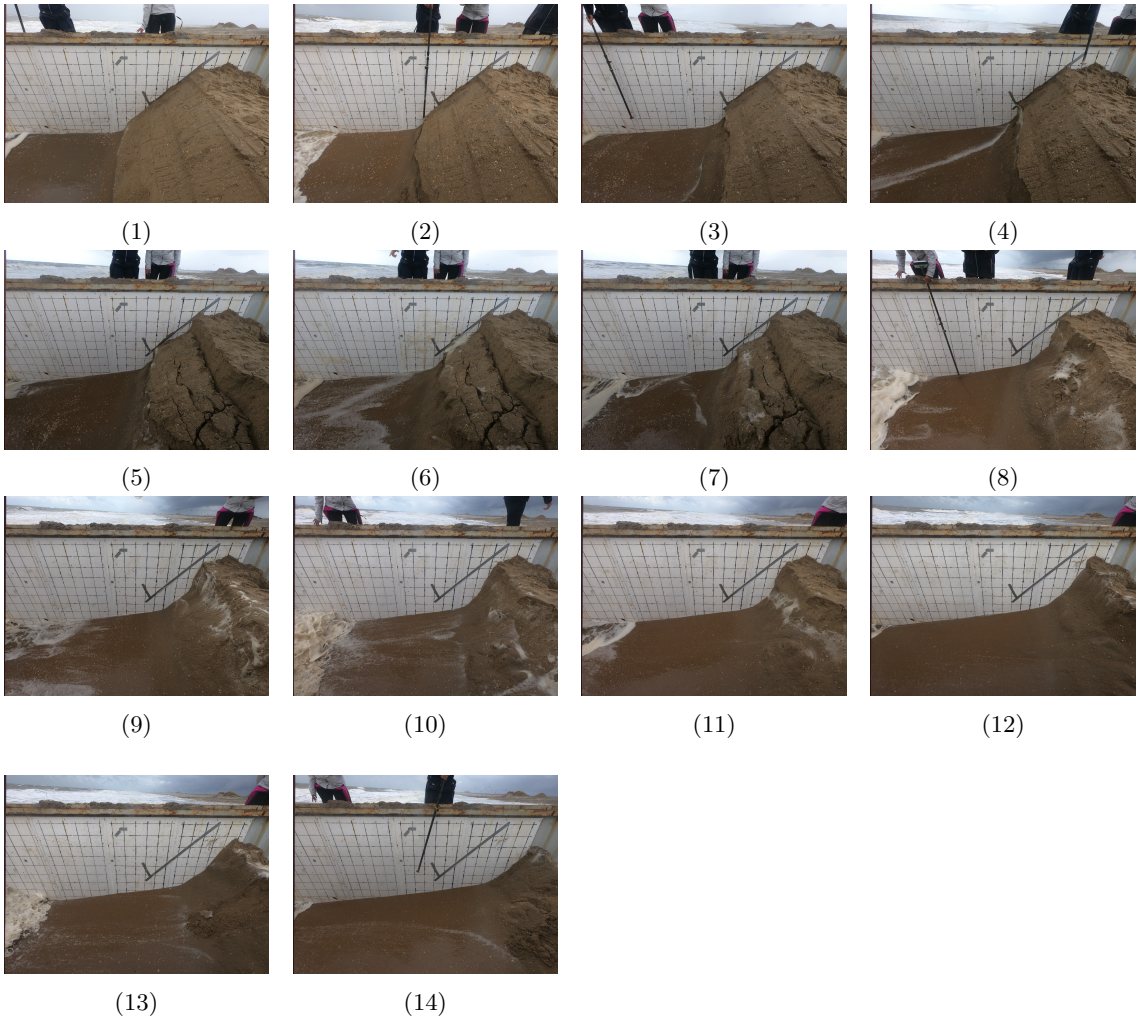

Figure 56: Erosion events Green container 26-09.

E Literature review effect of dune vegetation on dune erosion

Dune vegetation

The effect of vegetated slopes of dunes is commonly related to the ability to enhance dune formation, however the potential of dune vegetation to mitigate against erosion remains questionable. Traditional measures against dune erosion are more and more questioned, whether these are the only options and nature based solutions become more popular with a rising need. Therefore the potential of dune vegetation as such a nature based solution should be studied more comprehensively.

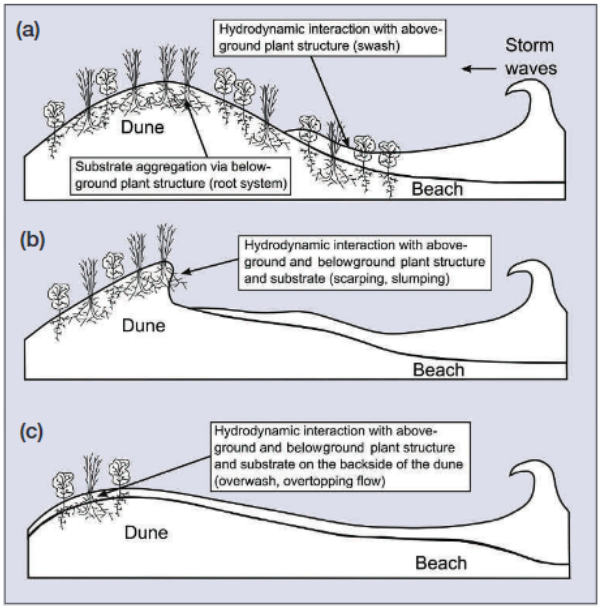

Figure 57: Interaction between vegetation and waves: swash interaction (a), Scarping of the dune during collision regime (b) (R. A. Feagin et al., 2015).

A distinction is made between above ground and below ground vegetation. The effect of above ground vegetation is related to the hydrodynamic altering of the flow, resulting in an increase in friction. This increase in friction leads to a greater dissipation of wave energy and, consequently, to a smaller run-up and a decrease in sediment absorption. The effect of below ground vegetation is expressed in the increase of soil stability. The roots anchor the soil, increasing grain-to-grain cohesion, the shear strength and increasing the critical slope reducing slumping (Heineke, 2022; R. A. Feagin et al., 2015).

In addition, secondary processes, as uprooting, burying, destruction and over strengthening, also have an effect on the robustness of the dune. Uprooting of below ground vegetation is induced by mobilization of sediment due to the hydrodynamic altering of the flow around the above ground vegetation. Burial of vegetation reduces the surface roughness and increases the erosion. Furthermore, destruction of vegetation by avalanching of dune scarps can lead to an expanded erosion rate. Lastly, over strengthening of the dunes is associated with retention of sediment resulting in steep foreshores resembling reflective beaches (Heineke, 2022).

Many experiments have already been dedicated to the question, regarding the relationship between dune vegetation and dune erosion volume. However, most experiments are limited by scale effects and limitations of laboratory simulations. Outcomes of studies contradict each other, leaving the question still unresolved.

Previous studies

Several studies describing the effect of dune vegetation on dune erosion have been dedicated (e.g. Kobayashi et al., 2013;Figlus et al., 2014;Martinez et al., 2016;Silva et al., 2016;Mendoza et al., 2017;R. Feagin, 2022). Kobayashi et al. investigated the effect of vegetation on dune erosion simulating dune vegetation with wooden dowels. In 2013 he conducted experiments in a wave flume. His experiments concluded that run up is reduced for a vegetated covered fore slope in the swash zone. However he also obtained an increase of sand mobilization in the vegetation zone and an overall increase of offshore sediment transport.

Figlus et al. covered the front slope of the dune with real vegetation. He obtained a reduction in erosion volume for slopes covered with vegetation of 33%. In addition, he found a relationship between the maturity of the plants and the reduction of dune erosion. His research concludes that mature and densely planted vegetation reduces erosion volume and scarp formation. Moreover, his experiments showed that it is essential to represent the vegetation with real live plants, since the interaction between above and below ground vegetation plays a dominant role.

Martinez et al., Silva et al., 2016 and Mendoza et al. conducted experiments in wave flumes with real vegetation. All studies found that dunes covered by vegetation experienced less erosion than dunes without vegetation (Heineke, 2022).

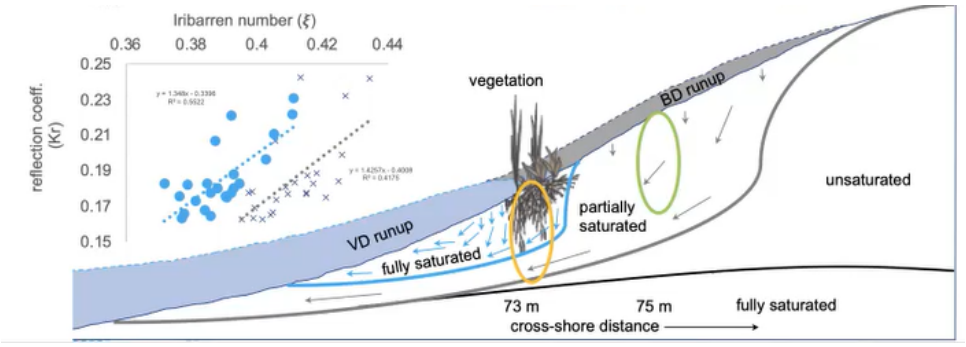

Figure 58: Dune erosion Vegetated dune (VD) compared to Bare dune (BD) (R. Feagin, 2022).

In contrast to the other studies, recent experiments by R. Feagin in 2022 showed that vegetation accelerates wave erosion during extreme events by depositing the formation of a slope, causing the dune to transition more quickly into a wave collision regime. He planted vegetation on the dunes and allowed it to grow for 6 weeks. He explained his findings by the attenuated wave run up, increase of reflected wave energy, excess runup moisture concentrations and initiated micro slope failures. As the vegetated dune retards the run up leads to altering of the flow. This leads to higher saturation levels at the top of the soil. Since the pressure in the lower layers is considerably less, this pressure build-up at the top of the soil will cause clumps to fall off the dune. For dunes without vegetation, the water will flow up and down undisturbed, leading to a more partially saturated dune and less falling clumps.

As shown in the previous studies, briefly explained above. There remains some uncertainty about how to simulate vegetation in experiments and studies results in differing outcomes. Therefore, it can be stated that it is important to do more research into potential ways of simulating dune vegetation as accurately as possible in order to provide a true reflection of reality in which the interaction between above and below ground vegetation can be simulated.

Current implementation dune vegetation in models

This section describes the current implementation of vegetation in the models DUROS+ and Xbeach. DUROS+ provides no option to implement vegetation into the model. For Xbeach four vegetation approaches are briefly discussed based on recently conducted research about these approaches by Heineke, 2022.

DUROS+ is limited to 1D erosion processes and is not able to model non-standard dunes (den Heijer et al., 2012). The equation on which the model is based does not take vegetation into account (Equation 2).

In XBeach, two approaches can represent the process of hydrodynamic change of flow through above ground vegetation, namely the roughness approach and the vegetation model. The other two approaches, the avalanching module and the root model, represent the process of soil stabilization by the below-ground vegetation.

The roughness approach takes vegetation into account by modifying the bed friction coefficient (cf) for vegetated areas. Heineke found that application of this model resulted in insignificant contribution to the effect of erosion volumes. The vegetation module incorporates the effect of vegetation by incorporating a dissipation term. This term relates shortwave dissipation to vegetation layers, stem diameter, density, and height. The use of the vegetation model has not yet been validated and, like the roughness approach, resulted in an insignificant effect on erosion volumes. Within the Avalanching module, the critical slope can be modified (Equation 5), in this way the effects on soil stabilization due to the root system of below ground vegetation can be simulated. Heineke stated that increasing the critical slope represents the best , simulation of dune vegetation of the four approaches. The root model simulates vegetation by increasing the critical velocity for sediment pickup, thereby reducing erosion volumes This model improves the ability of the model to simulate vegetation and could be applied in combination with the avalanche simulation module.


TU Delft
Witteveen + Bos